CHEMICAL REVIEWS

Volume 102, Number 5 May 2002

Organometallic Chemistry on Silicon and Germanium Surfaces

Jillian M. Buriak*

Department of Chemistry, 1393 Brown Laboratories, Purdue University, West Lafayette, Indiana 47907-1393

Received July 10, 2001

Contents

I. Introduction 1272
II. Flat and Porous Surfaces 1272
  A. Flat Single-Crystal Silicon and Germanium 1272
    1. Flat Silicon 1272
    2. Flat Germanium 1273
  B. Porous Silicon and Porous Germanium 1273
    1. Porous Silicon 1273
    2. Porous Germanium 1273
III. Reactive Surface Precursors 1274
  A. Si–H_x- and Ge–H_x-Terminated Surfaces 1274
    1. Si–H_x-Derivatized Flat Single-Crystal Silicon 1274
    2. Si–H_x-Derivatized Porous Silicon 1275
    3. Ge–H_x-Derivatized Flat, Single-Crystal Germanium 1275
    4. Ge–H_x-Derivatized Porous Germanium 1275
  B. Si–X (X = Cl, Br, I) and Ge–Cl-Terminated Surfaces 1276
    1. Si–Cl Termination of Flat Single-Crystal Silicon 1276
    2. Si–Br Termination of Flat Single-Crystal Silicon 1276
    3. Si–X Termination of Porous Silicon (X = Cl, Br, I) 1276
    4. Ge–Cl Termination of Flat Single-Crystal Germanium 1276
  C. Si(100) and Ge(100)-2 × 1 Dimer Surfaces 1277
IV. Wet Chemical Approaches to Si–C Bond Formation 1278
  A. Hydrosilylation Involving a Radical Initiator 1278
  B. Thermally Induced Hydrosilylation 1279
    1. Alkenes 1279
    2. Alkynes 1282
  C. Photochemical Hydrosilylation (UV) 1282
  D. Photochemical Hydrosilylation (White Light) 1285
  E. Hydrosilylation and Related Reactions Mediated by Metal Complexes 1288
  F. Reactions of Alkyl/Aryl Carbanions with Hydride- and Halide-Terminated Surfaces 1290
  G. Electrochemical Grafting on Hydride-Terminated Surfaces 1292
  H. Mechano–Chemical Functionalization of Non-Hydride-Terminated Silicon 1293
V. Wet Chemical Approaches to Ge–C Bond Formation 1293
  A. Halogenation/Alkylation Routes 1294
  B. Hydrogermylation Routes 1294
VI. UHV (Ultrahigh Vacuum) Approaches to Si–C Bond Formation 1295
  A. [2+2] Reactions of Alkenes and Alkynes with the Si(100)-2 × 1 Surface 1295
  B. [2+2] Reactions of Other Carbon-Containing Unsaturated Molecules with the Si(100)-2 × 1 Surface 1299
  C. Diels Alder ([4+2]) Reactions of Dienes with the Si(100)-2 × 1 Surface 1299
  D. Reaction of Methyl Halides with the Si(100)-2 × 1 Surface 1301
  E. STM-Initiated Reactions on Silicon Surfaces 1301
VII. UHV Approaches to Ge–C Bond Formation 1302
  A. [2+2] Reactions of Alkenes with the Ge(100)-2 × 1 Surface 1302
  B. Diels Alder ([4+2]) Reactions of Dienes with the Ge(100)-2 × 1 and Ge/Si(100)-2 × 1 Surfaces 1302
VIII. Further Functionalizing Functionalized Surfaces 1303
  A. C–H Bond Activation of Terminal Methyl Groups 1303
  B. Amide and Sulfonamide Bond Formation 1303
  C. Ester Hydrolysis 1303
  D. Ester Reduction and Cleavage 1303
  E. Ester Formation 1305
  F. Hydroboration of Olefins 1305
  G. Polymerization 1305
IX. Conclusions 1306
X. Acknowledgments 1306
XI. References 1306

* To whom correspondence should be addressed. E-mail: buriak@purdue.edu.

10.1021/cr000064s CCC: $39.75 © 2002 American Chemical Society
Published on Web 03/08/2002

Jillian Buriak was born in Toronto, Canada, in 1967. She received her A.B. degree from Harvard University in 1990 and pursued undergraduate research with Professor Andrew R. Barron. After teaching high school sciences in the Fiji Islands on a Catherine Innes Ireland Fellowship from Radcliffe College, she commenced her doctoral studies in 1991 with Professor John A. Osborn at the Université Louis Pasteur in Strasbourg, France. After completion of her Ph.D. degree in 1995, she carried out two years of postdoctoral research with Professor M. Reza Ghadiri at The Scripps Research Institute in La Jolla, CA. In 1997 she joined the faculty at Purdue University as Assistant Professor of Inorganic Chemistry and was promoted to Associate Professor in 2001.

I. Introduction

There is a rapidly growing interest in the surface chemistry of the group(IV) semiconductors, silicon and germanium, not only for the many technological applications presently in use and envisioned for the future, but from a fundamental perspective.[1,2] Much remains to be understood about the surface reactivity of these materials, despite the ubiquitous presence of silicon in microelectronics. New and fascinating reactions with organic molecules appear regularly in the literature which are continually transforming perceptions and perspectives of the surface reactivity of both silicon and germanium. While oftentimes the reactivity on a surface parallels that of solution-phase molecular silanes and germanes, there are many cases where perturbations or electronic effects from the underlying bulk can have dramatic consequences on the reaction pathway and outcome. In other situations, the electroactive behavior of the semiconductors can be utilized to drive surface chemistry, thus permitting access to reactions that are unknown in molecular systems. This incredible diversity is just now coming to light, despite a lack of detailed understanding of the subtle effects underpinning the observed reactivity.

It may seem initially surprising that the surface chemistry of silicon in 2002 has many questions associated with it, because of the worldwide domination of silicon in integrated circuits (ICs) and computing applications.[3] Surface oxide has served admirably well as the main passivation route for silicon devices since the 1960s due to its stability and ease of synthesis. There is, however, a strong drive to control and tailor the interfacial characteristics of this material, not only to address future IC roadblocks related to size considerations,[4] but also for a host of novel applications. As the size of devices on silicon chips decreases to the 100 nm regime and below,[5] the ratio of surface atoms/bulk becomes increasingly important, and thus, ideal manipulation of surface states is critical.[6] In addition, the Si/SiO_2 interface on silicon can be unacceptably electrically defective and is insulating which may be a problem if a direct electronic connection is required.[7] Silicon-chip-based devices for applications other than microelectronics also demand control over the interfacial characteristics, such as microarray technology moving to the forefront of genomics, proteomics, and sensing[8−12] lab-on-chips and μ-TAS (total automated systems),[13,14] and MEMS and NEMS (micro- and nanoelectromechanical systems).[15] Monolayers based on silicon−carbon bonds may provide the answer to many of these problems since the vast resources of organic and organometallic chemistry can be tapped to permit access to a broad range of functionalities.[16,17] The Si−C bond is both thermodynamically and kinetically stable due to the high bond strength and low polarity of the bond.[18]

Germanium, while overlooked as a microelectronics material since its use to build the first transistor in 1947,[19] is presently being revived due to predicted potential in high-speed and optoelectronic Si/Ge heterostructures.[20,21] The Semiconductor Industry Association (SIA) has postulated that these silicon−germanium layers may potentially provide one extra generation of performance when existing silicon-based CMOS FETs (complementary metal oxide semiconductor field effect transistors) reach their lowermost size limit.[22] Elemental Ge is also an important semiconductor from a technological standpoint: electron mobility is twice that of silicon,[23] and the increasing preponderance of Ge-based detectors[24] is awakening a long dormant interest in pure germanium materials. The fact that germanium lacks a stable oxide has always been viewed as a disadvantage in the past; Ge−C bond formation provides, however, a viable alternative that may prove convenient for further usage of germanium-based devices.

The field of silicon− and germanium−carbon bond formation on these semiconducting surfaces is divided into the 'wet chemical' and ultrahigh vacuum (UHV) groups. Both research areas are summarized here because while at first glance appearing somewhat dissimilar, they provide different perspectives on the same material, under distinct conditions. As more is understood about the organometallic surface chemistry of germanium and silicon, it is expected that insights gleaned from one method will more thoroughly complement the other.

II. Flat and Porous Surfaces

A. Flat Single-Crystal Silicon and Germanium

1. Flat Silicon

Due to their wide use in microelectronic applications, single-crystal silicon wafers of high purity are commercially available and relatively inexpensive. The most common surface orientations are Si(100) and Si(111) (vide infra), although other Si(*hkl*) orientations are known.[1,2,25] Upon exposure to air, single-crystal silicon becomes rapidly coated with a thin, native oxide that can be removed chemically with fluoride ion or thermally under UHV conditions. Depending upon the desired electronic properties,

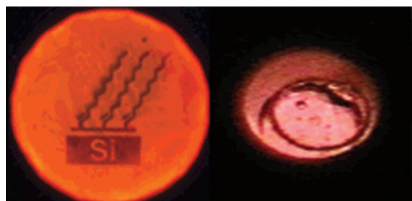

Figure 1. Two 1 cm diameter porous silicon samples emitting light through photoluminescence (left) and electrochemiluminescence (right).

silicon wafers are doped in a controlled fashion with electron-donating (P, As, Sb: n-type) or -withdrawing (B: p-type) impurities to render the intrinsic material more highly conducting. Due to the incredible strides made by the semiconductor industry in the areas of photolithography and etching, micro- and nanoscale three-dimensional structures on silicon wafers can be made with relative ease.

2. Flat Germanium

Limited use of germanium renders it substantially more expensive than silicon. On a square inch basis, prime grade Ge(100) is approximately 500 times costlier than prime grade Si(100). Doped and intrinsic Ge(100), (110), and (111) wafers are available commercially, and other stable orientations are known and their reactivities studied.[26] The GeO_2 interface is disordered and water soluble, one of the main obstacles for both fundamental studies and technological applications.

B. Porous Silicon and Porous Germanium

1. Porous Silicon

In 1990, Canham made the important discovery that nanocrystalline porous silicon can emit visible light through photoluminescence at room temperature.[27] Porous silicon samples emitting orange-red light under photo- and electroluminescence conditions are shown in Figure 1.

This discovery was quickly followed up by electro- and chemiluminescence and a subsequent explosion of interest.[28−30] Porous silicon has elicited publication of over 3500 papers since 1990, which is testament not only to its technological potential, but to the fundamental interest in understanding the luminescence phenomena of this material.[31] Porous silicon has a highly complex nanoscale architecture made up of 1-dimensional crystalline nanowires and 0-dimensional nanocrystallites;[6,32] an SEM image is shown in Figure 2.

The major barrier preventing commercial applications of porous silicon is the instability of its native interface, a metastable Si−H termination (vide infra), and thus, surface chemistry has proven to be a crucial element for the technological success of this material.[33] The photoluminescence of porous silicon depends strongly upon the surface passivation, with certain functionalities (i.e., halogens, styrenyl and phenethynyl groups)[34−36] resulting in complete quenching of light emission. While highly debated in the literature, it is generally accepted that due to quantum confinement effects, radiative recombination of entrapped electron−hole pairs (excitons) within the boundaries of nanocrystallites/nanowires with diameters of 2 nm is favorable, leading to the observed luminescence.[6,37] Surface states associated with various interface species can have dramatic quenching effects if they provide sites for nonradiative recombination of the excitons ('smart' quantum confinement model).[38,39] The precision of organic chemistry promises to allow for fine-tuning of these important interfacial effects, leading ultimately toward an understanding of the role of surface states on semiconducting nanoparticles in general. The nature of the surface bond, sterics, conjugation, and electronics of organic substituents can all be modulated at will and should provide the following: (i) stable porous silicon surfaces, (ii) modifiable surface characteristics, and (iii) potential to interface with organic conductor/semiconductors/LEDs and biologically relevant molecules for an array of applications, such as sensing,[40−44] photonics,[45] and other analytical uses.[46] From a technological standpoint, light-emitting porous silicon is especially attractive because it could be readily integrated with existing silicon-based integrated circuit (IC) manufacturing processes. Other non-silicon-based light-emitting materials such as GaAs or organic light-emitting compounds will require extensive modification of the IC processes for their incorporation into silicon-based chips.

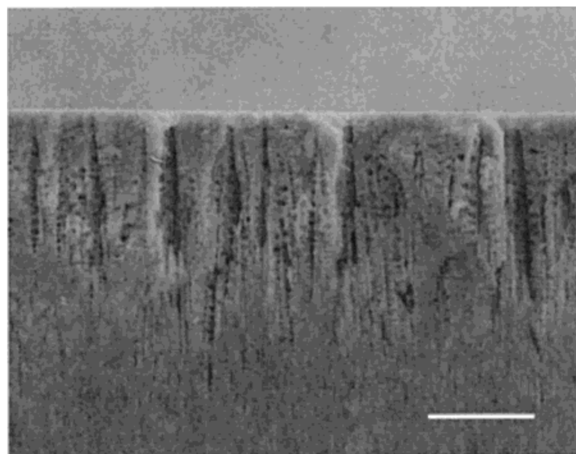

Figure 2. Cross-sectional scanning electron micrograph (SEM) image of a porous silicon sample. The anisotropy of the etch is clear, with the pores extending from the surface of the Si(100) wafer down into the bulk. This sample was etched from n-type Si(100) (P-doped, 0.75−0.95 Ω·cm) at 77.2 mA cm^{-2} for 1 min with a 1:1 solution of 49% HF(aq)/EtOH. Scale bar is 10 μm.

Porous silicon is an especially attractive testing ground for surface chemistry due to its high surface area which renders analysis relatively straightforward through conventional transmission Fourier transform infrared (FTIR) or diffuse reflectance infrared (DRIFT) spectroscopy. As a result, routine characterization of this material is practical and facile for most chemists.

2. Porous Germanium

While several thousand papers have been published on porous silicon, the total number related to porous germanium is less than 5.[47−50] It still remains unknown as to whether the properties of porous germanium are distinctly different from those of porous silicon. While weak red light emission has

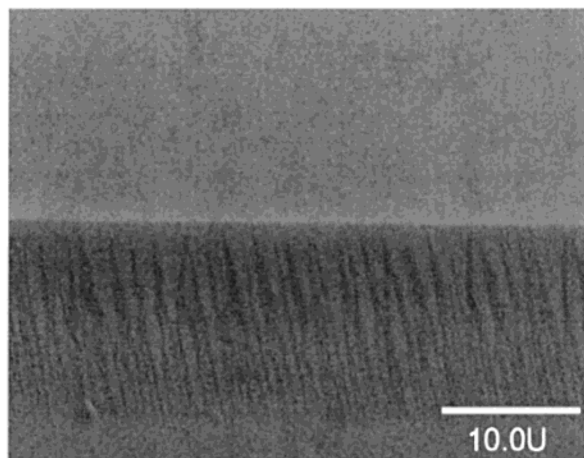

Figure 3. Cross-sectional SEM image of a porous germanium sample, derived from n-type Ge(100) with a 9° miscut, leading to tilting of the pores by 9° from the surface normal.

been reported from this material, the source has not been elucidated.[47,49] Initial reports utilized an anodic etch with an aqueous HF electrolyte/etchant, similar to known porous silicon preparations.[48-50] Because of the irreproducibility of these etches, a new bipolar etching procedure was published utilizing an aqueous HCl-based system.[47] Application of an initial positive bias to a Ge(100) wafer appears to produce a rough oxide interface which dissolves in the aqueous medium, due to the solubility of GeO_2 in water. A subsequent negative bias for 1 min results in the porous germanium structure, as shown by SEM (Figure 3). The anisotropic structure is titled 9° from the surface normal due to the 9° miscut of the wafer; this ensures that the observed structure is not an artifact of the cleavage procedure. Transmission FTIR spectroscopy can be carried out since the material has a wide IR window in the mid-IR region, like silicon. While much work remains to be done on this material, preliminary results suggest that porous germanium is tantalizingly different from porous silicon and thus may yield new and interesting new properties.

III. Reactive Surface Precursors

The surfaces of silicon and germanium have several different chemical handles through which functionalization may be carried out. The typical bond dissociation energies of various reactive groups on both surfaces and in molecular compounds are listed in Table 1.[51] Caution must be taken in using these values to predict reactivity. For instance, the Si−F bond is one of the strongest known between any two elements of the periodic table and yet is highly polarized in the direction $^{\delta+}$Si−F$^{\delta-}$; this enables facile substitution at the Si center upon nucleophilic attack

Table 1. Typical Bond Energies for Various Groups Related to Group(IV) Elements (kJ mol^{-1})

element	self	H	C	O	F	Cl	Br	I
C	292−360	416		336	485	327	285	213
Si	210−250 (bulk) 310−340 (disilane) 105−126 (disilene)	323	369	368	582	391	310	234
Ge	190−210 (bulk) 256 (digermane)	290	255		465	356	276	213

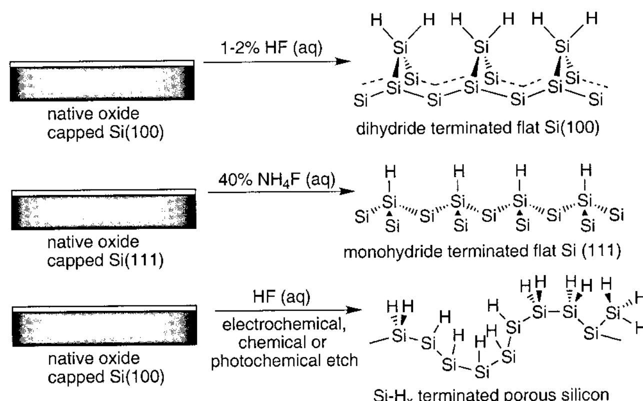

Figure 4. Fluoride-based etching conditions, leading to hydride-terminated flat and porous silicon surfaces.

and hence is kinetically very labile. As can be seen, the weakest bonds on the silicon and germanium surfaces are the Si−Si and Ge−Ge bonds, but if the surface is substituted with other groups, they may be less reactive due to steric considerations.

The different surfaces prepared and utilized for Si−C and Ge−C bond formation are described here. Wet chemical reactions require a metastable surface to successfully carry out surface chemistry: The precursor surface must be stable enough to handle at atmospheric pressure in the presence of solvent vapors, inert gas impurities, and other contaminants and yet reactive enough to undergo chemistry. Two surfaces shown to have this bipolar character are E−H and E−X (E = Si, Ge; X = Cl, Br, I) terminated silicon and germanium. The E−H-terminated surface is relatively stable in air for short periods; in contrast, the E−X-derivatized surface is much more reactive with respect to hydrolysis and E−OH formation and can generally only be handled under inert atmosphere. UHV, on the other hand, permits reactivity studies of surfaces much too reactive for even inert atmosphere handling. Practical information describing preparation and handling is given for both wet chemical and UHV surface precursors.

A. Si−H_x- and Ge−H_x-Terminated Surfaces

1. Si−H_x-Derivatized Flat Single-Crystal Silicon

The hydride-terminated surfaces in general offer many advantages, including their excellent chemical homogeneity (>99% H termination) and strong FTIR stretching modes (~2100 cm^{-1}) which can provide information as to surface flatness and makeup. Long-term use of an Si−H-terminated surface for many applications is precluded due to its propensity to oxidize, but it can be easily handled in air for minutes to tens of minutes without measurable degradation. Rapid and efficient preparation of Si−H hydride-terminated flat surfaces has been known for over 10 years, as outlined in Figure 4.[52,53] Treatment of commercial, native oxide-capped flat crystal silicon (100) wafers with dilute (1−2%) aqueous HF yields the (100) dihydride $=SiH_2$ surface, although surface roughness on the nanometer scale is observed.[52] Atomically flat areas of monohydride ≡Si−H termination can be achieved through use of a commercial silicon wafer of the (111) orientation, treated for 4−6 min with degassed 40% aqueous NH_4F.[52-54] The Si-

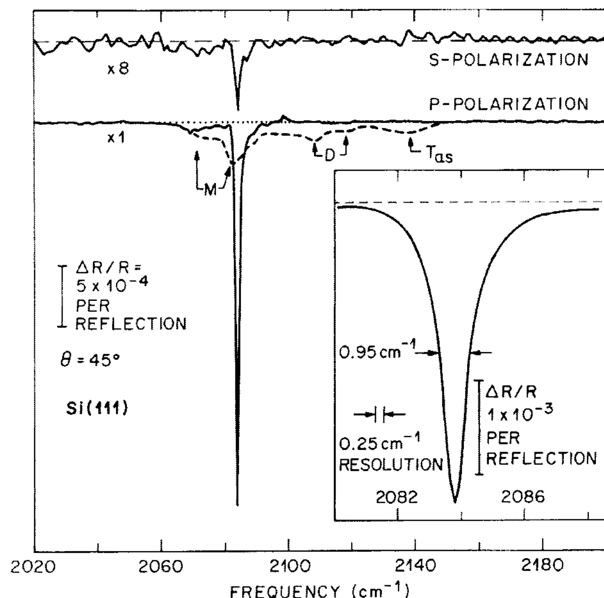

Figure 5. ATR-FTIR spectra of the hydride-terminated Si(111) surface, prepared through the 40% NH_4F (aq) etching procedure, taken with both s- and p-polarized IR light. The sharpness of the ν(Si−H) vibration at 2083.7 cm^{-1} clearly indicates the high degree of chemical homogeneity of this surface. (Reprinted with permission from ref 52. Copyright 1990 American Institute of Physics.) The authors are also thanked for permission to reprint this figure.

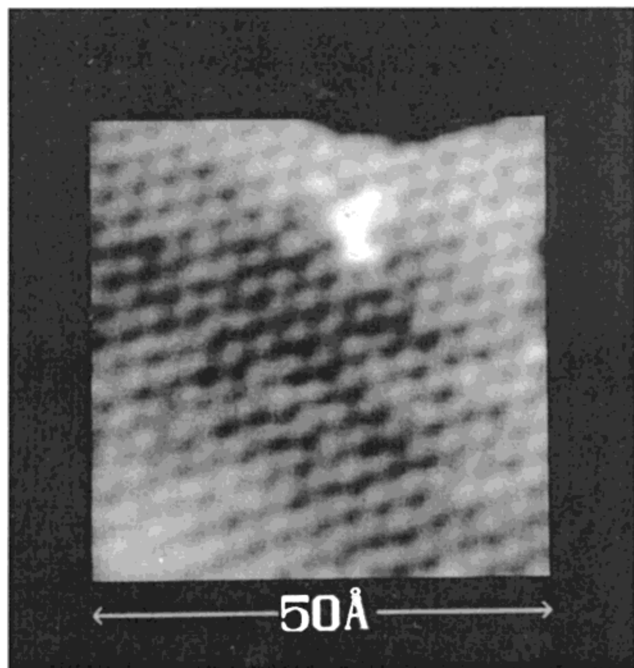

Figure 6. STM image of the flat Si(111)−H surface, prepared through etching with 40% NH_4F (aq). The gray scale represents a height change of 0.5 Å. (Reprinted with permission from ref 53. Copyright 1991 American Institute of Physics.) The authors are also thanked for permission to reprint this figure.

(111)−H monohydride surface has a very sharp, narrow stretch ν(Si−H) at 2083.7 cm^{-1} (line width = ∼1 cm^{-1}) as observed by attenuated total reflectance (ATR) FTIR which indicates an atomically smooth surface over nanometer-scale distances (Figure 5).[52] Atomic resolution of the surface silicon atoms can be observed by STM, as shown in Figure 6,

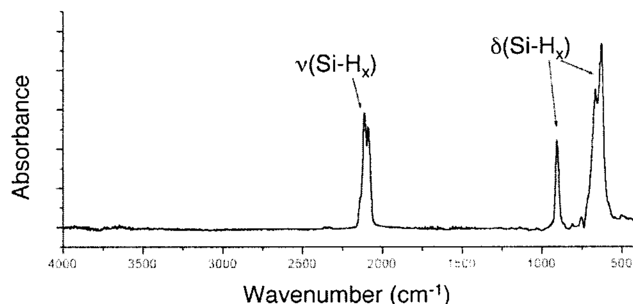

Figure 7. Transmission FTIR spectrum of hydride-terminated porous silicon. The only visible features correspond to Si−H_x stretches and bending modes.

confirming the flat, ordered surface produced by NH_4F etching.[53] In contrast, if dilute HF is used, the surface is rough, atomic resolution by STM is impossible, and the ν(Si−H) stretch is very broad.[55]

2. Si–H_x-Derivatized Porous Silicon

Porous silicon is easily prepared through simple galvanostatic,[56] chemical (stain),[57] or photochemical[58] etches from silicon wafers of a (100) orientation.[32] Aqueous solutions of HF are utilized, often with ethanol as a co-additive to reduce surface tension. A fortuitous result of the etching process is the native hydride termination of the surface, as shown in the transmission FTIR spectrum in Figure 7. The surface is terminated with $-SiH_3$, $=SiH_2$, and ≡SiH groups in a variety of different local orientations and environments due to the roughened surface morphology, as represented schematically in Figure 4.[59] The ν-(Si−H) band of porous silicon is broad (∼50 cm^{-1}), with a tripartite structure corresponding to the ≡SiH, $=SiH_2$, and $-SiH_3$ functionalities. All the freshly etched silicon hydride-terminated surfaces are chemically homogeneous (>99% H termination), essential for clean reactions. The electrochemical etching approach is most commonly used because of its ease and wide range of porosities and nanocrystallite sizes accessible. The etch is anodically assisted and thus appears to be driven by holes and oxidation of the silicon layer;[6] quantum confinement effects may also be important.[60]

3. Ge–H_x-Derivatized Flat, Single-Crystal Germanium

Hydride termination of flat Ge(100) single crystals via a wet chemical technique was first published only recently in 2000.[61,62] Immersion of a native oxide-terminated Ge(100) wafer in 10% aqueous HF for 10 min results in hydride termination with a surface roughness on the order of 3−4 nm. The roughness of this surface correlates with the broad ν(Ge−H) observed by ATR-FTIR centered around 2100 cm^{-1} with a line width of ∼50 cm^{-1} (Figure 8). More dilute solutions (2−5%) of aqueous HF resulted in weak ν-(Ge−H) stretches in the IR, and 25% aqueous HF caused deep pitting of the germanium surface. The Ge−H_x-terminated material is stable in air for up to 1 h, as shown by FTIR.

4. Ge–H_x-Derivatized Porous Germanium

Hydride-terminated porous germanium was first reported to be prepared by an electrochemical etch with HF; a broad stretch around 2100 cm^{-1} in the

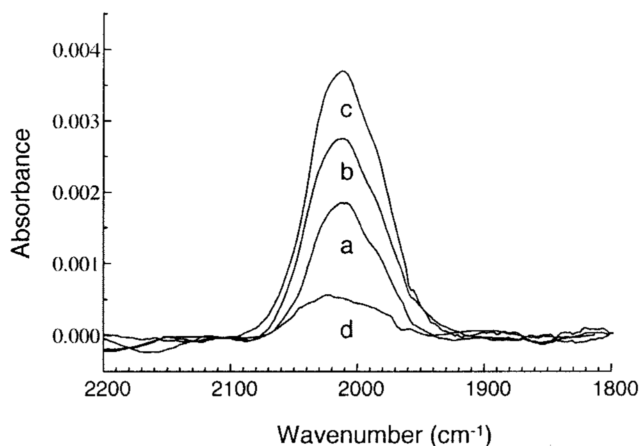

Figure 8. ν(Ge−H) vibrations observed by ATR-FTIR of hydride-terminated Ge(100). Surfaces prepared by etching with a 10% HF (aq) solution for (a) 2 min, (b) 5 min, (c) 10 min, and (d) 15 min. (Reprinted with permission from ref 61. Copyright 2000 American Chemical Society.)

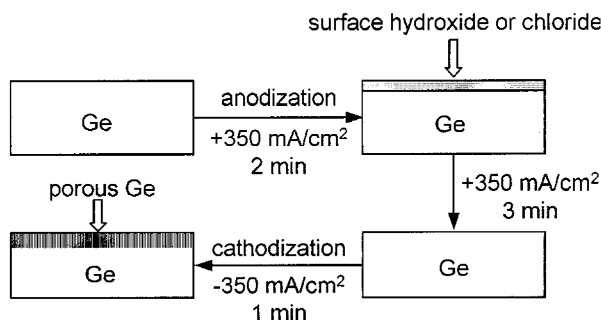

Figure 9. Bipolar electrochemical etching (BEE) procedure to produce porous germanium. The total 5 min of anodic etching in the aqueous HCl-based electrolyte serves to initially produce and then dissolve a porous germanium oxide layer. Subsequent etching for 1 min under a negative bias produces hydride-terminated porous germanium.

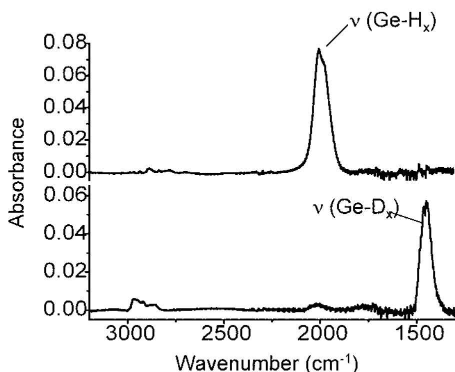

Figure 10. Transmission IR of porous germanium produced through BEE. The top spectrum utilized an aqueous HCl etchant, producing hydride termination with ν(Ge−H) at ~2100 cm^{-1}. A DCl/D_2O etchant yields the deuterated surface (bottom spectrum) with the expected isotopic shift.

FTIR spectrum was attributed to the ν(Ge−H).[48] Utilization of a unique bipolar electrochemical etch (BEE) with an HCl etchant/electrolyte has been shown recently to yield reproducibly hydride-terminated porous germanium structures, starting with Ge(100) wafers; the bipolar etching procedure is outlined in Figure 9.[47] The ν(Ge−H) vibration is broad, but two features are visible at 2044 and 2015 cm^{-1}. Use of a DCl solution results in a Ge−D_x-terminated surface with a ν(Ge−D) stretch centered around 1455 cm^{-1}, the expected isotopic shift. Figure 10 shows both the hydride- and deuteride-terminated surfaces.

B. Si–X (X = Cl, Br, I) and Ge–Cl-Terminated Surfaces

Halogenation of silicon and germanium surfaces through wet chemistry is outlined in Figure 11. In general, these surfaces are quite reactive and thus should be handled under an inert atmosphere. From a practical standpoint, however, all of the halide surfaces described here have been utilized for further surface chemistry, including Si−C, Si−O, and Ge−C bond formation, which points to their ease of preparation and good surface conversions.

1. Si–Cl Termination of Flat Single-Crystal Silicon

Si(111)−Cl surfaces have been prepared by treating the hydride-terminated Si(111) surface, synthesized through aqueous HF treatment, with PCl_5 for 20−60 min at 80−100 °C using benzoyl peroxide as a radical initiator in chlorobenzene.[63] X-ray photoelectron spectroscopy (XPS), AES, and HREELS support formation of Si−Cl bonds. UV irradiation from a lamp with lines at 254, 312, and 364 nm has also been shown to permit surface chlorination with PCl_5 at the boiling point of the chlorobenzene solvent, in the absence of the benzoyl peroxide initiator.[64] Cl_2 can be used with either photochemical (350 nm for 15 s −10 min or 300 W tungsten lamp for 2 min) or thermal (80 °C for 10 min) initiation to convert the Si(111)−H surface to Si(111)−Cl.[65−67]

2. Si–Br Termination of Flat Single-Crystal Silicon

Bromide termination of an Si(111) surface has been carried out by treating the hydride surface, prepared through etching with 40% NH_4F, with *N*-bromosuccinimide (NBS) in DMF for 20 min at 60 °C in the presence of benzoyl peroxide as the radical initiator.[65] Alternatively, neat CCl_3Br can be used under thermal conditions (80 °C for 30 min), with photolysis (300 nm UV for 20 min), or in the presence of benzoyl peroxide (60 °C for 30 min).[65]

3. Si–X Termination of Porous Silicon (X = Cl, Br, I)

Treatment of a freshly etched hydride-terminated porous silicon surface with molecular chlorine, bromine, and iodine under nitrogen or argon results in efficient Si−X (X = Cl, Br, I) bond formation in 30 min at room temperature.[68,69] In contrast to the preceding reactions on flat Si(111) surfaces, the hydrides remain intact and are not substituted by chloride; the weaker Si−Si bonds are cleaved and two new Si−X bonds are formed.

4. Ge–Cl Termination of Flat Single-Crystal Germanium

Exposure of an oxidized Ge (111) surface (pretreated with H_2O_2 and oxalic acid) to HCl gas at 87−90 °C for 20 min removes a small amount (~0.2 μm) of Ge(s) as $GeCl_4$(g), and results in a chloride-terminated surface.[70] In a simplified and gentler approach, treatment of the native oxide on a Ge(111) wafer with 10% aqueous HCl for 10 min results in chloride termination.[71] According to the authors, the Ge(111)−Cl surface can be handled in air with little degradation. The surfaces were analyzed by XPS and X-ray absorption near edge spectroscopy (XANES).

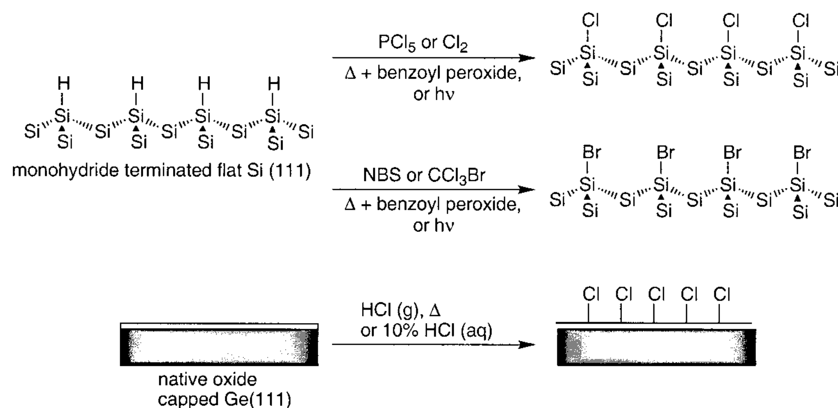

Figure 11. Summary of routes to produce halide-terminated flat silicon and germanium.

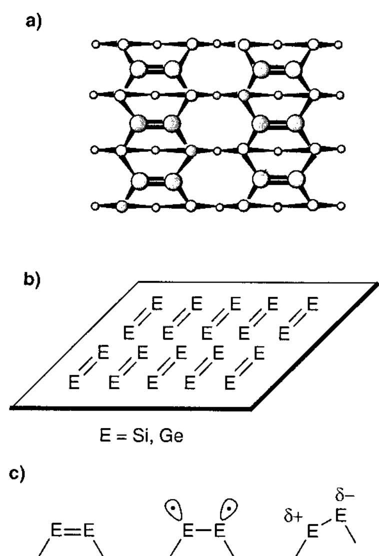

Figure 12. (a) Representation of the silicon–silicon or germanium–germanium dimers on the corresponding E(100)-2 × 1 (E = Si,Ge) surface. (b) Schematic of the E=E dimers on the E(100)-2 × 1 interface and their relative orientation in the *x* and *y* directions. (c) Possible characters of the silicon–silicon and germanium–germanium dimers: covalent σ- and π-bonding arrangement, singlet diradical, and tilted zwitterionic species.

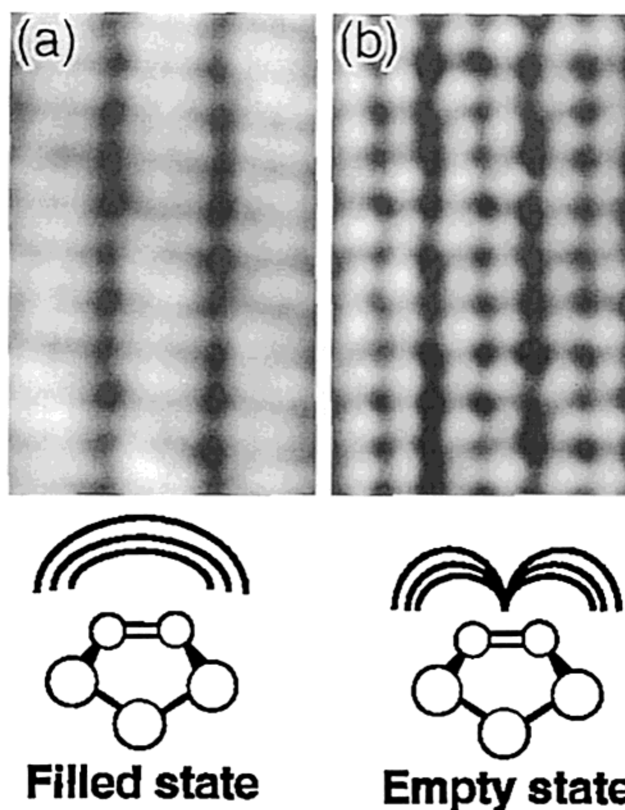

Figure 13. STM images of the silicon–silicon dimers, imaged with (a) $V_{sample} = -2.0$ V and (b) $V_{sample} = 2.3$ V. The filled and empty states of these highly ordered dimers can be probed by biasing the surface in the opposite directions. The dimensions of the figure are 2.3 nm × 7.7 nm. (Reprinted with permission from ref 2. Copyright 1996 American Chemical Society.) The authors are also thanked for permission to reprint this figure.

C. Si(100) and Ge(100)-2 × 1 Dimer Surfaces

Under ultrahigh vacuum (UHV) conditions (pressure < 10^{-10} Torr), highly reactive 'bare' single-crystal silicon surfaces can be prepared and studied.[1,2] The activity of these surfaces is very different from that of the metastable hydride and halide-terminated materials, providing entirely different insights into the structures and properties of flat group(IV) semiconductors. The surface atoms on thermally reconstructed Si and Ge(100)-2 × 1 surfaces pair into dimers connected by a σ and weak π bond, thus having essentially a double bond analogous to alkenes, disilylenes ($R_2Si{=}SiR_2$), and digermylenes ($R_2Ge{=}GeR_2$), as shown in Figure 12.[72] The exact nature of this bond is, however, debated since the low strength of the π bond may actually indicate that a diradical depiction is more accurate. In addition, it has been shown that the silicon–silicon and germanium–germanium dimers tilt on the surface, leading to zwitterionic character. In any case, the silicon and germanium dimers are highly reactive toward cycloaddition reactions with unsaturated bonds and have been exploited to produce ordered organic monolayers. Interestingly, use of 4° miscut off-axis Si(100) single-crystal wafers allows for highly rotationally oriented samples in which all the Si=Si dimers are pointed in the same direction, yielding anisotropic surfaces on a centimeter length scale. The high ordering of the dimers, showing both the filled and empty states, is shown in the stunning STM images of Figure 13; the filled and empty states were imaged by changing the tip bias.[2]

The Si(100)-2 × 1 dimer surfaces are prepared by first degassing the native oxide-terminated surface

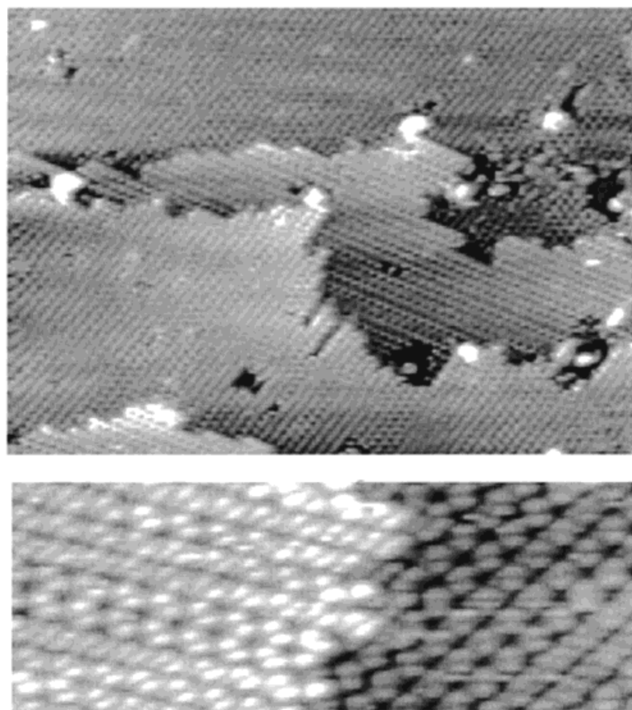

Figure 14. STM images of the Ge(100)-2 × 1 surface prepared by the technique described in section III.C. The top image is 52 nm × 38 nm and the bottom 14 nm × 6 nm. (Reprinted with permission from ref 75a. Copyright 1999 Elsevier.) The authors are also thanked for permission to reprint this figure.

at temperatures greater than ~ 875 K and then flash annealing.[73,74] Surface pretreatments include extensive degassing overnight at high temperatures or Ar^+ sputtering at room temperature, both under UHV. The literature suggests that the Ge(100)-2 × 1 surface may be a bit more tricky to access due to the lattice mismatch between Ge and GeO_2 which leads to an inhomogeneous oxide layer. This problem has been addressed through a procedure involving wet chemical degreasing and oxidation, followed by a UV/ozone treatment, and then outgassing and flash annealing under UHV at 1000 K.[75] The surface shows ordered flat areas with dimensions >50 nm, as shown in Figure 14.

IV. Wet Chemical Approaches to Si–C Bond Formation

Over the past 8 years, an incredible diversity of approaches that can be categorized as 'wet chemical' or benchtop chemistry has arisen in the literature. The summary of the wet chemical approaches will start with a reaction motif known for decades in the molecular organosilicon literature, hydrosilylation, and then diverge into electrochemical and other routes toward Si–C bonds on surfaces.

A. Hydrosilylation Involving a Radical Initiator

Hydrosilylation involves insertion of an unsaturated bond into a silicon–hydride group. Alkyne and alkene hydrosilylation on Si–H-terminated surfaces yield alkenyl and alkyl termination, respectively, as shown in Figure 15. The first example of hydrosilylation of nonoxidized hydride-passivated silicon was carried out in 1993 on flat crystal Si(111)–H surfaces.[76] Insertion of alkenes into surface-bound Si–H groups, in the presence of the a diacyl peroxide radical initiator, provided high-quality alkyl monolayers in 1 h at 100 °C. Monolayers prepared from octadecene, yielding octadecyl groups on the surface, are densely packed and tilted approximately 30° from the surface normal. As a result of the good coverage provided by the film, the silicon surfaces demonstrate excellent stability and withstand extended boiling in aerated boiling chloroform, water, acid (2.5 M H_2SO_4 in 90% dioxane, v/v), and base (10% aqueous 1 M NH_4OH) and are resistant to fluoride (immersion in 48% aqueous HF). Under ambient conditions in air, little oxidation of the silicon surface is observed, indicating the usefulness of this approach for technological applications.

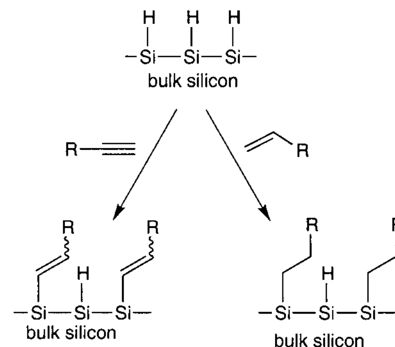

Figure 15. Schematic of hydrosilylation chemistry. Hydrosilylation involves the insertion of an unsaturated bond, here an alkyne or an alkene, into an Si–H bond, resulting in Si–C bond formation and formation of alkenyl or alkyl groups, respectively.

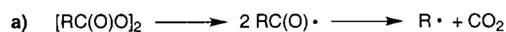

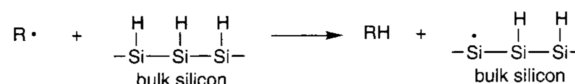

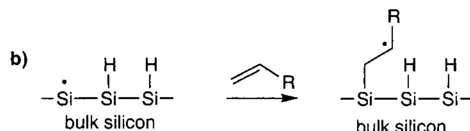

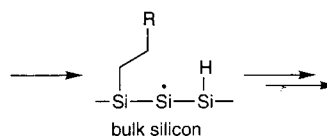

Figure 16. Mechanism for radical-based hydrosilylation. (a) Initation reaction in the presence of diacylperoxide, resulting in R• radicals. The R• can then abstract a hydrogen atom from the surface, forming a highly reactive silicon radical. (b) Reaction of the surface silicon radical with the alkene substrate and formation of the Si–C bond.

A radical mechanism was proposed for monolayer formation under these conditions, as shown in Figure 16. The initiator, the diacyl peroxide, undergoes homolytic cleavage to form two acyloxy radicals which decompose to carbon dioxide and an alkyl radical. The alkyl radical can then abstract H• from a surface Si–H group to produce a silicon radical.

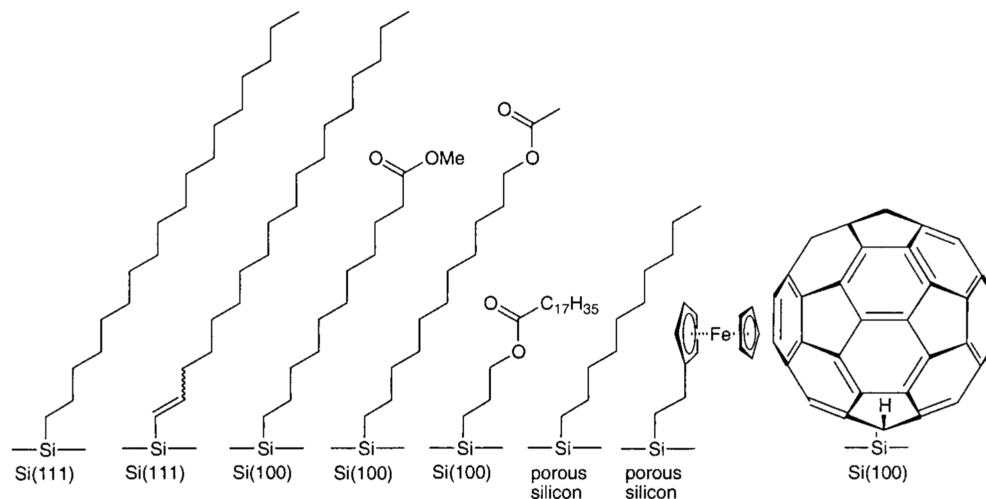

Figure 17. Examples of surface terminations produced by thermal hydrosilylation.

Because silyl radicals are known to react extremely rapidly with olefins, formation of a silicon carbon bond is the next probable step.[77] The carbon-based radical can then abstract a hydrogen atom either from a neighboring Si−H group or from the allylic position of an unreacted olefin.

The majority of studies carried out by this group involved octadecene, but the ω-Cl-terminated olefin, 11-chloroundec-1-ene, produced good-quality monolayers with chloride termination. As suggested by the authors, further functionalization of the surface through the chloride is possible. The use of the bromide-terminated olefin, 11-bromoundec-1-ene, however, produced a poorly organized monolayer, perhaps due to the incompatibility of the Br with the radical nature of the reaction.

B. Thermally Induced Hydrosilylation

1. Alkenes

Control experiments carried out by Chidsey and coworkers during their investigations of diacylperoxide-initiated olefin hydrosilylation on Si(111) surfaces indicated that the reaction could occur in the absence of diacylperoxide initiator at higher temperatures (≥150 °C), almost certainly through homolytic Si−H cleavage, $Si{-}H \rightarrow Si^{\bullet} + H^{\bullet}$. This yields the silicon surface-based radical (dangling bond) which can then react via the mechanism outlined in Figure 16b.[78] Aliphatic monolayers produced on hydride-terminated Si(111) and Si(100) through the thermal hydrosilylation of alkenes are stable up to 615 K under vacuum, which indicates that organic monolayers on silicon can be thermally resistant.[79]

Hydride-terminated Si(100) was shown to react in a similar fashion.[80] Working at 200 °C, a number of different olefins were examined for their propensity to form stable monolayers. A 2 h contact time produced closely packed monolayers when long-chain aliphatic alkenes (12−18 carbons) were used as judged by X-ray reflectivity, ATR infrared spectroscopy, and contact angle measurements. Examples of surface terminations accessible through the thermal hydrosilylation route are shown in Figure 17.

A major limitation of the thermal hydrosilylation approach is the large excess of alkene required.[81] For instance, up to several milliliters of neat alkene are required to modify the entire surface of a silicon parallelopiped ($50 \times 10 \times 1$ mm^3) for ATR analysis *each time.* While simple alkenes such as 1-hexadecene are not particularly expensive, more exotic substrates and those which are not commercially available and thus need to be synthesized are potential limitations. To circumscribe this restriction, a range of alkenes dissolved in inert, high-boiling hydrocarbons were examined. 1-Hexadecene (10%) in solvents such as *n*-decane, anisole, toluene, xylene, cumene, *tert*-butylbenzene, and mesitylene was compared with the results obtained with neat 1-hexadecene, the reference sample; contact angles with water provided the benchmark. On the Si(100) hydride surface, both refluxing *tert*-butylbenzene and mesitylene solutions gave high advancing contact angles (Θ_a) of 108° and 109° with water, comparable to that obtained with neat 1-hexadecene ($\Theta_a = 109°$). The receding contact angles (Θ_r) were also high and similar to each other. The effect of concentration of 1-hexadecene in the various high-boiling solvents on contact angles of the monolayers is shown in Figure 18. Amazingly, a solution concentration as low as 2.5% of 1-hexadecene in mesitylene still has Θ_a and Θ_r that compare well with neat 1-hexadecene, while the other solvents show greater decreases or start out with lower contact angles, even at higher concentrations of 25%. The apparent advantage of mesitylene as opposed to the other high-boiling solvents tried is that this molecule does not result in pinhole defects in the monolayer as a result of its large size, as opposed to *n*-hexadecane which intercalates into the forming monolayer. This work is very useful because it reveals that even dilute solutions of alkene (2.5%) in mesitylene, a 40-fold reduction in absolute quantity, can result in ordered monolayers via thermal hydrosilylation; neat alkene is not required.

Because the spectroscopic techniques measure only macroscopic properties of the organic monolayers, molecular modeling of Si(111) alkyl-terminated surfaces, the product of alkene hydrosilylation, was carried out to try to extract molecular- and atomic-level information.[82,83] The modified surface was described as a repeating box using the polymer-consistent force field (PCFF), as shown in Figure 19.

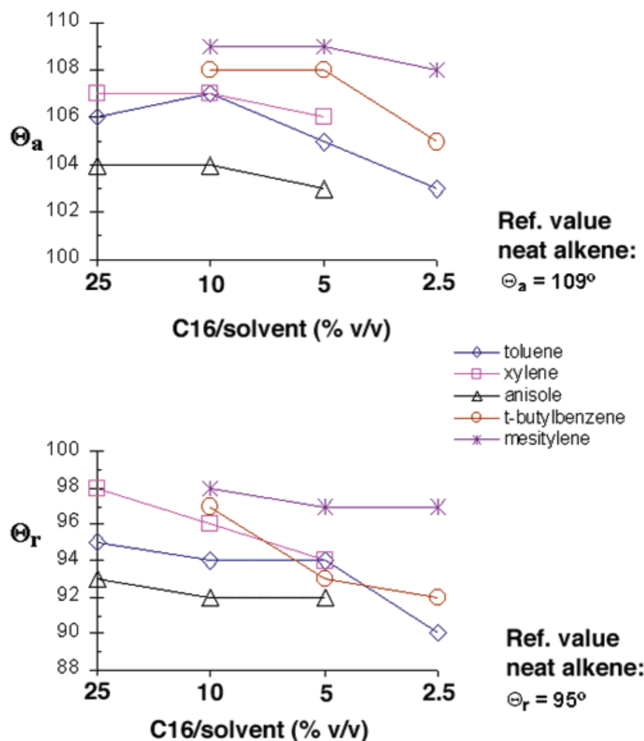

Figure 18. Effects of different hydrocarbon solutions of hexadecene on the contact angles of water of the resulting alkyl-terminated Si(100) surface, formed through thermal hydrosilylation. (Top) Advancing contact angles, Θ_a. (Bottom) Receding contact angles, Θ_r. (Reprinted with permission from ref 81. Copyright 1999 American Chemical Society.) The authors are also thanked for permission to reprint this figure.

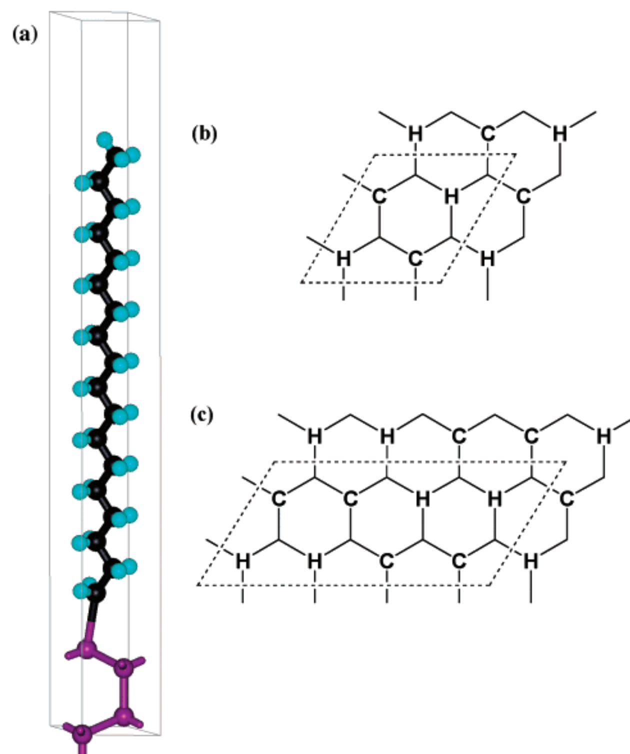

Figure 19. (a) Structure of the basis unit utilized to model the alkylated Si(111) surface. (b and c) Two different unit cells used to construct the repeating boxes to make up a larger Si(111) surface. C and H represent alkyl and hydride groups, respectively, and the dashed lines the unit cells. (Reprinted with permission from ref 82. Copyright 2000 American Chemical Society.) The authors are also thanked for permission to reprint this figure.

Substituting 50% of the surface hydrides with alkyl chains resulted in calculations which correspond with experimental data, specifically the tilt angle of the chains as determined by ATR-FTIR and X-ray reflectivity. On the basis of the substitution patterns (unit cells) of Figure 19, the PCFF-optimized structures are shown in Figure 20. Different percent coverages result in monolayers that do not fit the experimental evidence. For instance, lower substitution values of 33.3% result in highly disordered monolayers in which the alkyl chains attempt to compensate for the extra space by tilting 60° from the surface normal and bending, twisting, or adopting banana-like configurations, behavior not substantiated by the ATR-FTIR spectroscopy and X-ray reflectivity data. Substitution of 100% of the surface hydrides with alkyl chains results in a tilt angle of ~1°, serious deformations of the surface Si−C bonds, and substantial interpenetration of the van der Waals volumes, a highly unfavorable situation. The authors conclude that about 50−55% of the surface hydrides on an Si(111)−H surface are replaced during thermal hydrosilylation, as this appears to be the optimal substitution percentage based on their theoretical calculations. These results substantiate the suggestions made by Chidsey and co-workers, that the alkyl chains on the Si(111) structure cannot pack with complete substitution of the apical Si−H functionalities (1 × 1 structure); an average pattern more similar to a 2 × 1 substitution motif is more likely, which is equivalent to ~50% substitution.[76]

This molecular modeling work was followed up by further molecular mechanics and molecular dynamics simulations at various temperatures.[84] Because the film thickness, tilt angle, and conformation of alkanethiols on Au(111) surfaces are temperature dependent, simulations of alkyl monolayers on silicon were carried out over a temperature range of 50−500 K. As the temperature increases, both the system and molecular tilt angles decrease, rendering the monolayer thicker as a result, as shown in Figure 21. As would be expected, the number of gauche defects along the methylene chain also increases with temperature, with as many as 35% at 500 K, according to these simulations.

Thermally induced hydrosilylation of alkenes and an alkyne has been applied to Si−H-terminated porous silicon surfaces.[85−87] It was initially reported that refluxing porous silicon for 18−20 h at 110−180 °C in an aliphatic alkyne or alkene yields alkyl monolayers.[85] They showed that an ethyl ferrocene surface could be produced via hydrosilylation of vinyl ferrocene and carried out cyclic voltammetry (CV), providing insight into the electronic properties of these functionalized porous silicon layers. The surfaces demonstrate good stability to chemically caustic conditions, with little oxidation appearing upon boiling in aqueous base (pH 12 solution of KOH) for 1 h; hydride-terminated porous silicon dissolves in minutes under these conditions.

Further investigation of thermal hydrosilylation of 1-decene on porous silicon was examined, and the

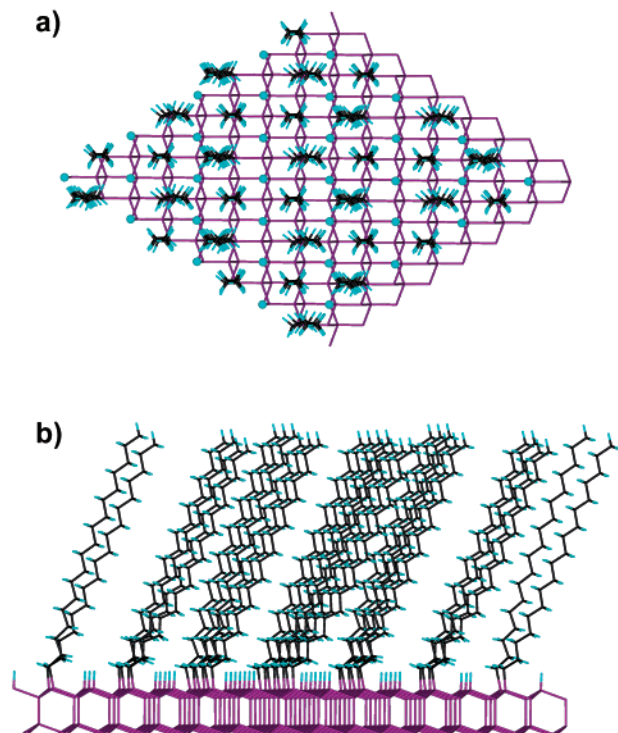

Figure 20. PCCF-optimized structure of the alkyl monolayer formed on Si(111)−H based on the unit cell in Figure 19b. (a) The top view shows the alterning Si−C and Si−H groups on the surface. (b) The side view clearly shows the tilt of the alkyl groups at this level of surface substitution (~50%). (Reprinted with permission from ref 82. Copyright 2000 American Chemical Society.) The authors are also thanked for permission to reprint this figure.

derivatized surfaces were characterized by atomic force microscopy (AFM), diffuse reflectance FTIR (DRIFT), transmission FTIR, Raman, and XPS.[86] About 30−50% of the surface hydrides are consumed in the reaction as calculated based on transmission FTIR spectra, with little accompanying oxidation. The Raman spectra taken before and after the thermal hydrosilylation indicate that the nanoscale structure of the porous silicon skeleton is not affected by the high temperatures and extended time of the reaction. The hydrosilylation takes place throughout the porous structure since the Auger depth profiles show consistent carbon incorporation. The surfaces are chemically robust, as indicated by a range of chemically demanding conditions, including sonication and boiling in chlorinated solvents, boiling protic acid and base, long-term aqueous HF immersion, and steam treatment.

One of the most interesting aspects of this paper is the mechanisms proposed as alternatives to a radical-based reaction, as outlined in Figure 22.[86] The 'standard' radical mechanism is shown in Figure 16b, which is initiated by Si−H bond homolysis or an adventitious radical remaining from the etching process. The first alternative mechanism proposed (path a) involves F^- catalysis, since residual fluoride from the etch is always present. Nucleophilic attack of a surface silicon atom by F^- results in a pentavalent intermediate which could transfer a hydride to the double bond to give the carbanion. This carbanion then attacks the polarized Si center ($^{\delta+}Si-F^{\delta-}$), releasing F^- and forming the Si−C bond. The second alternative mechanism (path b) is based on the π-electron-rich double bond attacking a surface silicon atom in a nucleophilic center to form a pentavalent silicon atom, followed by hydride transfer (a [1,3] shift) to the carbocation. At this point, few experiments have been carried out in the literature which would help to distinguish between them.

Thermal hydrosilylation has been utilized to graft C_{60} to a hydride-terminated Si(100) surface, as shown in Figure 17.[88] Cyclic voltametry of these C_{60}-modified surfaces indicate the surfaces are quite stable and almost certainly chemically bonded; cycling several times does not result in a decay in current density,

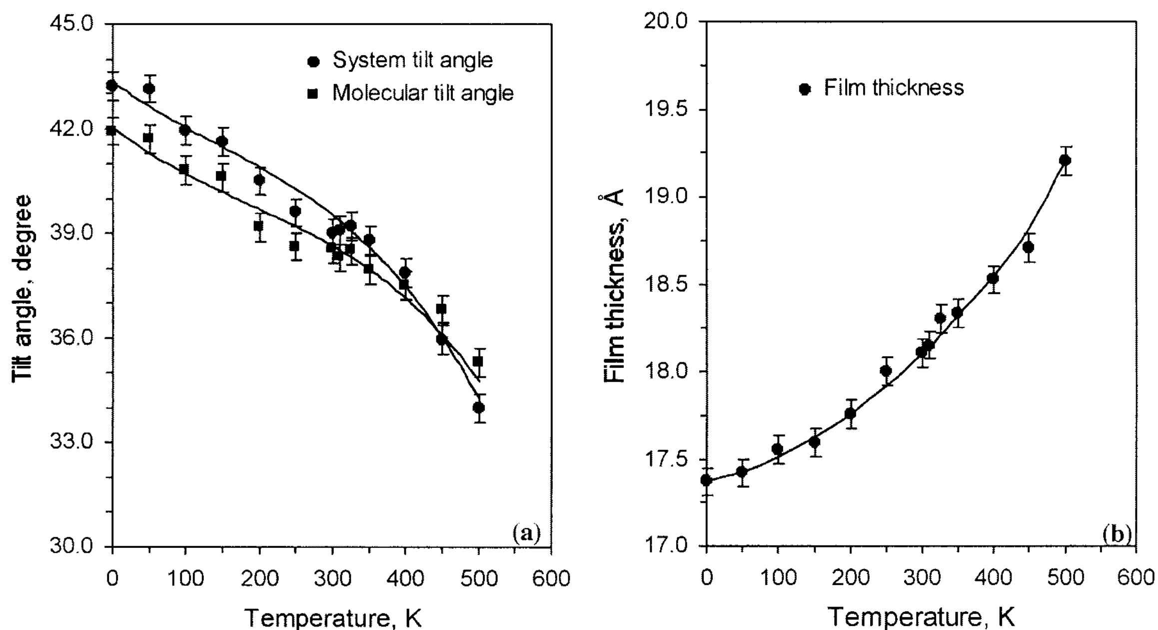

Figure 21. Dependence of C_{18} alkyl monolayers on Si(111) from MD simulations at various temperatures: (a) system and molecular tilt angles and (b) film thickness. (Reprinted with permission from ref 84. Copyright 2001 American Chemical Society.) The authors are also thanked for permission to reprint this figure.

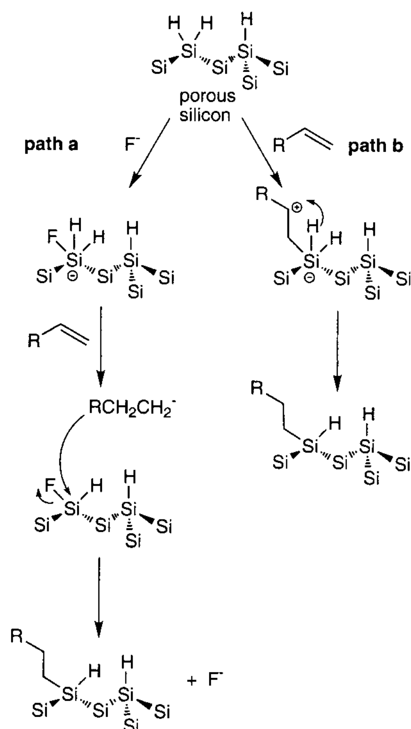

Figure 22. Two alternative mechanisms to the radical-based mechanism proposed for thermal hydrosilylation.[85] Path a involves a fluoride-assisted mechanism, resulting from residual fluoride derived from the HF etch. Path b is based upon direct nucleophilic attack of a surface silicon by the alkene.

as observed with a hydride-terminated silicon sample. On the basis of integration of the cyclic voltammograms, the surface coverage is about 10% that of a full monolayer, based on what would be expected for a close-packed monolayer. The authors conclude that such surfaces may be of interest for photovoltaic and sensor applications.

2. Alkynes

Chidsey mentioned earlier that alkyne hydrosilylation on Si(111)–H surfaces was successful, in the presence of a diacylperoxide radical initiator at 100 °C, and reported observing a vibration at 1600.8 cm^{-1} by FTIR.[89] This stretching frequency correlates perfectly with a monosilicon-substituted double bond (vide infra, section IV.E), and thus, they formed an alkenyl-derivatized surface under these conditions, shown schematically in Figure 15. On hydride-terminated Si(100) surfaces, however, formation of alkenyl monolayers is not observed by ATR-FTIR.[90] Very stable and ordered organic layers are formed at 165 °C for 2 h with high contact angles (with water, $\Theta_a = 108°-110°$) and tilt angles of ~30°–35° from the surface normal, suggesting that the monolayers are very similar to those formed from alkene hydrosilylation. The lack of an observable SiC=C stretch, clearly seen on the Si(111) surface and on porous silicon (vide infra, section IV.E), however, points toward bis-silylation, therefore reducing the bond order of the C–C triple bond to a single bond. In contrast to the alkene hydrosilylation monolayers, the X-ray reflectivity data of the alkyne-reacted surface required introduction of an intermediate

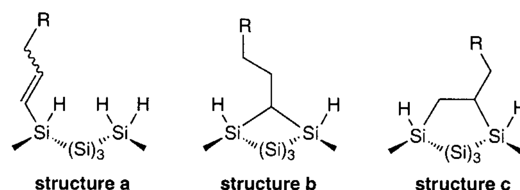

Figure 23. Three proposed possible products of alkyne hydrosilylation on hydride-terminated Si(100). Structure a is the monohydrosilylation product, and structures b and c are the 1,1- and 1,2-bridged bis-hydrosilylation products.

layer between the organic monolayer and the bulk silicon substrate. The calculated electron density of this layer is higher than that of both the alkyl layer and the bulk silicon, which indicates a high density of electronegative atoms at this interfacial region. SiO_2 is discounted because the electron density of silicon dioxide is comparable to that of Si and thus cannot account for the increase. Instead, a bis-silylated alkyne is proposed in which a carbon atom is bonded to two silicon atoms, as shown in Figure 23. Two possible bis-silylated structures are possible, a methine-bound carbon (1,1-bridge, structure a) and an ethylene chain (1,2-bridge, structure c), in contrast to the usual hydrosilylation product, structure a.

To provide insight into the two possible binding configurations, the 1,1- and 1,2-bridge, quantum mechanical B3LYP/6-31G(d) calculations on a 32-atom cluster were carried out.[90] An alkenyl (monohydrosilylated) surface was also examined for comparative purposes. The 1,1-bridged species has the lowest energy, 4.7 and 7.3 kcal mol^{-1} lower than the two possible 1,2-bridging configurations. It is also 20 kcal mol^{-1} lower in energy than the alkenyl surface. The authors conclude that not only is the 1,1-bridge structurally feasible, but it is actually energetically the most favorable structure. They do note, however, that because of the high-temperature reaction conditions and surface roughness (vide supra) of the Si(100) hydride-terminated surface, both the 1,1- and 1,2-bridged species may be present. Perhaps detailed spectroscopic studies (FTIR and solid-state NMR) could differentiate between these two groups.

There is some discrepancy as to the surface termination produced upon alkyne hydrosilylation on hydride-terminated porous silicon. Initial reports suggested that alkyne hydrosilylation does not produce surface-bound vinyl groups based upon transmission FTIR data,[85] presumably because it undergoes two consecutive hydrosilylations (bis-silylation) or forms a 1,1- or 1,2-bridged species. Other work has indicated that the surface-bonded alkenyl group, presumably an intermediate, can be observed at shorter (1–2 h) reflux times at higher temperatures (>150 °C).[91] Further work is required to better understand this reaction on porous silicon.

C. Photochemical Hydrosilylation (UV)

It is known in the organic and organometallic literature that UV irradiation can promote hydrosilylation of unsaturated compounds[92] due to homolytic cleavage of Si–H bonds, as is the case with thermal induction. UV photoinduction, however, takes place at room temperature and thus provides a way to

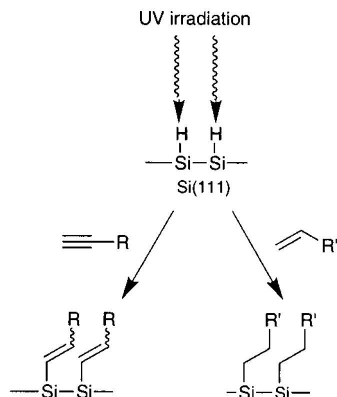

Figure 24. Schematic for UV-mediated alkene hydrosilylation on Si(111)−H.

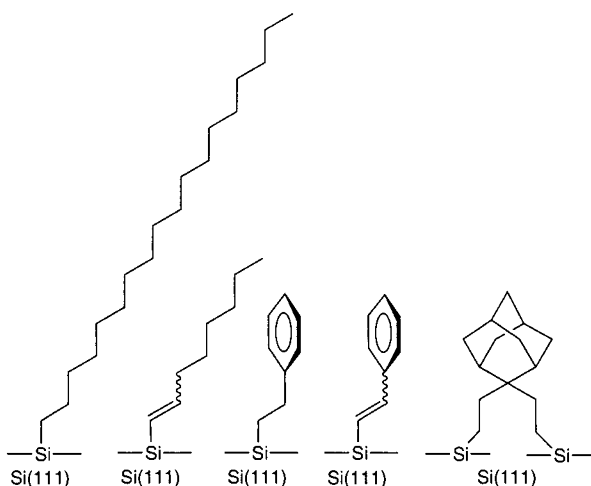

Figure 25. Examples of surfaces produced through UV-mediated hydrosilylation on Si(111)−H.

avoid thermal input that could be harmful to delicate or small features on a silicon chip. Minimal input of thermal energy would be preferable in any IC manufacturing process (thermal budget). Irradiation of a hydride-terminated Si(111) surface with UV light (185 and 253.7 nm) in the presence of an aliphatic alkene like 1-pentene or 1-octadecene brings about hydrosilylation in 2 h at room temperature, as shown in Figure 24.[93,94] A range of alkenes and alkynes were successfully tried, including 1-octene, 1-octadecene, 1-octyne, styrene, and phenylacetylene, with the alkenes yielding alkyl monolayers and the alkynes yielding alkenyl monolayers; examples of surfaces prepared are shown in Figure 25. The XPS spectrum of an Si(111)−H surface irradiated with an Hg lamp (254 nm) in the presence of 1-octene leads to a coverage of 0.44 eight-carbon adsorbates per surface silicon atom, about one alkyl group per two silicons, as proposed to be ideal based on molecular modeling.[82−84] The thickness of this monolayer was measured by ellipsometry to be 9 Å, as predicted. Hydrosilylation of 1-octadecene, forming an octadecyl surface, showed an asymmetric methylene stretch of 2917 cm^{-1} which indicates a highly ordered film. Alkyne hydrosilylation leads to alkenyl-terminated surfaces, as indicated by the observed absorbance in the ATR-FTIR spectrum for 1-octyne at 1601 cm^{-1}, corresponding to a monosilicon-substituted vinyl group. XPS analysis also substantiates this conclusion as a slightly higher energy component of the carbon signal is seen and is absent for the 1-octene reacted surface. As shown in Figure 26, maximum coverage by alkenes and alkynes is obtained in about 1 h of UV irradiation with the Hg lamp. It was later shown that irradiation of an Si(111)−H surface with longer wavelengths, up to 385 nm, could be used to promote alkene hydrosilylation, but irradiation had to be prolonged for 20−24 h, with an accompanying increase in temperature to 50 °C.[95]

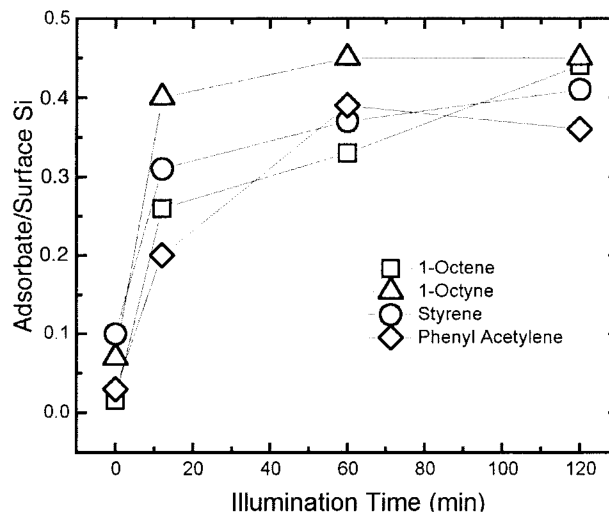

Figure 26. Ratio of adsorbate/surface Si as a function of time for UV-mediated hydrosilylation for various eight-carbon substrates using a Hg lamp. The reactions are essentially complete after 60 min. (Reprinted with permission from ref 94. Copyright 2000 American Chemical Society.) The authors are also thanked for permission to reprint this figure.

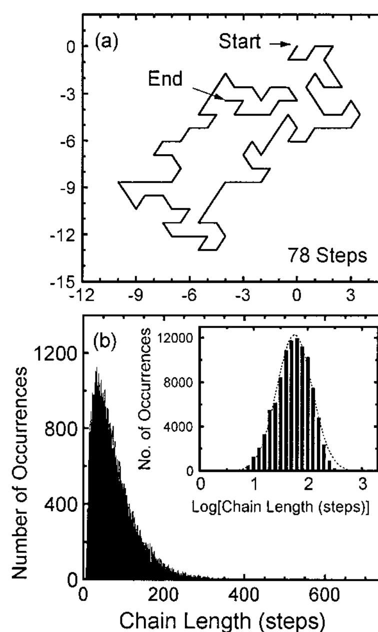

Figure 27. (a) Self-avoiding random walk on a triangular lattice, similar to that of a flat Si(111)−H surface. (b) Monte Carlo simulation of this process over 10^5 cycles and, as shown in the inset, the number of occurrences of a walk versus the log of the number of steps. (Reprinted with permission from ref 94. Copyright 2000 American Chemical Society.) The authors are also thanked for permission to reprint this figure.

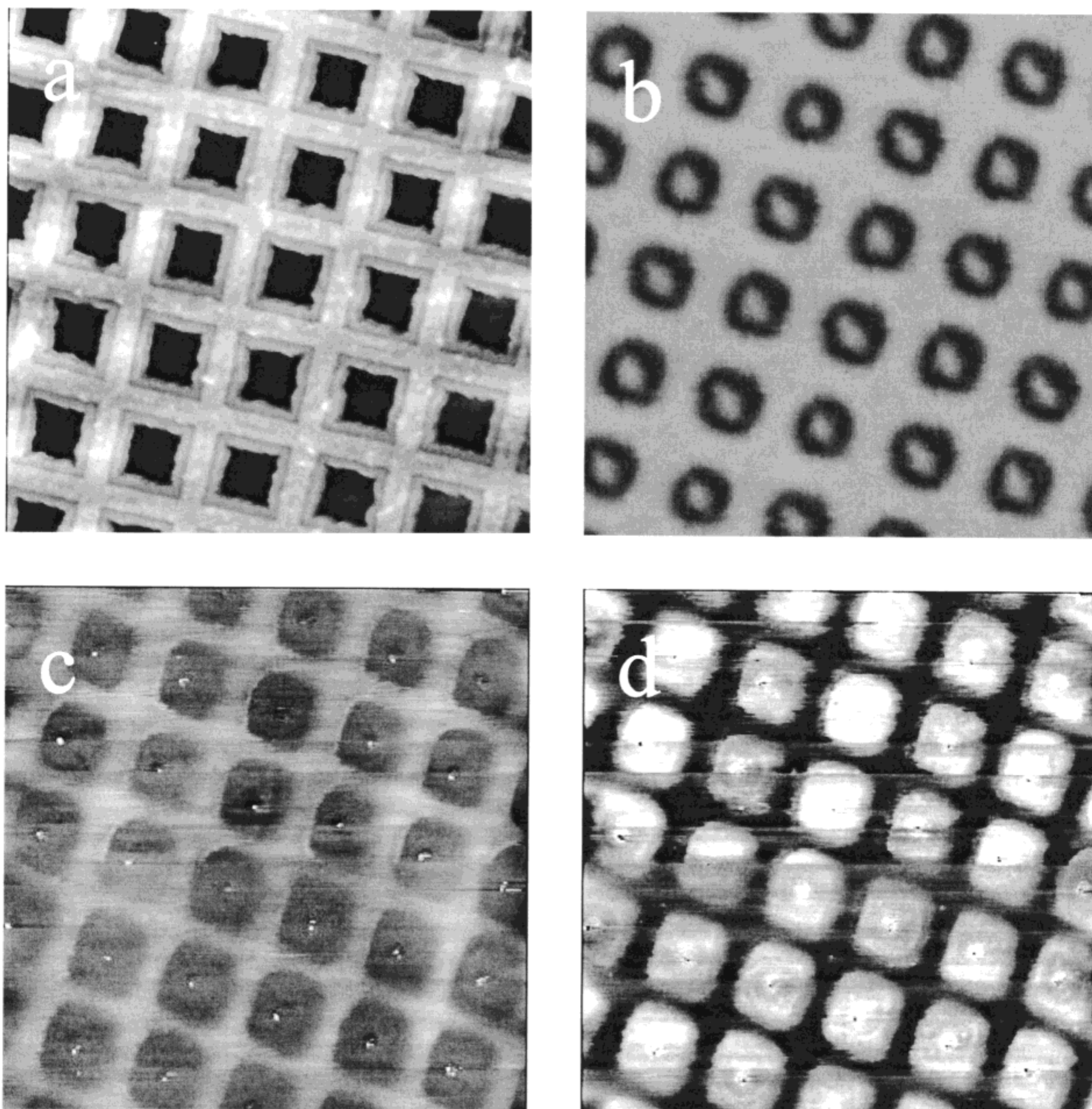

Figure 28. 140 μm × 140 μm images of (a) an AFM tapping mode image of the gold wire grid, (b) CCD optical image of the Si(111) surface following patterning and exposure to water vapor, (c) AFM height image of the patterned surface, and (d) AFM image taken in frictional force mode. (Reprinted with permission from ref 99. Copyright 2001 American Chemical Society.) The authors are also thanked for permission to reprint this figure.

The mechanism proposed is radical based, with homolytic Si−H bond cleavage initiating the reaction to form a silicon radical (dangling bond),[96] similar to that shown in Figure 16b.[94] Because silicon radicals are known to react very rapidly with unsaturated carbon−carbon bonds,[77,97] Si−C bond formation is expected to be a facile step, forming the surface-bound carbon-based radical on the β-carbon. Abstraction of a neighboring hydrogen completes the hydrosilylation. On the basis of the bond strengths of the weakest Si−H bond on a silicon surface, the monohydride ≡Si−H group (~3.5 eV), it appears that a minimum of 3.5 eV UV ($\lambda < 350$ nm) is required to efficiently perform Si−H bond homolysis.[94] In fact, direct single-photon-induced homolysis requires deep UV (157 nm, 7.9 eV), although multiphoton processes have been observed using near UV light.[98] Irradiation of the Si(111)−H surface in air results in fast and efficient loss of hydrides, as observed by ATR-FTIR, only at wavelengths shorter than 350 nm, again pointing to the threshold near this wavelength for Si−H bond activation on this surface.

The radicals are almost certainly surface-based radicals since polymerization of styrene and phenylacetylene, two readily polymerizable substrates under radical conditions, is not observed. To model this radical chain reaction on the surface, a Monte Carlo simulation of a self-avoiding random walk on a triangular lattice (like the Si(111) surface) was examined, as shown in Figure 27a.[94] The average number of steps taken during this random walk was calculated to be 77.2 ± 5. Figure 27b shows the distribution of steps calculated from 100 000 simulations.

The use of this UV irradiation method invites photopatterning, which was undertaken to induce

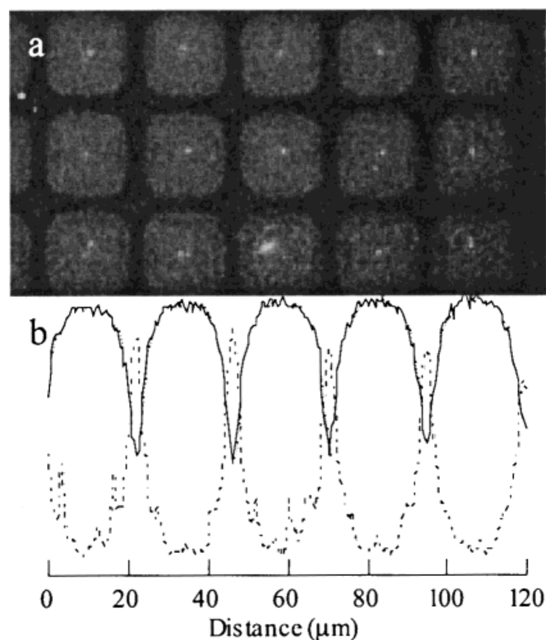

Figure 29. (a) SEM image of the functionalized surface. (b) Scanning Auger electron spectroscopy (SAES) of the functionalized surface which depicts the relative abundance of carbon (- - -) and oxygen (—) as a function of distance. (Reprinted with permission from ref 99. Copyright 2001 American Chemical Society.) The authors are also thanked for permission to reprint this figure.

hydrosilylation in spatially defined areas on a flat silicon surface.[99] Using the observation that irradiation of an Si(111)−H surface in air with 254 nm results in loss of hydrides and concomitant oxide formation,[94] irradiation through a commercially available gold grid with 10 μm wires results in micrometer-scale oxide features on the surface. The unexposed areas, however, remain Si−H terminated and can undergo further chemistry. Immersion of this oxide/Si−H-patterned surface in deoxygenated 1-decene and irradiation of this entire surface at 300 nm for 3 h induces hydrosilylation and results in an oxide/alkyl pattern. AFM and CCD optical images of these patterned surfaces are shown in Figure 28. The SEM and scanning Auger electron spectroscopy (SAES) images of the patterned surface are shown in Figure 29. The SAES spectrum clearly shows the alternation of carbon and oxygen as one moves laterally across the pattern. Through this very simple method hydrophobic and hydrophilic domains can be created, which can, as the authors suggest, be extended to DNA and protein microarray synthesis.

Very recently, the electronic properties and electron-transfer characteristics of the UV hydrosilylated Si(111)−H monolayer surfaces were examined.[100,101] Two different monolayers were investigated, alkyl and fluoro, which were contrasted with an alkoxy monolayer formed by reaction of an alcohol with the Si(111)−H surface. The alkyl monolayer has the highest number of organic adsorbates per surface silicon atom (0.43), compared to the fluorinated alkyl (0.27) and alkoxy (0.21) monolayers. Electrochemical experiments were carried out using aqueous 3 mM potassium ferrocyanide, 3 mM potassium ferricyanide, 1 mM potassium chloride, and a platinum reference electrode. As shown in Figure 30, an Si-

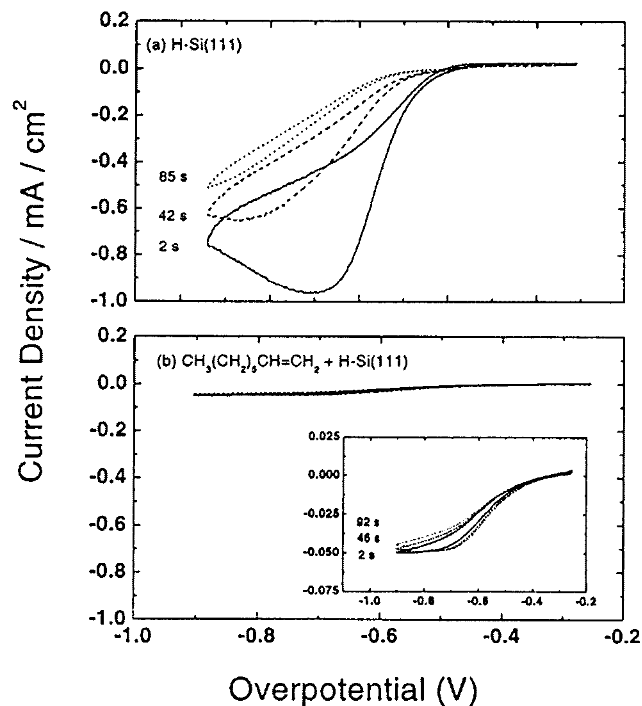

Figure 30. Three successive cyclic voltammograms using a $K_3Fe(CN)_6$/$K_4Fe(CN)_6$/KCl (aq) electrolyte of (a) an Si(111)−H electrode and (b) an octyl-terminated Si(111) electrode. (Reprinted with permission from ref 100. Copyright 2001 American Chemical Society.) The authors are also thanked for permission to reprint this figure.

(111)−H surface has a diffusion-limited peak at ∼−0.7 V whereas the octyl-terminated surface shows significant blocking of the current. Interestingly, the octyl-terminated silicon electrode can be cycled several times (Figure 30b), whereas the Si(111)−H surface current decreases significantly. Clearly, the hydride-terminated surface is oxidizing under these conditions, forming an SiO_2 barrier. The blocking behavior of the octyl surface is most effectively and reproducibly observed using THF as the solvent and a decamethylferrocene/decamethylferrocenium couple. A distance dependence of electron transfer could be determined, along with a β value of about 1.0 per methylene unit. A study of the dependence on monolayer thickness reveals a direct correlation, suggesting no significant contribution from electron transfer through pinhole defects.[101]

UV-induced hydrosilylation has also been utilized on Si(111)−H surfaces to prepare functionalized surfaces for chemical vapor deposition (CVD) of diamond.[102] Hydrosilylation of 2,2-vinyladamantane results in an adamantyl-coated monolayer bonded through Si−C bonds (Figure 25). CVD of carbon produced a reasonable diamond film.

D. Photochemical Hydrosilylation (White Light)

In contrast to flat, hydride-terminated silicon surfaces, a simple white-light source can induce hydrosilylation of alkenes and unconjugated alkynes on Si−H-terminated photoluminescent porous silicon surfaces at room temperature in minutes.[103,104] Illumination with an ELH bulb (GE slide projector bulb) of moderate intensity (22−44 mW/cm²), filtered

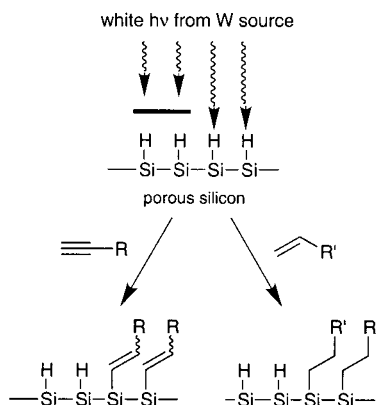

Figure 31. Schematic representation of the white-light-promoted hydrosilylation reaction. Use of simple white light of moderate intensity from a tungsten source and a mask can pattern the surface with various chemical groups, bound through Si−C bonds.

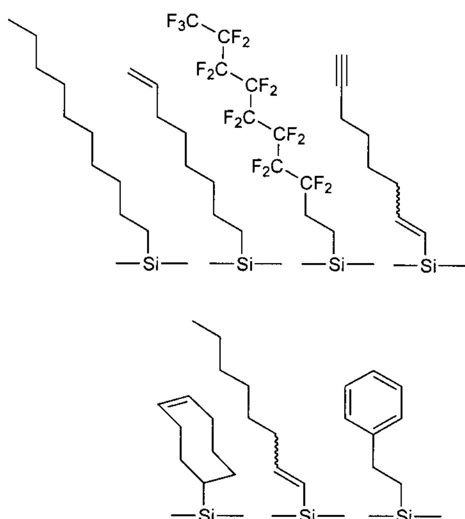

Figure 32. Examples of surface terminations produced through the white-light-promoted hydrosilylation reaction.[103,104]

through a 400−600 nm window to eliminate all UV and IR of a photoluminescent porous silicon sample wetted with an alkene or alkyne brings about surface hydrosilylation in 30 min as demonstrated schematically in Figure 31. Examples of surfaces produced through this method are shown in Figure 32. *The reaction requires the porous silicon samples to be photoluminescent* and is not dependent upon morphology or doping, as long as red light emission is observed upon UV irradiation. The reaction appears to give a substantial portion of *trans*-alkene product when alkynes are hydrosilylated due to observation of the strong *trans*-olefinic out-of-plane mode, $\gamma_w(-CH{=}CH-)_{trans}$ at ∼970 cm^{-1}. Because the reaction is photoinduced, photopatterning can be easily carried out with simple optical apparatus to prepare spatially defined areas of differing chemical functionalities. For instance, use of a f/75 reducing lens and a mask produced with a high-quality laser printer can achieve features as small as 30 μm. Examples of photopatterning on porous silicon produced from n-type silicon crystal wafers are shown in Figure 33.[103] As demonstrated with Figure 33b−d, long aliphatic substituents on the surface, here dodecyl groups, can sufficiently protect the surface from boiling alkali. The remaining, unpatterned areas of Si−H termination dissolve rapidly under these conditions in what can be viewed as a lithographic process. Dodecyl-terminated samples will tolerate boiling for 30 min in aerated aqueous KOH (pH 10) solution, conditions under which freshly etched (Si−H terminated) porous silicon will dissolve in seconds. Figure 34 shows a porous silicon sample under photoluminescence conditions that has been photopatterned through three separate steps with decene, styrene, and cyclooctadiene (COD), leading to spatially defined regions of decyl, phenethyl, and cyclooctenyl groups.[104]

The light-mediated reaction appears very gentle and, depending upon the chemical groups incorporated, can preserve most or all of the intrinsic photoluminescence of the porous silicon (Figure 35). Dodecyl groups, having no unsaturation, maintain almost all the photoluminescence, whereas dodecenyl termination bound to the surface through a vinyl group preserves ∼60%. Styrenyl termination, formed through phenylacetylene hydrosilylation, induces complete quenching of the photoluminescence intensity. A small red shift of the photoluminescence of about 10 nm is observed in the dodecyl termination. This functionalization with alkyl groups could, therefore, be important for preparation of optoelectronic porous silicon devices and sensors.

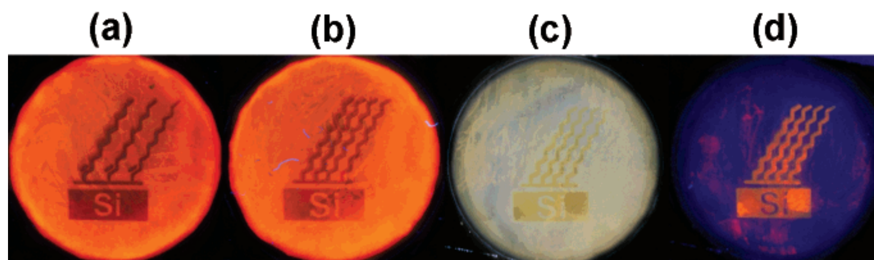

Figure 33. Photographs of 12 mm diameter porous silicon samples prepared through light-promoted hydrosilylation of 1-dodecyne (dodecenyl surface) and 1-dodecene (dodecyl) through masking procedures. (a) The dodecenyl surface appears as the darkened, red-shifted patterned area when illuminated with a 365 nm hand-held UV lamp. The other areas of the wafer are unfunctionalized (native Si−H termination). (b) Dodecyl surface (red-shifted patterned area) upon illumination with 365 nm light. (c) Sample from b after boiling in an aerated, aqueous KOH (pH 12) solution for 15 s. The unfunctionalized porous silicon (grey area) has dissolved, while the hydrosilylated surface (golden area) remains intact. (d) Illumination of the surface from (c) with a 365 nm hand held UV lamp. The PL of the hydrosilylated area remains intact while most of the unfunctionalized PL is destroyed. (Reprinted with permission from ref 103. Copyright 1998 Wiley-VCH.)

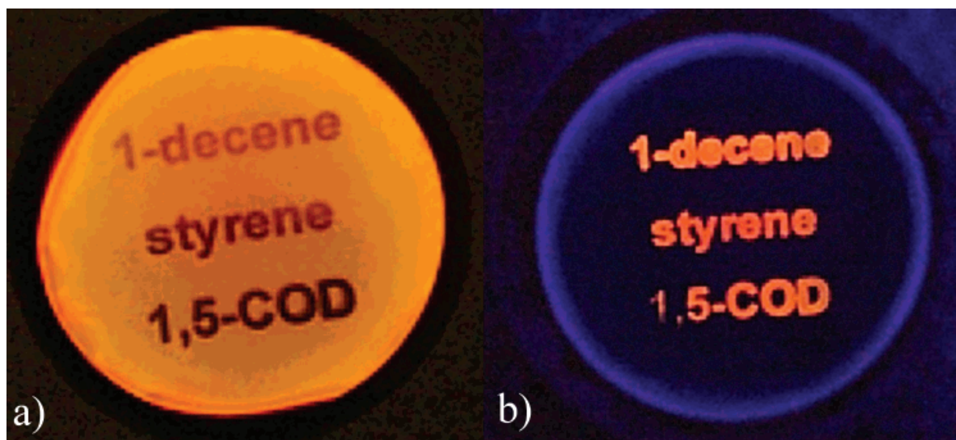

Figure 34. 1 cm diameter porous silicon samples, prepared via etching procedure A, photoluminescing under UV (365 nm) irradiation. (a) A triply photopatterned porous silicon structure. The words "1-decene", "styrene", and "1,5-COD" are the areas reacted with these same reagents via a masking procedure. The area that spells out "1-decene" is a decyl-functionalized surface; the "styrene" area is a phenethyl surface; the "1,5-COD" area is a cyclooctenyl surface. The reacted areas are slightly red shifted and darkened as compared to the PL of the unreacted regions of the sample. (b) The same sample after lithographic development using boiling pH 12 KOH solution, showing isolated regions of photoluminescent derivatized porous silicon. The underivatized (Si−H terminated) areas dissolve with the basic treatment and lose photoluminescence while the alkyl-terminated areas are protected and retain their light emitting properties. (Reprinted with permission from ref 104. Copyright 2001 American Chemical Society.)

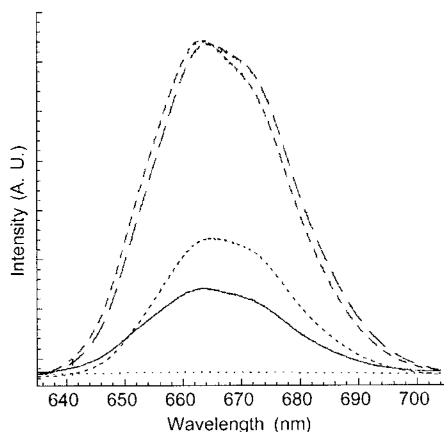

Figure 35. Photoluminescence spectra of various terminations on porous silicon in order of decreasing intensity: Si−H (- - -), dodecyl (— — —), phenethyl (···), octenyl (—), styrenyl (- - -). (Reprinted with permission from ref 104. Copyright 2001 American Chemical Society.)

Because of the relatively low energy of the white-light illumination ($\lambda > 400$ nm) and photoluminescence requirement for successful hydrosilylation, excitons generated in situ are proposed to drive the surface chemistry, as opposed to Si−H homolysis, seen with UV irradiation (vide supra, section IV.C). The excitons are also responsible for photoluminescence,[105] which provides the crucial link between the observed hydrosilylation reactivity and light emission. In Figure 36, a proposed mechanism for the light-promoted hydrosilylation reaction begins with the formation of a complex between an adsorbed alkene and the surface-localized hole. Attack by an alkene or alkyne nucleophile at an electrophilic silicon center proceeds directly and irreversibly to form the Si−C bond, resulting in a carbocation stabilized by a β-silyl group.[106] The high strength and low polarity of the nascent Si−C bond should limit the reversibility of this step. The strongly acidic

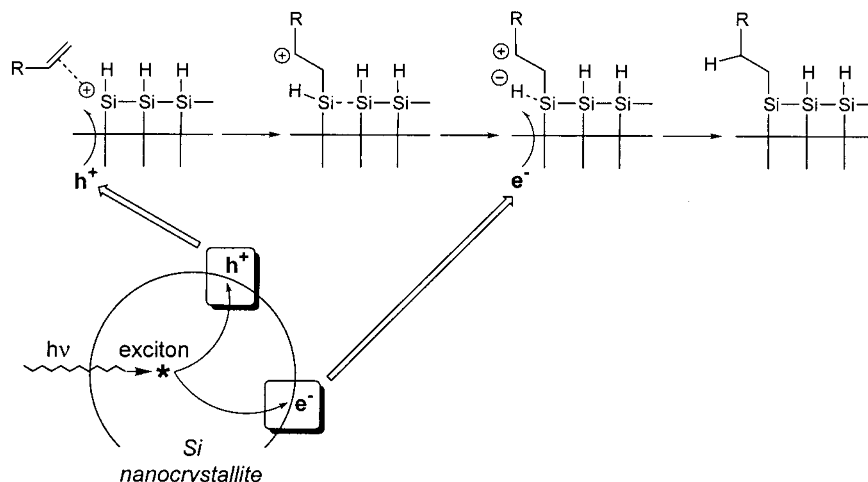

Figure 36. Proposed mechanism for the exciton-mediated hydrosilylation event. An unbound exciton produced by light absorption leads to a surface-localized supra-band gap positive charge. This surface charge can then interact with an alkene and form a silylated β-carbocation upon Si−C bond formation. This carbocation can then abstract a hydride (formally H$^{\bullet}$ + electron from exciton) from an adjacent Si−H bond, yielding the neutral organic termination. (Reprinted with permission from ref 104. Copyright 2001 American Chemical Society.)

carbocation can then abstract a hydride from an adjacent hydridic Si−H bond, forming a stronger and less polar C−H bond. This hydride could be formally the product of a hydrogen atom and the electron half of the original exciton e^-/h^+ pair. This hydride abstraction step by a β-silyl carbocation is proposed in mechanisms related to solution-phase hydrosilylation.[106,107] Experiments with known photoluminescence quenching agents such as ferrocene, 9,10-diphenylanthracene, and decamethylruthenocene were examined and found to prevent white-light-promoted hydrosilylation.

This work is of interest in that it has no parallels with the chemistry of either bulk silicon surfaces or molecular silanes. It functions purely as a result of the nanoscale size of the features in porous silicon and is tied intimately with the unique photoluminescence of this material.

E. Hydrosilylation and Related Reactions Mediated by Metal Complexes

Because Pt(0) complexes and colloids are extremely effective catalysts for the hydrosilylation of alkenes with soluble, molecular silanes,[108] their potential was examined on hydrogen-terminated flat Si(100) surfaces.[109] Using 3,4-dichlorobutene as the olefin and platinum(0)−divinyltetramethyldisiloxane as the catalyst precursor, chloride incorporation (from the Cl-containing olefin) on the surface was observed by XPS and surface mass spectrometry (TOF−SIMS) after 45 min at room temperature. In situ ATR-FTIR spectroscopy indicated consumption of surface SiH_2 groups, supporting a hydrosilylation mechanism. The platinum complex also catalyzes oxidation of the silicon surface, although this competing reaction could be reduced by minimizing trace water and utilizing a large excess of olefin.

Other workers have found that late-transition-metal complexes can be problematic with respect to hydrosilylation and attempted bis-silylation on Si−H-terminated porous silicon.[110,111] Exposure of freshly etched porous silicon to Wilkinson's catalyst, $RhCl(PPh_3)_3$ (hydrosilylation catalyst), and the palladium complexes $PdCl_2(PEt_3)_2$ or $Pd(OAc)_2$/1,1,3,3-tetramethylbutyl isocyanide (bis-silylation catalyst) in the presence of alkynes[112] resulted in blackening of the surfaces due to apparent metal deposition which thoroughly quenched the photoluminescence.[110] Substantial oxidation was also noted even if considerable precautions were taken. Karstedt's catalyst, a Pt-based complex well-known for solution-phase hydrosilylation,[113] can only be used either with a partially oxidized hydride-terminated porous silicon surface or when the reaction is carried out in the presence of air, resulting in concomitant oxidation of the surface which then undergoes hydrosilylation.[111] On the other hand, if $Rh_2(OAc)_4$ is used as a catalyst with heating to promote insertion of carbenes from diazo compounds into surface Si−H bonds, little oxidation by transmission IR is observed which suggests that this method may have synthetic utility, although stability tests, photoluminescence measurements, and reaction efficiencies remain to be carried out.[111]

To avoid late transition metals and their potential for accompanying problems of oxidation and metal reduction on porous silicon, a Lewis acid was utilized to mediate hydrosilylation of alkynes and alkenes.[114,115] Lewis acid-catalyzed or -mediated hydrosilylation reactions seemed ideal for functionalization of porous silicon because of the mild reaction conditions involved and high selectivity and specificity of the corresponding solution-phase reaction.[116] $AlCl_3$ is an effective catalyst for alkenes as well, which suggested that Lewis acid-mediated surface chemistry would not be limited to alkynes.[117] Since $EtAlCl_2$ is soluble in nonpolar solvents whereas $AlCl_3$ is not, it was chosen as the Lewis acid to avoid multiphasic reactions on the surface of porous silicon.[118] A wide range of alkynes and alkenes were smoothly hydrosilylated on Si−H-passivated porous silicon at room temperature (Figure 37), yielding vinyl- and alkyl-terminated surfaces, respectively. In solution using molecular silanes and alkynes, *trans*-addition is observed, leading to a *cis*-alkene. While difficult to substantiate, it appears that *cis*-alkenes are also formed on the surface because of the lack of the strong *trans*-olefinic out-of-plane mode, $\gamma_w(-CH{=}CH-)_{trans}$ at ~970 cm^{-1}; this vibration is seen in the white light-promoted hydrosilylation route and thus is observable.[104] While not definitive, it appears that the chemistry on the surface is similar to that in solution with molecular silanes. By using an excess of $EtAlCl_2$, alkynes with coordinating functional groups (ester, hydroxy, and cyano groups) could also be incorporated onto the surface. One equivalent of the Lewis acid complexes the coordinating group and the remainder mediates the hydrosilylation reaction. We found, thus far, the reaction to be independent of silicon doping and morphology. Importantly, the reaction does not change the porous structure of the nanoscale architecture of the material, as indicated by surface area measurements before and after the reaction (BET and BJH methods).

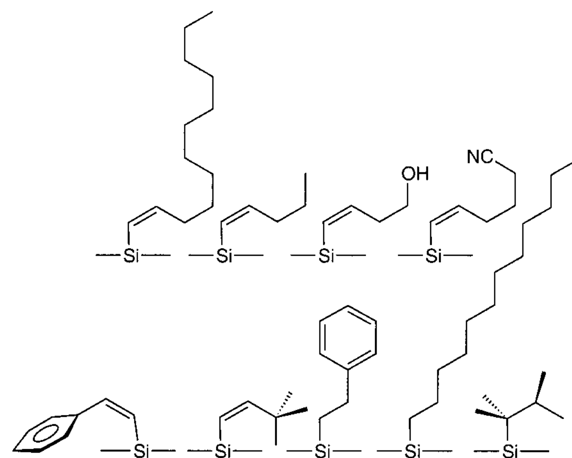

Figure 37. Examples of surfaces on porous silicon prepared through Lewis-acid-mediated hydrosilylation.[114,115]

To clearly prove that hydrosilylation of alkynes is indeed occurring, detailed transmission IR, efficiency and reactivity studies, stability studies, and solid-state ^{13}C NMR were carried out. Difference IR spectra, taken in a Teflon etching/reaction cell which doubles as an IR cell, indicate consumption of Si−H stretches ν(Si−H) centered around 2100 cm^{-1}, as shown in Figure 38 for the hydrosilylation reaction

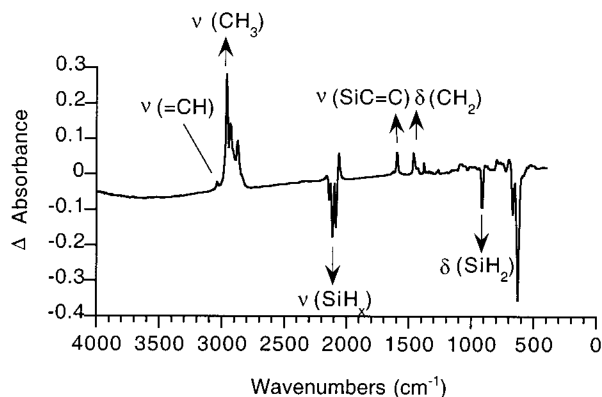

Figure 38. Difference transmission FTIR of porous silicon undergoing Lewis-acid-mediated hydrosilylation with 1-pentyne; the features below the baseline indicate disappearance of ν(Si–H$_x$) intensity, and those above correspond to the pentenyl termination.[115]

Table 2. Relative Efficiencies [Decrease in ν(Si–H$_x$) Intensity] of the Lewis-Acid-Mediated Hydrosilylation Reaction of Various Substrates as Determined by Transmission FTIR[a]

	hydrosilylated substrate	average efficiency **E** %
1	1-pentyne	19
2	1-dodecyne	17
3	2-hexyne	14
4	1-pentene	28
5	1-dodecene	28
6	*cis*–2-pentene	20
7	*trans*–2-hexene	11
8	2,3-dimethyl-2-pentene	11

[a] Conditions: The efficiency is an average of 2–4 runs, with an error of ±5% of the calculated efficiencies.

with 1-pentyne. Because there is no apparent oxidation or appearance of oxide back-bonded silicon hydrides at higher energy, integration of the ν(Si–H) (A_o) before and after the hydrosilylation reaction (A_1) yields the percent of hydrides consumed during the reaction or efficiency (*%E*). It is important to note that this is a *semiquantitative* method at best, allowing only for relative comparisons since IR intensities have not been shown to be linear in concentration.

$$\%E = (A_o - A_1)/A_o$$

As shown in Table 2, the average efficiency of the reaction depends on the substrate, with terminal alkenes giving the highest incorporation or *%E* levels, 28%. This indicates that ~70% of the surface hydrides remain intact. Carrying out the reaction again on a sample will not bring about greater %E values. For instance, a hydride-terminated porous silicon sample hydrosilylated with 1-pentyne has a %E of 19%; repeating the reaction will not increase this value.

Alkynes, when hydrosilylated, give the monohydrosilylated product, alkenyl substitution. The ν(SiC=C), a fairly intense band, is observed at 1595 cm^{-1} and has the exact energy for a monosilicon-substituted C=C, as compared to molecular organosilanes.[110,114,115] To prove that this stretch is indeed an alkenyl vibration, the sample was exposed to BH_3·

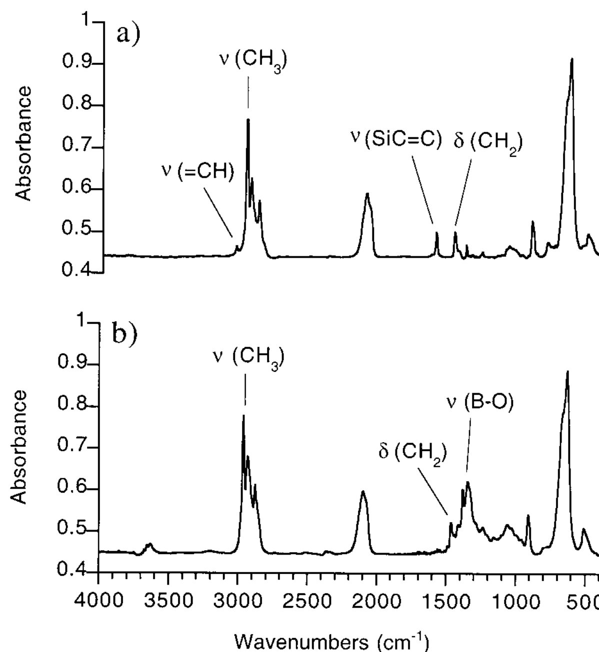

Figure 39. Transmission FTIR spectra of (a) a pentenyl-terminated surface prepared through Lewis-acid-mediated hydrosilylation of 1-pentyne on porous silicon and (b) the sample upon hydroboration with THF·BH_3, resulting in complete disappearance of the ν(SiC=C) at 1595 cm^{-1}.

THF, which will reduce alkenes to boroalkyls. Exposure of a pentenyl-terminated surface, formed from 1-pentyne hydrosilylation, to a commercial 1.0 M THF solution of BH_3·THF for 16 h at room temperature leads to quantitative disappearance of this band, shown in Figure 39.[114,115] The stretch at 1595 cm^{-1} therefore appears spectroscopically to be a surface-bonded vinyl group and in addition reacts as expected.

To complement the FTIR studies, solid-state ^{13}C NMR spectra of the 1-pentyne and 1-pentene hydrosilylation reactions on free-standing porous silicon samples were taken.[115] As a reference, these substrates were hydrosilylated in solution with tris(trimethylsilyl)silane, leading to organosilanes that should be similar to our proposed surface-bound structures. The molecular equivalent to the 1-pentyne product is shown below.

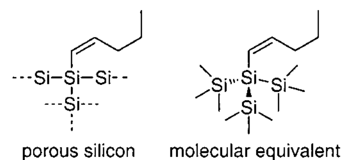

Figure 40a shows the ^{13}C NMR spectrum of the molecular equivalent in $CDCl_3$ and Figure 40b the product of 1-pentyne hydrosilylation on free-standing porous silicon. The spectra are very similar, with peaks present in both samples at δ ~150 and 120 ppm, corresponding to the olefinic carbons. In fact, ^{29}Si satellites visible in the molecular equivalent ^{13}C NMR spectrum indicate that the peak upfield at δ ~120 ppm is the silicon-bonded carbon. The three peaks upfield in the aliphatic region of the spectrum correspond to the propyl tail of the organic group.

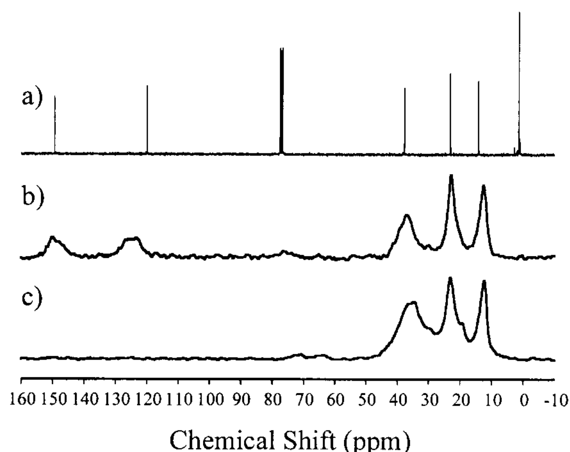

Figure 40. (a) Solution-phase ^{13}C NMR in $CDCl_3$ of the product of hydrosilylation of 1-pentyne with tris(trimethylsilyl)silane, catalyzed by $EtAlCl_2$. (b) ^{13}C CP-MAS solid-state NMR spectrum of porous silicon reacted with 1-pentyne in the presence of $EtAlCl_2$. (c) ^{13}C CP-MAS solid-state NMR spectrum of the porous silicon sample after exposure to BH_3·THF, resulting in complete disappearance of the peaks associated with the surface bonded vinyl group. (Reprinted with permission from ref 115. Copyright 1999 American Chemical Society.)

Similar to the FTIR study, hydroboration of this surface leads to complete consumption of the vinyl stretches, again proving the olefinic nature of these spectroscopic signals (Figure 40c).

The hydrophobic, alkyl- and alkenyl-terminated surfaces are very stable under highly demanding chemical conditions. The dodecenyl-functionalized surface will resist several hours of boiling in pH 12 aqueous KOH solutions. Higher pH levels, 13−14, can be tolerated for 5 min, conditions under which porous silicon dissolves in seconds. Long-term stability studies in ambient laboratory air indicate much lower rates of surface oxidation, based on observation of the appearance of oxide back-bonded $Si-H_x$ stretches by FTIR. In addition, the dodecenyl surfaces have been shown to be stable in simulated body fluids, suggesting that they may be bioinert in vivo.[119,120]

The effectiveness of the Lewis-acid hydrosilylation chemistry was examined on Si(111)−H surfaces.[121] In contrast to the ease of the room-temperature reaction on porous silicon, flat hydride-terminated silicon requires heating to 100 °C for 18 h. In the absence of catalyst under these conditions, low coverages are observed by XPS. The $\nu_{as}(CH_2)$ vibration of a decyl-terminated surface, a good indicator of monolayer order, is 2923 cm^{-1}, which in this case suggests a monolayer that is intermediate between a completely disordered liquid layer and a well-packed crystalline interface.

F. Reactions of Alkyl/Aryl Carbanions with Hydride- and Halide-Terminated Surfaces

The use of alkyl Grignard and alkyllithium nucleophiles on silicon surfaces was first investigated under electrochemical conditions.[122] Silicon−methyl-terminated porous silicon derived from p-type single-crystal silicon can be accessed through treatment of the native Si−H-passivated surface with a methyl Grignard or methyllithium organometallic when the silicon is positively biased. It is proposed that the silicon hydride groups are consumed through a transmetalation reaction, forming silicon−methyl groups and either MgHX or LiH as byproducts of the reaction. The stability of the surfaces increases an order of magnitude with respect to accelerated air oxidation at 100 °C as determined by FTIR spectroscopy. In a more recent paper, the same authors apply a positive bias to Si(111)−H in the presence of methyl Grignard and observe $Si-CH_3$ termination and complete disappearance of the hydride stretch by ATR-FTIR.[123]

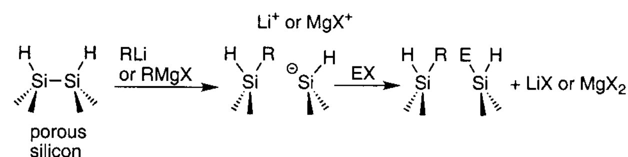

Figure 41. Proposed mechanism for carbanion addition (organolithium and Grignard reagents) to porous silicon and hydride-terminated Si(100) surfaces.[124−127] Cleavage of weak Si−Si bonds upon attack of the carbanion produces a silyl anion which can be further reacted with an electrophile (EX).

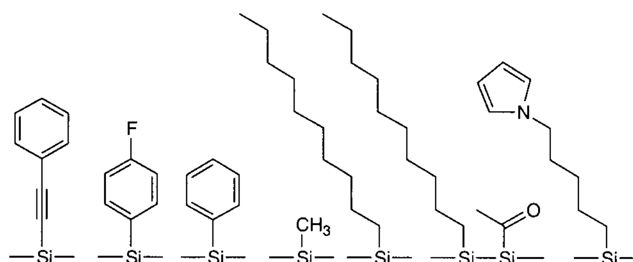

Figure 42. Examples of porous silicon surfaces produced through the addition of carbanions in the form of organolithium and Grignard reagents.

The addition of organolithium[124−126] and Grignard reagents[127] to porous silicon was subsequently investigated without an electronic bias on porous silicon and was found to proceed efficiently at room temperature. The range of carbanion nucleophiles that could be bound to the surface of porous silicon through Si−C bonds was extended, and detailed mechanistic studies were carried out. The mechanism proposed for silicon−carbon bond formation involves attack of the weak Si−Si bond by the carbanion nucleophile, as shown in Figure 41.[124,125,127] The resulting silyl anion on the porous silicon surface can be further reacted with an electrophile (EX), offering the possibility to form mixed surfaces. Examples of porous silicon surfaces prepared by this method are shown in Figure 42.

The effects of carbanion functionalization on the photoluminescence of porous silicon have also been investigated in some detail. Methyl termination has little effect on the photoluminescence intensity of p-type porous silicon.[122] A conjugated alkyne, on the other hand, results in irreversible quenching of the intrinsic photoluminescence that cannot be recovered by rinsing with HF solutions.[124,125] It was found, however, that simple phenyl or 4-fluorophenyl termination[127] resulted in only minor quenching, which points to the interesting possibility of using the

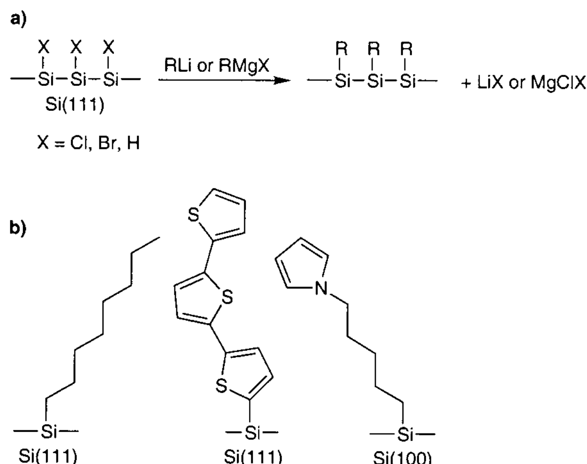

Figure 43. (a) Outline of the reaction of carbanions (organolithium and Grignard reagents) to flat halide- and hydride-terminated Si(111) surfaces, and (b) examples of three functionalized surfaces produced through this approach.

surface functionalities to tune the photoluminescence and underlying optoelectronics of the material.

The first approach to functionalize flat single-crystal silicon with carbanions involved a two-step halogenation/alkylation route.[63] Chlorination of a hydride-terminated flat Si(111) crystal with PCl_5 for 20−60 min at 80−100 °C produced a chloride-terminated silicon surface. Transmetalation with an alkyllithium or Grignard at 80 °C for 30 min to 8 days yields LiCl or MgXCl and an alkyl group bound to the silicon surface through an Si−C linkage, as shown in Figure 43. Surfaces with long alkyl termination are more resistant to oxidation under ambient conditions and to boiling in aerated chloroform and water. Thermal desorption and XPS experiments indicate that ≡Si−OR linkages are not formed which provides support for the expected Si−C bond formation event.

The effects of the two-step chlorination/alkylation reaction on recombination velocities on the Si(111) surface were measured using a contactless rf conductivity apparatus, and it was found that alkyl termination can stabilize the electronic properties of the bulk silicon.[128] Freshly etched Si(111)−H in strong acid has a very slow recombination velocity, <20 cm s^{-1}, but with 30 min of exposure to air, it increases dramatically. An octyl-terminated surface, prepared by reacting the chloro surface with octyl Grignard, also has a slow recombination velocity, <25 cm^{-1}, but this value remains basically unchanged after 4 weeks. The time-resolved photoconductivity decay spectra for freshly etched Si(111)−H, Si(111)−H exposed to air for 30 min and the octyl-terminated surface exposed to air for 504 h are shown in Figure 44. Mean carrier lifetimes showed little decrease in the octyl surface for up to 700 h.

In an application of the two-step halogenation/alkylation reaction, a bromination/alkylation approach was utilized to produce monolayers of oligothiophenes on Si(111) surfaces.[129] Reaction of the Si(111)−Br surface with a lithiated thiophene for several hours to 2 days at 60 °C led to stable interfaces. The surfaces were studied by XPS, ATR-FTIR, Auger electron spectroscopy, and near-edge X-ray absorption fine structure (NEXAFS).

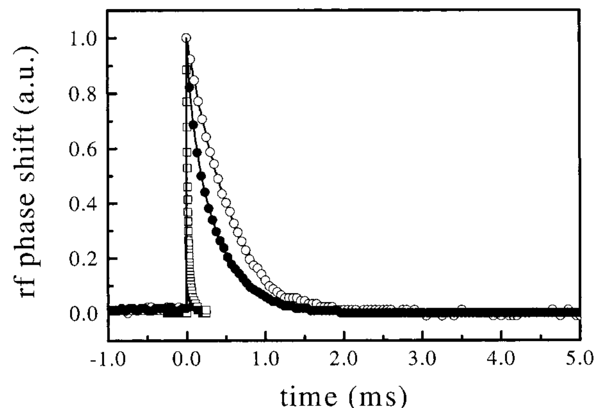

Figure 44. Time-resolved photoconductivity decay of Si(111)−H surfaces in contact with sulfuric acid (○) and after exposure to air for 30 min (□). The time constants for these decays are remarkably different—491 μs for the sulfuric acid-immersed sample and 14 μs for the air-exposed sample. A methyl-terminated Si(111) surface, on the other hand (●), after exposure to air for 504 h, yields a time constant of 342 μs. (Reprinted with permission from ref 128. Copyright 2000 American Institute of Physics.)The authors are also thanked for permission to reprint this figure.

In an interesting variation of this chemical approach, chloro-terminated silicon,[130] germanium,[131] and mixed silicon−germanium nanoparticles,[132] prepared through a Zintl phase synthesis route, where alkylated with alkyllithium reagents. Silicon nanoparticles were prepared by refluxing a reactive Zintl salt, Mg_2Si or NaSi, with $SiCl_4$ in glyme for up to 36−48 h; at this point the clusters are Si−Cl terminated. Upon addition of an alkyl Grignard or alkyllithium reagent, Si−C bond formation occurs, accompanied by MgXCl or LiCl precipitation. The alkyl termination of the particles was analyzed by solution-phase ^{13}C, ^{29}Si, ^{23}Na (in the case of NaSi) NMR and FTIR. Alkyl-terminated germanium nanoparticles were prepared via similar route, using NaGe and $GeCl_4$, followed by alkylation with an alkyllithium or Grignard reagent. Finally, mixed Ge/Si nanoparticles with a Ge core and an alkyl-terminated silicon shell were prepared by refluxing Mg_2Ge and $SiCl_4$ in triglyme, followed by a metathesis reaction with an alkyllithium reagent, forming the Si−C bonds which stabilize the clusters. In addition to stabilizing the clusters, the alkyl termination renders the nanoparticles soluble in organic solvents.

Recent work has shown that hydride-terminated Si(100) surfaces may be alkylated directly (without halogenation pretreatment) with butyl-, hexyl-, phenyl- and 5-(*N*-pyrrolyl)pentyllithium reagents in THF at room temperature.[126] The Si(111)−H surface has also been shown to be alkylated directly with decylmagnesium bromide after 16 h exposure in diethyl ether with slight heating.[121] While the reaction of porous silicon- and hydride-terminated Si(100) with a carbanion reagent is proposed to proceed via cleavage of weak Si−Si bonds,[124,125,127] this is not as probable on the Si(111) face.[121] ATR-FTIR reveals that no Si−H remains on the Si(111)−H surface, suggesting that the reaction proceeds via silicon−

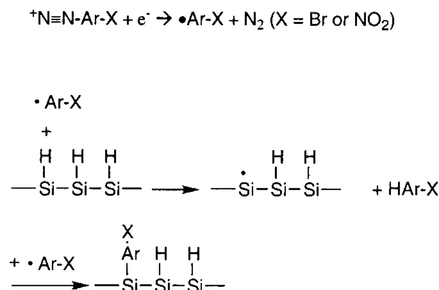

Figure 45. Mechanism for electrochemical diazonium reduction and formation of R• radicals. The radicals can then abstract a surface hydride, leading to formation of a surface silicon radical which can then combine with another R•, forming the Si−C bond.

hydride cleavage. The surfaces prepared via this route are very stable to a range of treatments, including sonication and boiling in chloroform, boiling in water, and extended exposure to fluoride and hydroxide.

G. Electrochemical Grafting on Hydride-Terminated Surfaces

Electrochemistry has also been used to produce close-packed phenyl monolayers on hydride-terminated flat n-type Si(111) surfaces, as shown in Figure 45.[133] Application of a negative potential of about 1 V to a dilute HF solution containing a 4-nitro or bromobenzene diazonium salt results in production of an aryl radical and dinitrogen. The aryl radical can then abstract a surface hydride to form silicon radicals, which can react with another aryl radical to form the silicon−carbon bond. The covalent nature of the phenyl bonding to the surface is demonstrated by the stability of the surfaces to aqueous 40% HF solutions and XPS and Rutherford backscattering (RBS) measurements. Because this reaction utilizes the electrode nature of the semiconducting silicon, no clear reaction parallels can be found for soluble, molecular silanes. One important advantage of this approach is that the process is cathodic, thus making the surface electron rich during the reaction, which renders it less susceptible to nucleophilic attack by water, suppressing oxidation.

Commercially available and structurally diverse alkyl iodides or bromides can be electrochemically reduced in situ, leading to Si−C bond formation on hydride-terminated porous silicon.[134] Solutions (0.2−0.4 M) of the alkyl halide and 0.2 M $LiBF_4$ (electrolyte) in dry, deoxygenated acetonitrile or acetonitrile/THF mixtures, upon application of a cathodic current of 10 mA cm^{-2} for 2 min at room temperature, result in efficient coverage. The same chemistry appears to work on flat hydride-terminated silicon as the surfaces become much more corrosion resistant upon exposure to base. The reaction and surfaces prepared via this method are shown in Figure 46. The proposed mechanism may involve reduction of the alkyl halide to the alkyl radical and halide anion, followed by abstraction of a surface H• by the alkyl radical, forming a surface silicon radical (dangling bond). At this point, three possible things could happen: (i) R• could react directly with Si•, forming the Si−C bond,

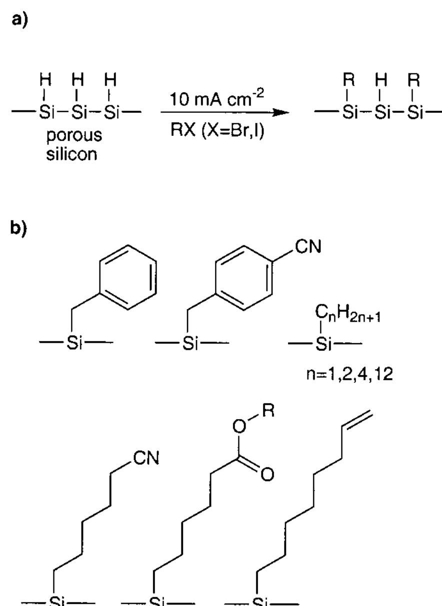

Figure 46. Examples of porous silicon surfaces produced through in-situ cathodic reduction of alkyl bromides and iodides.

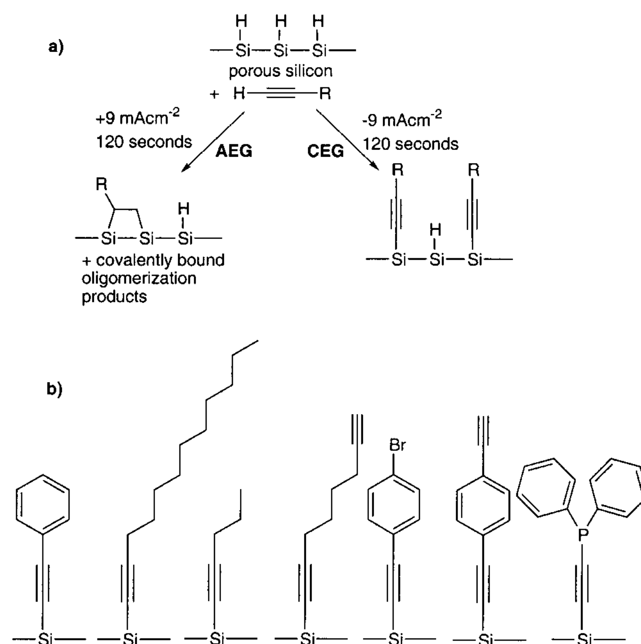

Figure 47. (a) Outline of cathodic (CEG) and anodic (AEG) electrografting on hydride-terminated porous silicon. (b) Examples of surface terminations produced via this route.

(ii) reduction of the Si• with an electron to form Si^- could react in a nucleophilic fashion with RX, leading to Si−R bond formation and release of X^-, or (iii) in situ reduction of R• to R^-, the carbanion, which could attack weak Si−Si bonds (vide supra, section IV.F).

Alkynes can also be grafted to Si−H-terminated porous silicon samples under negative bias (cathodic electrografting, or CEG), as outlined in Figure 47a.[135] The alkyne is bonded through an Si−C bond directly and in contrast to hydrosilylation is not reduced. Examples of surface terminations prepared by this method are shown in Figure 47b. The surface-bonded alkyne C≡C vibration can be observed by transmission FTIR at 2179 cm^{-1} for a pentynyl- or octynyl-derivatized surface; the C≡C stretch of the molecular

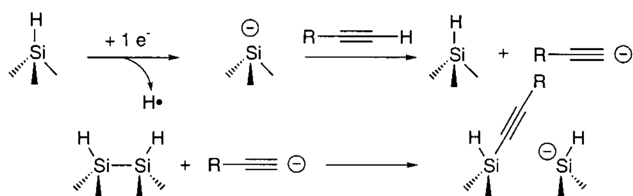

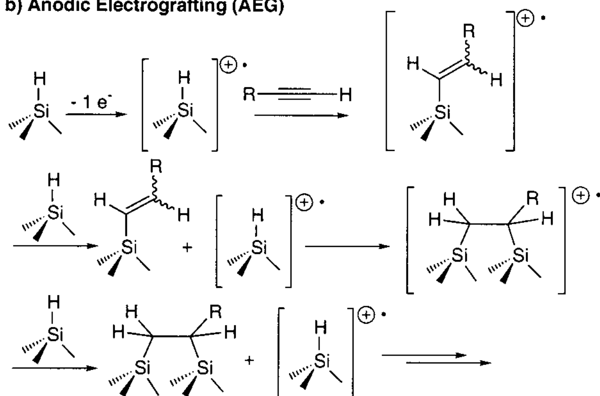

Figure 48. Proposed mechanisms for (a) CEG and (b) AEG Si−C bond formation on hydride-terminated porous silicon.

analogue 1-trimethylsilyldodec-1-yne appears at 2176 cm^{-1}. To definitively prove the alkynyl nature of this vibration, the pentynyl surface was subjected to hydroboration conditions. Exposure to disiamylborane, a borane-based reducing agent known to stop at the borylalkene stage, leads to a new stretch at 1580 cm^{-1} and complete disappearance of the alkyne stretch. The new vibration at 1580 cm^{-1} is of the correct energy to be a silylated, borylated double bond; the molecular equivalent, 1-trimethylsilyldodec-1-yne, when hydroborated with the same reagent has a double bond stretch at 1584 cm^{-1}. These reactivity studies prove that alkynes are grafted to the surface as a triple bond. The cathodic electrografting approach allows for many of the synthesized organic molecular wires to be grafted directly to a silicon device for testing and characterization. Positive bias (anodic electrografting, or AEG) was also tried and found to lead to Si−C bond formation but with total reduction of the bond order of the alkyne to aliphatic groups as judged by the lack of C≡C and C=C stretching modes in the transmission FTIR.

The proposed mechanisms for both CEG and AEG are shown in Figure 48.[132] CEG may involve a concerted reaction between a silicon−hydride, whose hydridic nature is even more pronounced under the effect of the negative bias, and an alkyne C−H, leading to $^1/_2H_2$. On the other hand, formation of a surface-bound silyl anion could deprotonate an alkyne, leading to a carbanion which has been shown to attack the weak Si−Si bonds on the surface, forming the Si−C bond. Indeed, carrying out the reaction in the presence of HCl in ether shuts down the reaction, possibly due to protonation of the silyl anion. AEG may be the result of a cationic hydrosilylation mechanism, previously postulated for molecular silanes and alkynes under electrochemical conditions.[136] Bis-

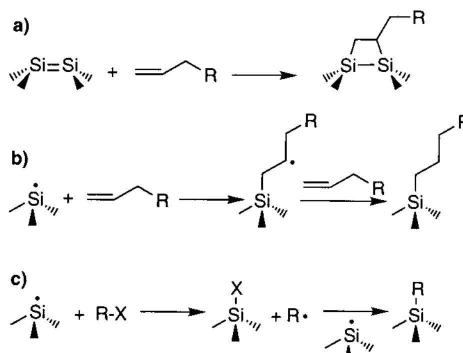

Figure 49. Possible reactive groups formed upon grinding or scribing silicon surfaces (Si=Si dimers and silicon radicals). Upon exposure to alkenes or alkyl halides, Si−C bond formation may occur through the pathways shown here.

silylation or cationic polymerization[137] appears to be occurring with the vinyl intermediate since no unsaturation is observed by transmission FTIR.

H. Mechano−Chemical Functionalization of Non-Hydride-Terminated Silicon

The only wet chemical surface functionalization strategy not utilizing a hydride-terminated silicon surface is a mechano-chemical process where the native oxide interface is physically abraded in the presence of alkenes or alkynes or alkyl halides under ambient conditions.[138−140] Grinding of silicon powders or abrasion of a flat silicon surface appears to result in highly active surface species, including Si=Si bonds and dangling bonds (radicals). In the presence of alkenes or alkynes, the Si=Si bonds could react in a [2+2] fashion, as observed under UHV conditions (vide supra, section VI.A), as shown in Figure 49a. The silicon radicals, however, could lead to a monosilylated product, outlined in Figure 49b. In the presence of alkyl halides, it is proposed that the silicon radicals abstract X• through homolytic cleavage of the C−X bond, resulting in an alkyl radical which can then react with a second silicon radical, forming the silicon−carbon bond (Figure 49c).

As a demonstration of the practical importance of this process, Figure 50 portrays 28 hydrophobic corrals that were scribed into an Si(100) wafer in the presence of 1-hexadecene.[139] The corral interiors still terminated with the native silicon oxide are hydrophilic, whereas the scribed lines are hydrophobic, due to being functionalized with long alkyl chains. When immersed in water, the water only clings to the hydrophilic corral interiors, even when the sample is turned 90° to vertical. The fact that this approach utilizes the native oxide surface and can be carried out in air makes it a promising methodology for a variety of applications.

V. Wet Chemical Approaches to Ge−C Bond Formation

In contrast to the chemistry on silicon surfaces, germanium surfaces remain scarcely studied for Ge−C bond formation. In fact, only three groups, over almost 40 years, have examined the wet organome-

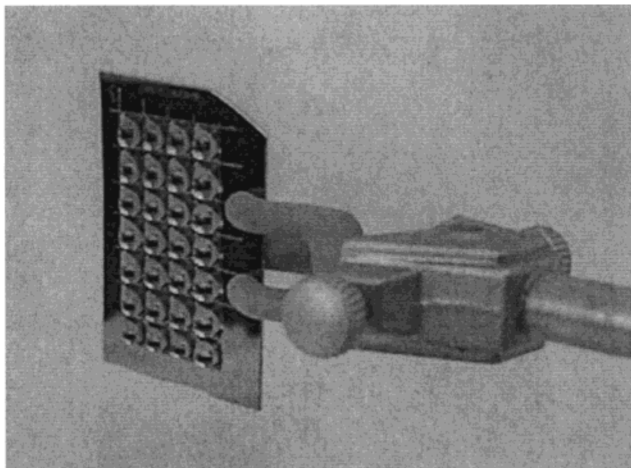

Figure 50. Photograph of water droplets held in a set of 28 hydrophobic corrals produced by scribing Si(100) with a diamond scribe in the presence of 1-hexadecene. Upon exposure of this wafer to water, water accumulates in the hydrophilic regions of the corral interiors and is repelled from the hydrophobic (hexadecyl terminated) borders. Water droplets are unable to escape from the corrals, even when the sample is turned on its side, as shown. (Reprinted with permission from ref 139. Copyright 2001 American Chemical Society.)

tallic chemistry of germanium (another 3 have looked at the UHV reactivity, vide infra). While it appears that the wet chemistries of silicon and germanium parallel each other, much more work remains to verify this hypothesis.

A. Halogenation/Alkylation Routes

In 1962, workers at RCA Laboratories published a paper entitled "The Stabilization of Germanium Surfaces by Ethylation", where they treated a Ge−Cl-terminated (111) surface with ethyl Grignard.[70] They were interested in preparing an interface that had a nonabrupt transition from the substrate to surface layer [since both Ge and C are group(IV) elements] that was made up of molecules capping each Ge atom, was chemically inert, was electronically insulating, and was transparent to visible light. Exposure of the chloride surface to an ethyl Grignard at room temperature resulted in an instantaneous reaction (as determined by radiotracing studies). Rinsing of this surface with aqueous solutions removed the Grignard hydrolysis products and magnesium salts, leaving a highly hydrophobic surface. The authors conclude that this procedure is effective in 'reproducibly preparing a surface essentially completely occupied with strongly held ethyl groups'. These researchers were so ahead of their time!

The radiotracing studies provided an indication of surface coverage and thermal stability.[141] ^{3}H-labeled ethylbromide was used to make the Grignard reagent. One ethyl group per surface Ge was reached, as the authors predicted should be the case in a perfect surface using a conceptual model, but since they did not carry out SEM to determine surface roughness, it is not clear whether an increase in surface roughness, and thus surface area, is actually responsible for higher levels of tritiated ethyl groups. The surfaces are stable to heating in air to 200 °C

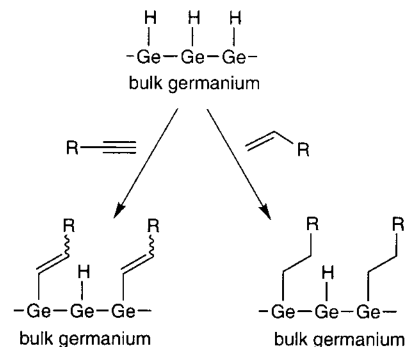

Figure 51. Outline of hydrogermylation on hydride-terminated Ge(100) surfaces.

but decompose rapidly at higher temperatures. The effects of these monolayers on the electronic properties of the Ge were also studied by the same authors.[142] These three papers represent a remarkable piece of work which was unfortunately forgotten until the mid-1990s, when interest in the wet surface chemistry of semiconductors became more important from a technological standpoint.

The work of the RCA group was extended to a broader range of Grignard reagents in 1998 and used a much gentler chlorination procedure.[143] Heating a solution of the alkyl Grignard and a Ge chloride wafer under inert atmosphere for 6 h (ethyl Grignard) to 7 days (octadecyl Grignard) leads to highly hydrophobic surfaces which were analyzed by ATR-FTIR and XPS. The pentadecyl surface is stable 30 min in boiling in water or 20 min in 20% aqueous HCl. Organolithium reagents did not lead to good monolayer formation, perhaps due to their high reactivity and potential for hydrolysis.

B. Hydrogermylation Routes

Hydrogermylation, similar to hydrosilylation, involves the insertion of an unsaturated carbon−carbon bond into a surface-bound Ge−H bond, leading to Ge−C formation, as outlined schematically in Figure 51. There are only two reports to date in the literature concerned with hydrogermylation of alkynes and alkenes on germanium hydride-terminated surfaces. The first, on hydride-terminated Ge(100) surfaces, was published in 2000 and utilizes the optimal conditions found for hydrosilylation on flat and porous silicon.[61] Since the Lewis acid $EtAlCl_2$ mediates the room-temperature hydrosilylation of alkynes and alkenes on porous silicon,[114,115] identical conditions were applied to hydride-terminated flat Ge(100). Alkynes were allowed to react for 1 h and alkenes 12 h, leading to alkenyl- and alkyl-terminated monolayers, respectively, bonded through Ge−C bonds. When 1-pentyne is hydrogermylated, the resulting surface is capped with pentenyl groups, as evidenced by the appearance of the ν(GeC=C) vibration at 1594 cm^{-1} as observed by ATR-FTIR. To definitively prove the carbon−carbon double-bond nature of this stretch, the surface was exposed to hydroborating conditions (BH_3·THF). As shown in the ATR-FTIR spectrum shown in Figure 52, quantitative disappearance of GeC=C vibration is noted, indicating that this feature does indeed correspond

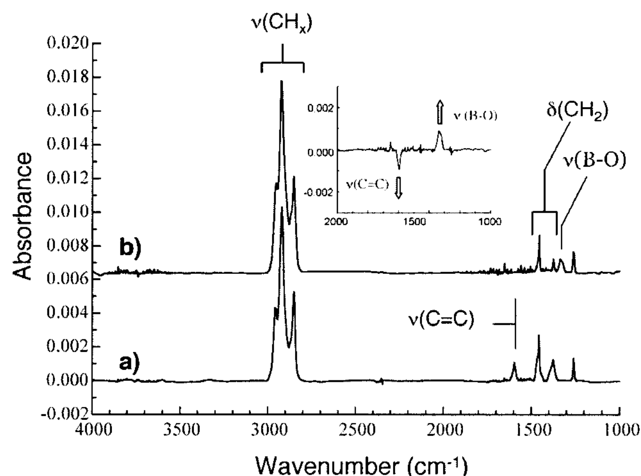

Figure 52. ATR-FTIR spectra of (a) 1-dodecenyl-terminated Ge(100) prepared by Lewis-acid-mediated hydrogermylation on hydride-terminated Ge(100) with 1-dodecyne, and (b) hydroboration of this surface with BH_3.THF. The inset in b shows the difference spectrum upon hydroboration. (Reprinted with permission from ref 61. Copyright 2000 American Chemical Society.)

to a surface-bonded vinyl group. Like hydrosilylation on porous silicon, alkenes can also be hydrogermylated, yielding an alkyl-terminated surface, following a 12 h reaction period. Contact angles (water) of the surfaces produced through Lewis acid chemistry are lower than other methods (thermal, UV, see below) although the ATR-FTIR spectra are identical, probably due to the effect of residual $EtAlCl_2$ which hydrolyzes in air, making the surface more hydrophilic.

Because thermal alkene hydrosilylation has proven to be effective on silicon surfaces (see section IV.B), it was attempted on the flat, germanium hydride-terminated interface. Heating of a neat alkene or alkyne at 200 °C for 2 h resulted in monolayer formation, as shown by contact angles and ATR-FTIR. Alkynes could be diluted to 25% (v/v) in mesitylene, also producing similar monolayers. Alkenes, on the other hand, showed very low incorporation when diluted in mesitylene, even at 33% (v/v) concentrations, possibly due to their lower reactivity. The ν(Ge−H_x) vibrations disappear under these conditions, implying that the germanium−hydride bonds are not stable upon heating and will desorb hydrogen if a hydrogermylation reaction does not proceed. UV (254 nm) induced hydrogermylation was also shown to occur with 1-hexadecene, leading to a hexadecyl-terminated surface in 2 h. Stability studies were carried out on all the hydrogermylated surfaces (HF soaking, boiling in chloroform and water); these experiments indicated that alkyl termination produced via the thermal hydrogermylation of alkenes gave the most stable interface.

Hydrogermylation was also carried out on hydride-terminated porous germanium.[47] Thermal hydrosilylation gave the greatest incorporation levels, compared to Lewis-acid-mediated hydrosilylation and Ge−Ge bond attack with Grignard reagents. A 20% solution of 1-dodecene in mesitylene was heated under a nitrogen atmosphere at 250 °C for 2 h, resulting in incorporation of decyl groups.

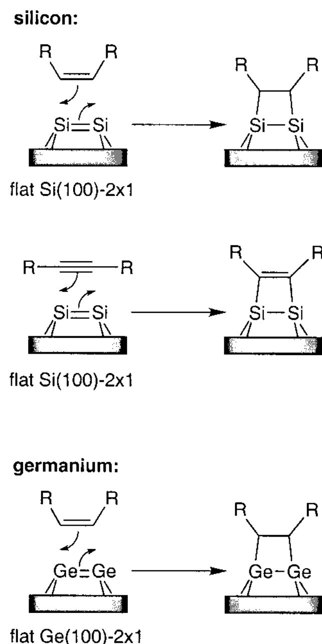

Figure 53. [2+2] cycloadditions on Si(100)-2 × 1 and Ge(100)-2 × 1 surfaces with alkenes and alkynes. The π bond of the silicon or germanium dimer is cleaved, and two new Si−C or Ge−C σ bonds are formed.

VI. UHV (Ultrahigh Vacuum) Approaches to Si−C Bond Formation

UHV surface functionalization strategies offer the possibility to study surfaces in conditions that are, as close as experimentally possible, perfect at the atomic level. Operating at pressures below 10^{-10} Torr, surfaces can be routinely heated to temperatures greater than 1000 K without oxidation, allowing access to unusual (and thermally stable) reconstructions that are otherwise attainable, even under inert atmosphere. In addition, working under UHV permits exquisite STM imaging of the surface-bonded molecules, examples of which are shown here. Molecular modeling of these interfaces has also been studied in detail because of the high order of the interface and will be mentioned.

A. [2+2] Reactions of Alkenes and Alkynes with the Si(100)-2 × 1 Surface

Research starting in 1986 on small unsaturated hydrocarbons such as ethylene, propylene, acetylene, and benzene has shown that they chemisorb to Si(100)-2 × 1 surfaces at room temperature and that the products are able to resist temperatures of up to 550−600 K.[144] The experimental work of many groups clearly indicates that alkenes add to clean Si(100)-2 × 1 surfaces to form a disilicon-substituted aliphatic $-CH_2CH_2-$ bridge through a formal [2+2] cycloaddition, as outlined in Figure 53. Two new Si−C σ bonds form due to cleavage of the π bonds in the alkene and disilylene, with the Si−Si σ bond remaining intact as shown by ATR-FTIR, XPS, EELS, photoelectron diffraction (PhD), and STM studies; concomitant rehybridization of the two sp^2 carbons to sp^3 takes place. Theoretical analyses of the [2+2] additions indicate that there is no stable

minimum for a structure with a broken Si–Si σ bond.[145] Acetylene reacts in a similar [2+2] fashion yielding a disilicon-substituted alkene and involves a change in hybridization at the carbon from sp to sp^2 in this case.[146] Computational studies have substantiated the [2+2] addition reaction of alkenes and alkynes to the surface and indicate breakage of the weak π bond, leaving the σ bond intact,[147] although there are still some questions remaining concerning adsorption geometries of acetylene.[148] Cycloaddition reactions, both [2+2] and [4+2] (vide infra), have been reviewed recently.[72]

Concerted [2+2] cycloadditions are normally symmetry-forbidden in molecular systems[149] and hence very slow, suggesting that a low-symmetry pathway may be accessible on the surface.[150] As shown in Figure 12, the weakness of the π bond may actually suggest more of a diradical character, with each silicon or germanium atom having associated with it an unpaired electron. The dimers can also tilt on the surface, leading to zwitterionic character, with each of the silicon atoms having a partial positive or negative charge.[151] The actual properties of the silicon and germanium dimers may be a combination of these three representations.[72] It is clear that a simple σ- and π-bonding picture of these dimers cannot explain the ease at which [2+2] cycloadditions occur. The tilting of the dimers on the surface, based on calculations, leads to bending of the Si=Si bond from a planar arrangement, causing charge polarization of the dimer and making the π^* orbital at one end susceptible to attack by nucleophiles, which leads to a much higher reaction probability.[72,74]

Olefins and alkynes with secondary functional groups, such as a second alkene, nitrogen, or aromatic group, can also undergo the [2+2] reaction, leading to a more highly functionalized surface.[152] A wide range of complex olefins react in this manner at moderate temperatures, including cyclopentene, 3-pyrroline, pyrrolidone, norbornadiene, 1,5-cyclooctadiene, 1,3,5,7-cyclooctatetraene, and styrene.[72,74,153–158] Beautiful STM images of the reaction products of 1,3,5,7-cyclooctatetraene addition, resolved down to the molecular level, are shown in Figure 54.[156] Ordering of the underlying silicon–silicon dimers and of the resultant organoterminated surface is evident from these images. This molecule is of special interest because it appears to add to the surface through a double cycloaddition, leaving two alkene groups per molecule exposed through which further chemistry could perhaps be carried out (Figure 54d).[152,156] Figure 55 shows the ordered surface formed from the [2+2] addition of one of the alkenes in 1,5-cyclooctadiene.[155] In this case, only one of the alkenes adds, leaving the other free.

When carrying out the [2+2] cycloadditions, chirality and stereospecificity issues become important when the alkene is chiral, prochiral, or disubstituted. In 1995, the absorption, desorption, and decomposition of both *cis*- and *trans*-2-butene on the Si(100)-2 × 1 surface were observed and contrasted.[159] While the sticking coefficients and adsorption rates of both molecules are very similar, temperature-programmed desorption studies reveal a difference in stability

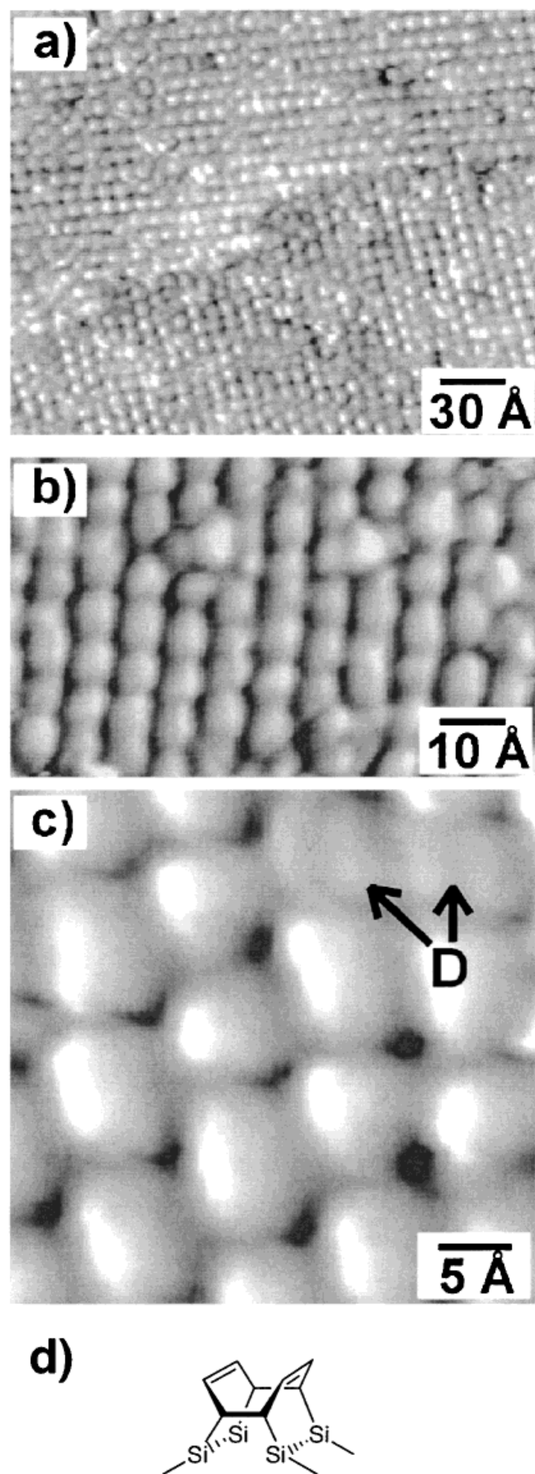

Figure 54. Scanning tunneling microscopy (STM) images of the silicon–silicon dimer-terminated Si(100) surface after exposure to 1,3,5,7-cyclooctatetraene to form the surface shown in d. Panel a demonstrates the long-range anisotropy and ordering of the surface. Panels b and c reveal the absorption pattern of the molecules. “D” refers to a minority species comprising <5% of the surface features. (Reprinted with permission from ref 156. Copyright 1998 American Chemical Society.) The authors are also thanked for permission to reprint this figure.

between the surfaces produced upon [2+2] addition of the butene stereoisomers, indicating that the molecules yield different surfaces as a result their *cis*- or *trans*-precursor structures, as drawn schematically in Figure 56. The surfaces formed from *cis*-

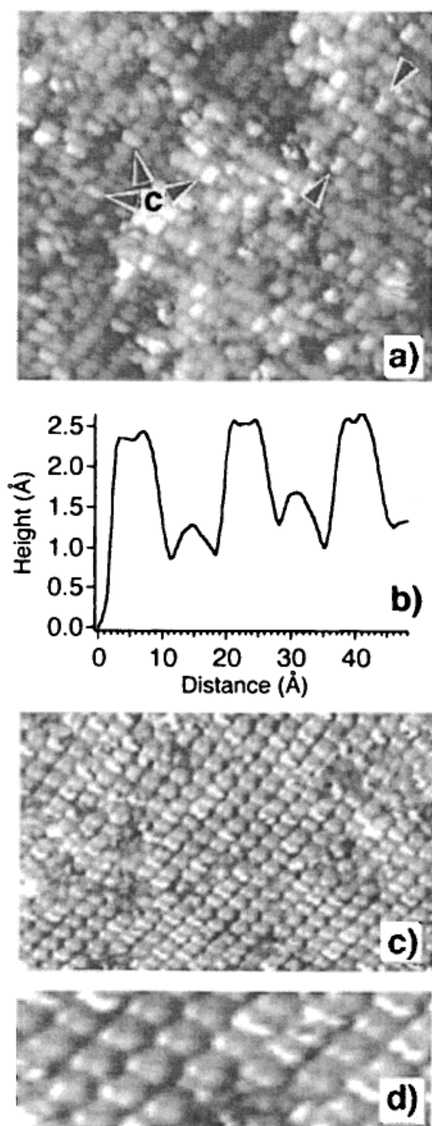

Figure 55. STM images of Si(001)-2 × 1 surface after exposure to 1,5-cyclooctadiene (COD). (a) The individual COD molecules and the underlying dimerized Si(001) surface can be observed at low coverage. (b) Height profile along the line indicated in a. (c) STM image obtained after saturation exposure showing highly ordered arrays of COD molecules on Si(001) surface. (d) Magnified view of saturation-coverage surface showing apparent internal structure of molecules on the surface. (Reprinted with permission from ref 155. Copyright 1997 American Chemical Society.) The authors are also thanked for permission to reprint this figure.

2-butene are slightly less stable. The reactivity of *cis*- and *trans*-1,2-dideuterioethylene by ATR-FTIR was examined and compared the stretching frequencies of the observed vibrations with calculated values (Gaussian 94).[150] On the basis of the frequency differences between the ν(C−H)$_s$ and ν(C−H)$_{as}$ modes, they could clearly differentiate between the surfaces formed from the *cis*- and *trans*-precursors. Each carbon atom becomes chiral, upon [2+2] addition, and therefore, the three possible stereoisomers would be (*R,R*), (*R,S*), and (*S,S*). They conclude that *cis*-1,2-dideuterioethylene yields the (*R,S*) surface and the *trans*-isomer the (*R,R*) or (*S,S*) surface.

STM studies later revealed a measurable degree of isomerization on the surface, ~2%, during the

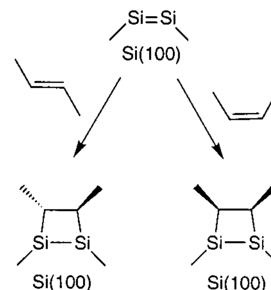

Figure 56. Addition of *cis*- and *trans*-2-butene to the surface bound silicon dimers lead to two different stereoisomers.

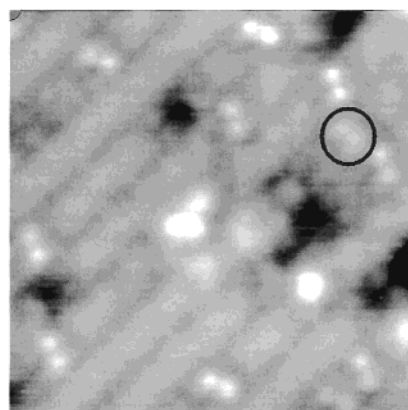

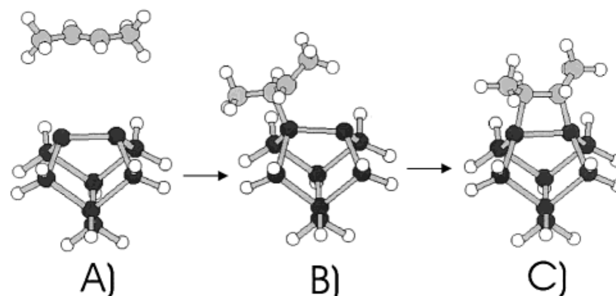

Figure 57. (Top) STM image (7.5 nm × 7.5 nm) of the Si(100)-2 × 1 surface upon exposure to *trans*-2-butene. The majority of the molecules retain their *trans*-configuration upon binding, but a small percentage (~2%) isomerize to the *cis*-form, as seen in the circled area. (Bottom) The steps involved in the [2+2] addition of *trans*-2-butene to a surface silicon dimer. (Reprinted with permission from ref 160. Copyright 2000 American Chemical Society.) The authors are also thanked for permission to reprint this figure.

[2+2] addition of *cis*- and *trans*-2-butene to the Si(100)-2 × 1 surface.[160] As shown in Figure 57, upon exposure of the surface to *trans*-2-butene, the STM image shows pairs of white protrusions which correspond to methyl groups, superimposed upon a row of silicon dimers (grey bars); the majority lie at an angle of 30° with respect to the dimer row.[161] These correspond with the *trans*-2-butene undergoing the [2+2] addition in a stereospecific fashion, as outlined in Figure 57, going from A → C. The circled area in the STM image of Figure 57, however, corresponds with a small population of organic groups in which the pair of methyl groups is inclined in a perpendicular fashion to the row of silicon dimers, as opposed to being tilted by ~30°. This is exactly the orientation observed when *cis*-2-butene is adsorbed,

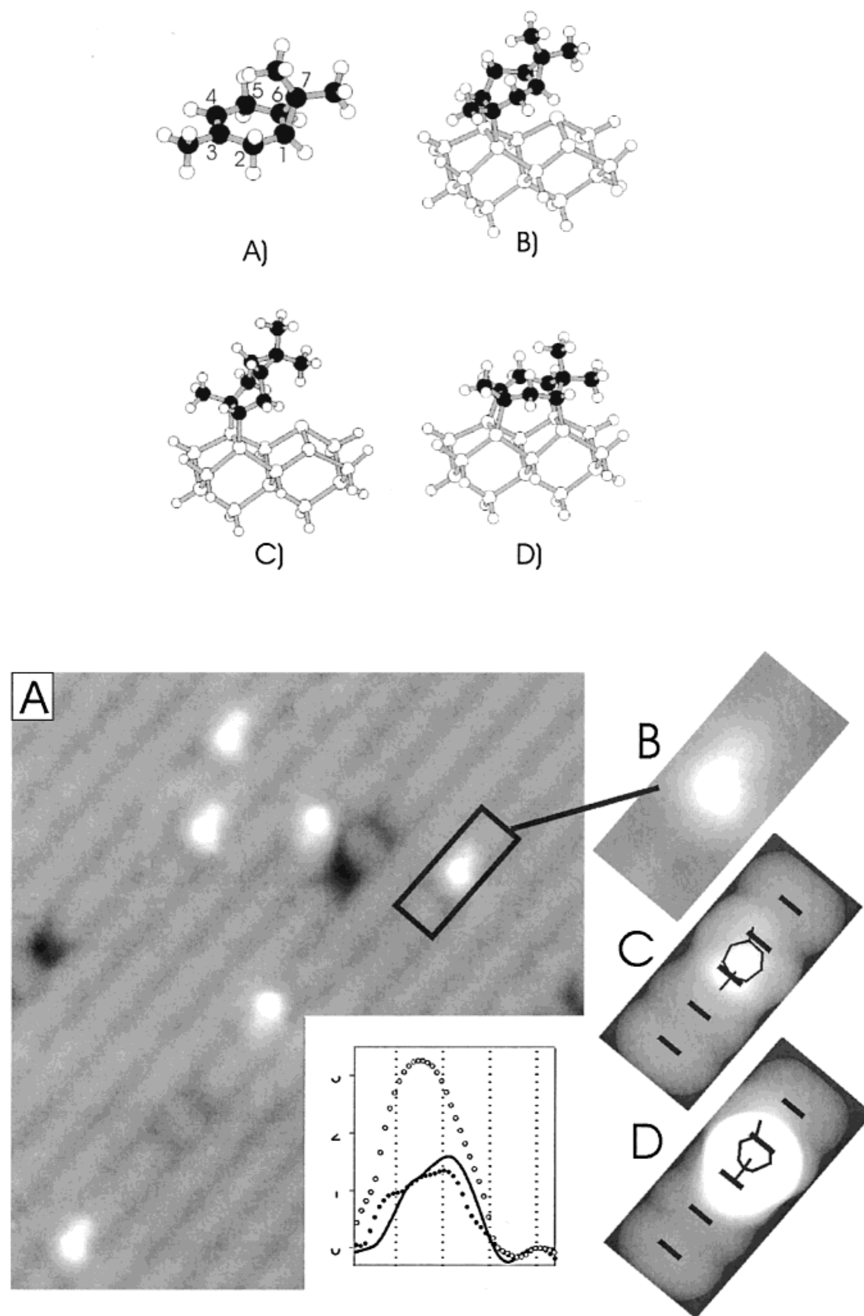

Figure 58. (Top) (A) The 1S(+)-3-carene molecule and different possible bonding geometries calculated for binding of this molecule to an Si(100)-2 × 1 dimer model cluster (B−D). Structures B and C are bonded exclusively through the alkene and structure D through both the alkene and the cyclopropyl group (bridging geometry). (Bottom) (A) STM image (10 nm × 10 nm) of the Si(100)-2 × 1 surface upon binding of 1S(+)-3-carene. An enlarged view of the molecule is shown in B. When simulated images are calculated for both the exclusive alkene binding and bridging geometries, as shown in C and D, only the bridging geometry matches the actual observed image of B; the other structures involving only binding through the alkene have a much higher predicted maximum. (Reprinted with permission from ref 73. Copyright 1999 American Chemical Society.) The authors are also thanked for permission to reprint this figure.

indicating that some isomerization is occurring on the surface. Through an examination of several hundred molecules, the fraction of *cis*-configured molecules was determined to be 2.1 ± 0.7%, significantly higher than the *cis*-contamination of the *trans*-2-butene material (0.2 ± 0.1%). The isomerization is observed on dimers belonging to a clean surface and is therefore not induced by defects. Because earlier work has shown that the *trans*-surface is thermodynamically more stable,[159] the authors conclude that the process is kinetically controlled. These observations have important mechanistic implications in that they eliminate the possibility for a concerted [2+2] cycloaddition; a stepwise mechanism with sufficient time (picoseconds) to rotate about the C−C bond after formation of the first Si−C bond is more likely.

In an interesting extension of this work, the same group examined the [2+2] addition of 1S(+)-3-carene (3,7,7-trimethylbicyclo[4.1.0]hept-3-ene), shown in Figure 58 (molecule A), to the Si(100)-2 × 1 surface.[73] Three possible surface bonding configurations are shown in Figure 58, two of which involve [2+2] addition of the olefin moiety (B and C) and a third involving both the [2+2] of the olefin and an opening

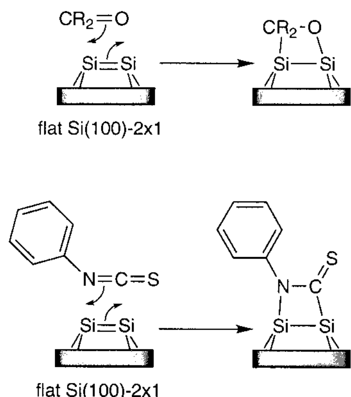

Figure 59. [2+2] cycloadditions of heteroatom-containing double-bonded molecules: carbonyls and phenyl isothiocyanate on the Si(100)-2 × 1 surface.

of the cyclopropyl ring (D). Comparison of STM images to calculations indicate that the third bonding motif, structure D in Figure 58, appears to occur in an enantospecific manner, resulting in a chiral surface. Because cyclopropane has been shown to not interact with the Si((100)−(2 × 1) interface, it is probable that once the [2+2] cycloaddition of the alkene portion of the molecule has occurred, the cyclopropyl fragment is held in close proximity, enabling the reaction to occur with ease.[1]

B. [2+2] Reactions of Other Carbon-Containing Unsaturated Molecules with the Si(100)-2 × 1 Surface

Carbonyl-containing compounds such as acetone, 2,3-butanedione and acetaldehyde have been shown to react irreversibly with the Si(100)-2 × 1 surface.[162,163] The [2+2] addition of a carbonyl yields one Si−C and one Si−O bond, as shown in Figure 59, while the [4+2] addition of a 1,2-dialdehyde such as biacetyl ($CH_3COCOCH_3$) could produce two Si−O bonds. If the surface is roughened, chemisorption of these molecules decreases dramatically, indicating the importance of the silicon−silicon dimers. Other products are also observed by XPS, even at low temperatures. It was initially concluded that the [4+2] addition of biacetyl does not take place; instead, a [2+2] addition product is formed, leaving an unreacted C=O bond, as based upon the observation of a vibration at 1670 cm^{-1} in the HREELS spectrum. Very recent theoretical work has suggested instead that the [4+2] addition occurs readily and that this vibration is the alkene stretch that remains after the hetero-Diels−Alder reaction.[164]

Phenyl isothiocyanate, despite several binding modes available, reacts preferentially through a 1,2-dipolar addition, involving the C=N group, forming an Si−C and Si−N bond, as outlined in Figure 59.[165] XPS, ATR-FTIR, and STM imaging were complemented by calculations, indicating that the phenyl ring plays no role in the surface interaction.

C. Diels Alder ([4+2]) Reactions of Dienes with the Si(100)-2 × 1 Surface

A Diels−Alder-like [4+2] reaction was first predicted theoretically[166] and then demonstrated experimentally on the Si(100)-2 × 1 surface;[167,168] the double-bond character of the silicon−silicon dimers enables them to act as a dienophile in a Diels−Alder [4+2] type reaction, as shown in Figure 60. Calculations indicate that the [4+2] reaction will be 15−29 kcal mol^{-1} more stable than the [2+2] addition product; the calculated structures of the [4+2] and [2+2] cycloaddition products of cyclohexadiene are shown in Figure 61.[166] Experiments indicate that chemisorption of 1,3-butadiene or 2,3-dimethyl-1,3-butadiene onto the Si(100)-2 × 1 surface at room temperature results in an efficient Diels−Alder reaction, forming two Si−C σ bonds and one unconjugated, internal olefin. The [4+2] products as well as the possible [2+2] reaction for 1,3-butadiene and 2,3-dimethyl-1,3-butadiene are shown schematically in Figure 62. FTIR spectroscopy, thermal desorption, near-edge X-ray absorption fine structure, and deuterium-labeling studies assisted in the determination of surface composition. While 80% of the 2,3-dimethyl-1,3-butadiene molecules undergo the [4+2] reaction, a minor fraction (20%) forms the [2+2] product.[169] In the case of 1,3-cyclohexadiene, 55% of the surface products arise from the [4+2] addition, 35% from the [2+2] addition, and 10% of unknown product. The [4+2] products are predicted to be thermodynamically more stable, but because surface temperature has little affect on product distributions, it is suggested that the reaction is under kinetic control. Computational studies on the reaction suggest that surface isomerization reactions connecting the [2+2] and [4+2] reactions are very unlikely, due to a high energy barrier.[170]

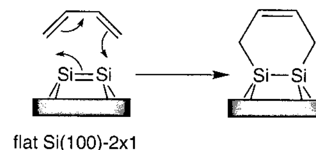

Figure 60. Diels−Alder ([4+2]) reaction of conjugated dienes with the Si(100)-2 × 1 surface. The π bond of the silicon or germanium dimer is cleaved, and two new Si−C or Ge−C σ bonds are formed, with a C=C double bond remaining in the organic product.

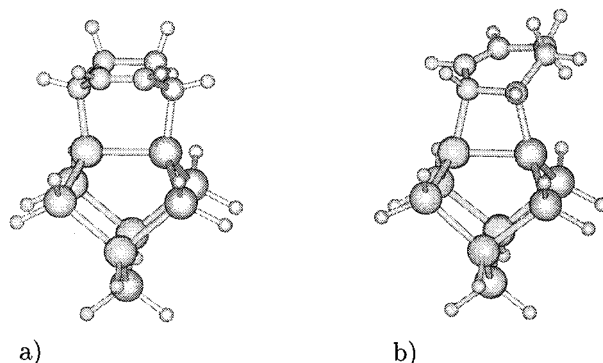

Figure 61. Calculated structures for the products of the [4+2] (a) and [2+2] (b) cycloaddition reactions of 1,3-cyclohexadiene with the Si(100)-2 × 1 surface, using an Si_9H_{12} cluster model. The largest spheres are Si, the middle C, and the smallest H. (Reprinted with permission from ref 166. Copyright 1997 American Chemical Society.) The authors are also thanked for permission to reprint this figure.

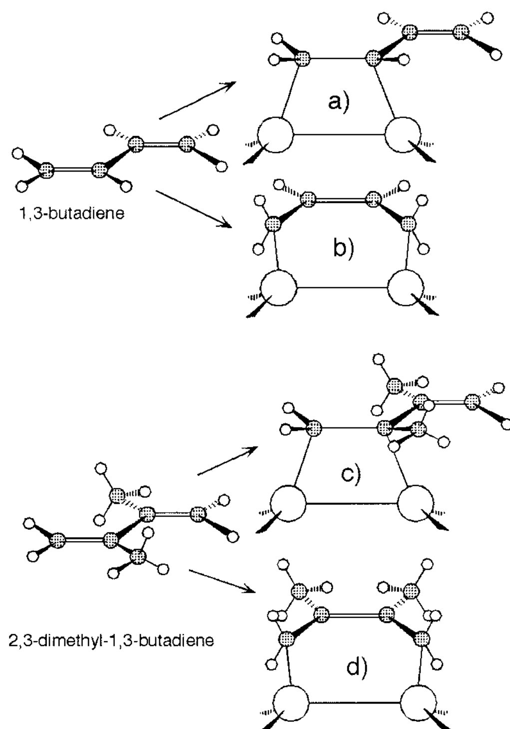

Figure 62. Possible products from the reaction of 1,3-butadiene and 2,3-dimethylbutadiene with the Si(100)-2 × 1 surface. The [4+2] addition products result in an internal C=C double bond, whereas the possible [2+2] addition only utilizes one alkene, leaving one terminal alkene untouched. (Reprinted with permission from ref 167. Copyright 1997 American Chemical Society.) The authors are also thanked for permission to reprint this figure.

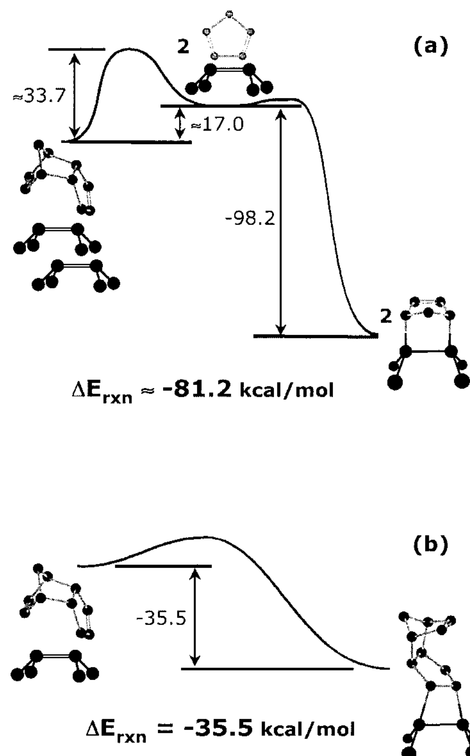

Figure 63. Potential energy diagrams for the (a) surface-catalyzed retro-Diels–Alder reaction for dicyclopentadiene and (b) the [2+2] cycloaddition only involving one alkene of dicyclopentadiene. (Reprinted with permission from ref 171. Copyright 1999 American Chemical Society.) The authors are also thanked for permission to reprint this figure.

An interesting approach examined the potential for the surface to catalyze a retro-Diels–Alder reaction of endodicyclopentadiene, formed via the Diels–Alder reaction of two cyclopentadiene molecules.[171] The [4+2] addition of cyclopentadiene is facile, and calculations indicate that dissociation of the endodicyclopentadiene into two cyclopentadiene molecules through the retro-Diels–Alder reaction will release a substantial amount of energy, favoring this pathway over a [2+2] addition pathway with just one of the C=C bonds, as outlined in Figure 63. Instead, the [2+2] pathway dominates, leading to incorporation of the endocyclopentadiene molecule intact, therefore indicating that the activation barrier for the retro-Diels–Alder reaction is simply too high at room temperature. The authors indicate that higher adsorption temperatures will be examined to facilitate this pathway.

In a detailed study, three similar cyclic C_6 hydrocarbons, 1,3-cyclohexadiene, 1,4-cyclohexadiene, and cyclohexene, were reacted with the Si(100)-2 × 1 surface and their products compared by ATR-FTIR, temperature-programmed reaction/desorption (TPR/D), and NEXAFS, as shown in Figure 64.[172] If the prepared surfaces are then hydrogenated, the same surface product, a 1,2-disilicon-substituted cyclohexane ring, is formed. Both 1,3- and 1,4-cyclohexadiene yield similar (but not identical) surfaces. The 1,4-cyclohexadiene molecule has either a lower absorption probability or surface coverage, however, perhaps suggesting that the [4+2] reaction occurs more readily than the [2+2], as this molecule cannot

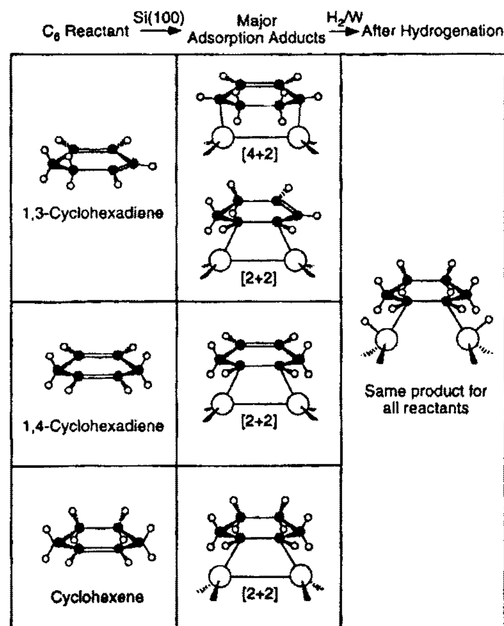

Figure 64. Reaction of three cyclic C6 hydrocarbons with the Si(100)-2 × 1 surface. After hydrogenation, the same surface can be accessed. (Reprinted with permission from ref 172. Copyright 2000 American Chemical Society.) The authors are also thanked for permission to reprint this figure.

undergo a Diels–Alder-like reaction. One double bond remains when the cyclohexadienes are reacted, eliminating the possibility of binding to two dimers (tetra-σ bonding), as has been implicated for ben-

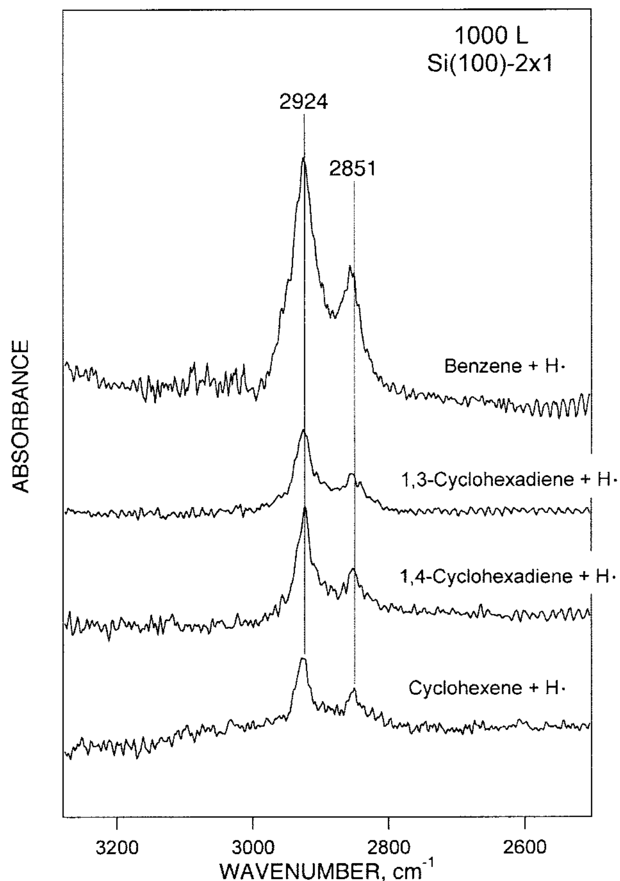

Figure 65. ATR-FTIR spectra of four cyclic C6 hydrocarbons after adsorption to the Si(100)-2 × 1 surface and subsequent hydrogenation. The spectra are essentially identical, indicating that the same termination is produced from different starting materials following the reaction with atomic hydrogen. (Reprinted with permission from ref 172. Copyright 2000 American Chemical Society.) The authors are also thanked for permission to reprint this figure.

zene.[173] NEXAFS verifies the existence of the C=C double bond through observation of the π^* orbital in the spectrum. This technique was also used to probe the orientation of the product of [4+2] cycloaddition products of 1,3-cyclohexadiene[172] and 2,3-dimethyl-1,3-butadiene.[174] The resulting products are oriented at an average angle of 35° and 41°, respectively, a similar value to that predicted theoretically.[160] When the cyclohexadiene surfaces are heated, benzene is released in both cases over a wide temperature range.

As outlined in Figure 64, the surfaces produced via the [4+2] cycloaddition reaction with 1,3- and 1,4-cyclohexadiene can be hydrogenated with atomic hydrogen, leading to the completely saturated cyclohexane fragment.[172] Figure 65 shows the ATR-FTIR spectrum of all the surfaces reacted with the C_6 hydrocarbons examined in this study, after exposure to a large excess of hydrogen atoms. Clearly, all the spectra are identical, indicating a common product on all the surfaces.

D. Reaction of Methyl Halides with the Si(100)-2 × 1 Surface

Methyl chloride, bromide, and iodide have been reacted with the Si(100)-2 × 1 surface and have

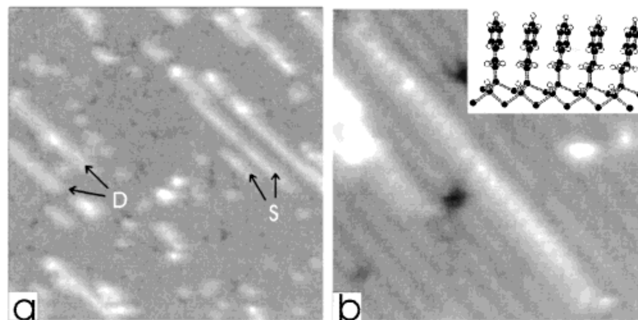

Figure 66. STM images (350 Å^2) of the styrene lines produced through the self-directed hydrosilylation reaction on a hydride-terminated Si(100) surface. (a) Exposure of a surface with a dilute concentration of silicon dangling bonds to styrene. Single (S) and double (D) lines are indicated. (b) STM image (90 Å^2) revealing molecular resolution of individual phenethyl groups on the surface, spaced 3.8 Å apart, as would be expected (see inset). (Reprinted with permission from *Nature* (http://www.nature.com), ref 182. Copyright 2000 Macmillan Magazines Ltd.) The authors are also thanked for permission to reprint this figure.

provided very useful handles to characterize the Si−CH_3 fragment by both STM and ATR-FTIR.[175−178] Upon exposure of the methyl halide to the silicon surface at room temperature, dissociative absorption occurs across a dimer, forming an Si−C bond and an Si−X (X = Cl, Br, I) bond. The sticking probability is near unity, and the methyl groups are thermally stable above 600 K, although it was shown that in the case of methyl chloride an annealing at 420 K induces island formation of the chlorides, as shown by STM. The $\nu(CH_3)$ modes observed by ATR-FTIR upon methyl iodide addition appear to represent only a small fraction of sites; these sites have a larger infrared absorption cross section than the major product.

E. STM-Initiated Reactions on Silicon Surfaces

The scanning tunneling microscope (STM) tip can be used to break bonds on a surface in a spatially defined manner.[179] For instance, Si−H bonds on a surface can be cleaved upon application of a tunneling current of ∼−6V (tip bias negative). This observation has been used to selectively break silicon−hydride bonds on a hydride-passivated Si(100)-2 × 1 surface, allowing for formation of depassivated areas 20 nm × 20 nm which are terminated with silicon dangling bonds.[180] Upon leakage of norbornadiene (bicyclo[2.2.1]hepta-2,5-diene) into the UHV chamber at room temperature, the alkene moieties react with the silicon radicals, forming Si−C bonds. The Si−H-terminated areas do not react with alkenes under these conditions. Thus, small areas of organic monolayers can be produced in spatially localized domains on the silicon surface.[181]

In an incredible piece of work, it was shown recently that under UHV conditions, stryene can be hydrosilylated by the Si(100)−H surface, continuing in a chain reaction that results in lines of phenethyl groups on the surface, as shown in Figure 66a.[182] A surface dangling bond is produced with the STM tip, leading to the surface-bonded radical. Exposure of a

surface with a dilute concentration of styrene leads to the growth of lines up to 13 nm long, corresponding to 34 adsorption sites (Figure 66b). The reaction proceeds through a radical mechanism, starting with the silicon-based dangling bond. Reaction of the styrene olefin with the Si radical results in an Si−C bond and a carbon-based radical β to the surface Si, α to the phenyl group. This radical can then abstract a neighboring hydrogen, reforming a silicon radical which then goes on to react with a second molecule of styrene, continuing the chain reaction. Growth appears to stop at defects such as missing dimers and is not affected by the STM tip itself. The intermolecular spacing between the phenyl rings of 3.8 Å is close enough to expect π-overlap, and thus, these structures may function as molecular wires, a hypothesis substantiated by calculations which suggest considerable electronic coupling between adjacent molecules. It is even suggested that by modifying both the reactant molecules and seed conditions, it may be possible to control growth direction, turn corners, and grow vertically as well as fabricate arrays of structures in a parallel fashion.

VII. UHV Approaches to Ge−C Bond Formation

A. [2+2] Reactions of Alkenes with the Ge(100)-2 × 1 Surface

It is only recently that Ge−C bond formation via the [2+2] cycloaddition reaction with alkenes has been examined. Cyclopentene and cyclohexene were shown to recently undergo a [2+2] addition reaction with the surface, similar to the observations made on Si(100)-2 × 1 surfaces, as shown in Figure 53.[183] The sticking coefficient of alkenes to the germanium surface is ~10% that of the silicon surface as determined by temperature-programmed desorption measurements and STM, although calculations suggest that the binding energy for cyclopentene is 27% higher on Ge than Si. This points to the greater thermodynamic stability of the organic [2+2] addition products on germanium but a higher activation barrier which makes the reaction more difficult (kinetic barrier). In contrast to the [2+2] addition product on silicon, the reaction with ethylene is reversible on germanium upon heating, although the desorption process in complicated by conversion of ~30% of the product into an undetermined structure which desorbs about 35 K higher in temperature.[184]

In contrast to Si(100)-2 × 1 surfaces at room temperature, acetone does not form the [2+2] product, leading to Ge−C and Ge−O bonds.[185] Instead, a dative bond between the carbonyl oxygen and Ge of a Ge=Ge dimer results, followed by enolization of the ketone and formation of a Ge−H bond. On the basis of these experimental results and complementary theoretical work, it was concluded that the enolization product is the thermodynamic product whereas the [2+2] addition is the kinetic product. Thus, in contrast to silicon, this reaction is under thermodynamic control, a very interesting observation which could help lead to greater selectivity in the formation of organic monolayers on semiconductor surfaces.

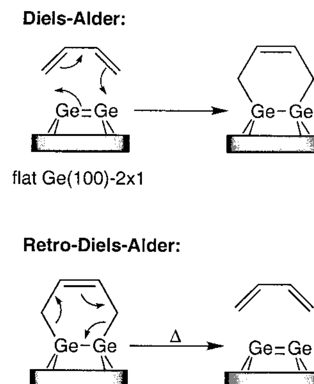

Figure 67. Diels−Alder and retro-Diels−Alder [4+2] cycloadditions of conjugated dienes to the Ge(100)-2 × 1 surface.

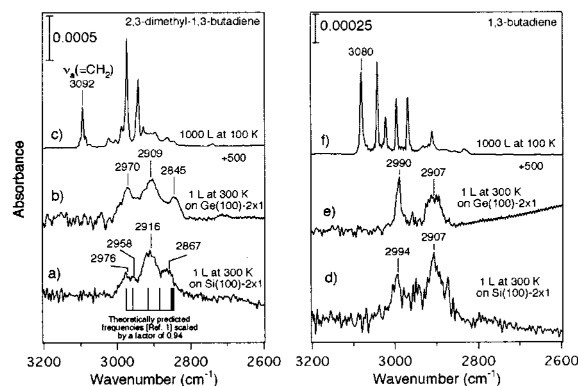

Figure 68. Infrared spectra of 2,3-dimethyl-1,3-butadiene (a) chemisorbed on Si(100)-2 × 1 at 300 K, (b) chemisorbed on Ge(100)-2 × 1 at 300 K, and (c) physisorbed in multilayers at 100 K and 1,3-butadiene (d) chemisorbed on Si(100)-2 × 1 at 300 K, (e) chemisorbed on Ge(100)-2 × 1 at 300 K, and (f) physisorbed in multilayers at 100 K. The theoretically predicted frequencies (in cm^{-1}) occur at 2846, 2850, 2854, 2885, 2916, 2958, and 2976. (Reprinted with permission from ref 186. Copyright 1998 American Chemical Society.) The authors are also thanked for permission to reprint this figure.

B. Diels Alder ([4+2]) Reactions of Dienes with the Ge(100)-2 × 1 and Ge/Si(100)-2 × 1 Surfaces

Following the successful demonstration of the [4+2] cycloaddition of conjugated dienes on the Si(100)-2 × 1 surface, the reaction was shown to proceed readily on the germanium equivalent.[186] In contrast to the silicon surface, however, a retro-Diels−Alder reaction occurs upon thermal annealing, as shown in Figure 67. ATR-FTIR of 2,3-dimethyl-1,3-butadiene and 1,3-butadiene reacted Si(100)-2 × 1 and Ge(100)-2 × 1 surfaces are shown in Figure 68; the similarities between the Si and Ge surfaces are clear, indicating that the same organic moieties form on both. When 1,3-butadiene is reacted with the Ge(100)-2 × 1 surface, two Ge−C σ bonds are formed; when this surface is heated from 350 to 650 K, clean evolution of 1,3-butadiene is observed by temperature-programmed reaction/desorption mass spectrometry. Auger electron spectroscopy (AES) indicates complete removal of all the chemisorbed carbon after thermal treatment. It has been suggested that the retro-Diels−Alder reaction may permit spatial modification through removal of areas of reacted surface via photoinduced or electron-induced chemistry.

Because of the importance of silicon−germanium materials for microelectronics,[22] the surface chemistry of this material is of interest, not only for technological applications but from a fundamental perspective as well. When germanium is grown on an Si(100) surface, at low and intermediate coverages, both Ge−Si and Ge−Ge dimers are observed.[187] Computational studies indicate that [4+2] cycloaddition reaction products of 1,3-butadiene on Si−Si, Si−Ge, and Ge−Ge are all more stable than the [2+2] products, due to ring strain in the latter.[188] With increasing Ge composition, however, the binding energies of the [4+2] cycloaddition products decrease due to the lower Ge−C bond strength.

Additional theoretical work which will help to elucidate the surface chemistry of germanium has been carried out, although to a much smaller extent than on silicon.[189] Perhaps with further work on this relatively unstudied material, similarities and differences between silicon, germanium, and Si/Ge [2+2] additions can be further elucidated.

VIII. Further Functionalizing Functionalized Surfaces

Because many of the surfaces prepared through wet chemical techniques have proven themselves to be very robust with respect to demanding chemical and oxidative conditions, further chemistry has been carried out on these interfaces to prepare more sophisticated surfaces for a variety of applications. Sensor design, surface-related assays, spectroscopic handles, and biological molecule interfacing and others were proposed as driving forces for this exciting area of research. As this work shows, traditional protecting group strategies may be viable options when preparing functional films on silicon (and by extension, germanium). These reactions are summarized in Figure 69. One interesting exception to the wet chemistry described here is a UHV example where polyimide films were prepared through a condensation reaction (section VIII.B, Figure 70).

A. C−H Bond Activation of Terminal Methyl Groups

In what were the first two papers in the field addressing functionalization of prepared monolayers bonded to unoxidized silicon surfaces through Si−C bonds, clean C−H activation of terminal methyl groups in an octadecyl monolayer on Si(111) was reported.[190,191] As outlined in Figure 69, part A, an Si(111)−$C_{18}H_{37}$ surface was illuminated with a 350 nm broadband lamp in the presence of 4′-[3-trifluoromethyl-3H-diazirin-3-yl]-benzoic acid *N*-hydroxysuccinimide ester (TBDA-OSu) for 15 min in CCl_4. This resulted in a hydrophobic surface containing a reactive terminal *N*-succinimide group which can be easily substituted with nucleophiles. A second reaction leads to a chlorosulfonyl-terminated octadecyl monolayer through a gas-phase reaction involving illumination with 351 nm UV light with chlorine gas in sulfur dioxide for 10 s. AFM studies reveal that these chemistries do not change the surface topology of the flat (111) surface.

B. Amide and Sulfonamide Bond Formation

The *N*-succinimide-terminated octadecyl monolayer on Si(111), described in section VII.A, was used to bind a DNA fragment containing an amino-modified C6 spacer at both 5′ ends, as shown in Figure 69, part B. Because the *N*-succinimide termination is hydrophobic, a trace of surfactant, such as Triton, helps to reduce surface tension and improve wetting when in contact with an aqueous solution. Use of the carboxylic acid-terminated monolayer, Si(111)−$C_{10}H_{20}$-COOH, with the coupling reagent diisopropylcarbodiimine, a base, and glycine methyl ester in chloroform resulted in amide bond formation at 50 °C for 18 h.[192] The newly formed peptide bond has a distinctive carbonyl stretch at 1680 cm^{-1}, as observed by ATR-FTIR. Sulfonamide groups were formed by reaction of Si(111)−$C_{18}H_{36}SO_2Cl$ (section VII.A) with a range of different primary and secondary amines, including ethylenediamine (thus leaving a free amine for further chemistry), a poly(ethylene oxide) chain, and a dendritic amine.[190,191] The surface formed with a primary amine, H_2NR, thus has the general formula of Si(111)−$C_{18}H_{36}SO_2NHR$, as characterized by XPS.

Under UHV conditions, polyimide thin films were prepared by reacting maleic anhydride with the Si-(100)-2 × 1 surface.[193] Instead of a [2+2] cycloaddition, C−H activation appears to be the dominant pathway, as shown in Figure 70. Phenylene diamine (PDA) was then dosed onto this surface, followed by pyromellitic dianhydride (PMDA); two amide bonds are formed in these two steps. Curing of the film at 430 °C to initiate imidization results in an intense vibration at 1160 cm^{-1} which is assigned to imide $(OC)_2NC$ modes of the expected product.

C. Ester Hydrolysis

Because of the difficulty of preparing a carboxylic acid-terminated monolayer with alkenes such as $CH_2{=}CHC_8H_{16}COOH$ via a hydrosilylation route due to concomitant silyl ester formation on the surface, a methyl ester was used in its place, $CH_2{=}CHC_8H_{16}$-$COOCH_3$.[80] Thermal hydrosilylation on a hydride-terminated Si(100) surface results in an Si(100)−$C_{10}H_{20}COOCH_3$ surface. Boiling in acidic water for 20−30 min resulted in cleavage of the ester, yielding a hydrophilic surface as determined by contact angles, as expected for a carboxylic acid-terminated monolayer. ATR-FTIR did indeed reveal the expected vibrations for a carboxylic group, but the low signal-to-noise in this region made a detailed analysis difficult. It was later shown that a 2.4 N HCl (aq) solution, when heated to 70 °C for 2 h, could also result in ethyl ester hydrolysis of Si(111)−$C_{10}H_{20}$-COOEt.[192] On the other hand, an acetate-terminated surface, Si(100)−$C_{11}H_{22}OC(O)CH_3$, could not be hydrolyzed under these conditions, perhaps due to the inaccessibility of the ester groups in this case.[80]

D. Ester Reduction and Cleavage

Thermal hydrosilylation of the acetate-containing alkene on hydride-terminated Si(100), $CH_2{=}CH$−$C_8H_{16}CH_2OC(O)CH_3$, yielded an acetate-terminated

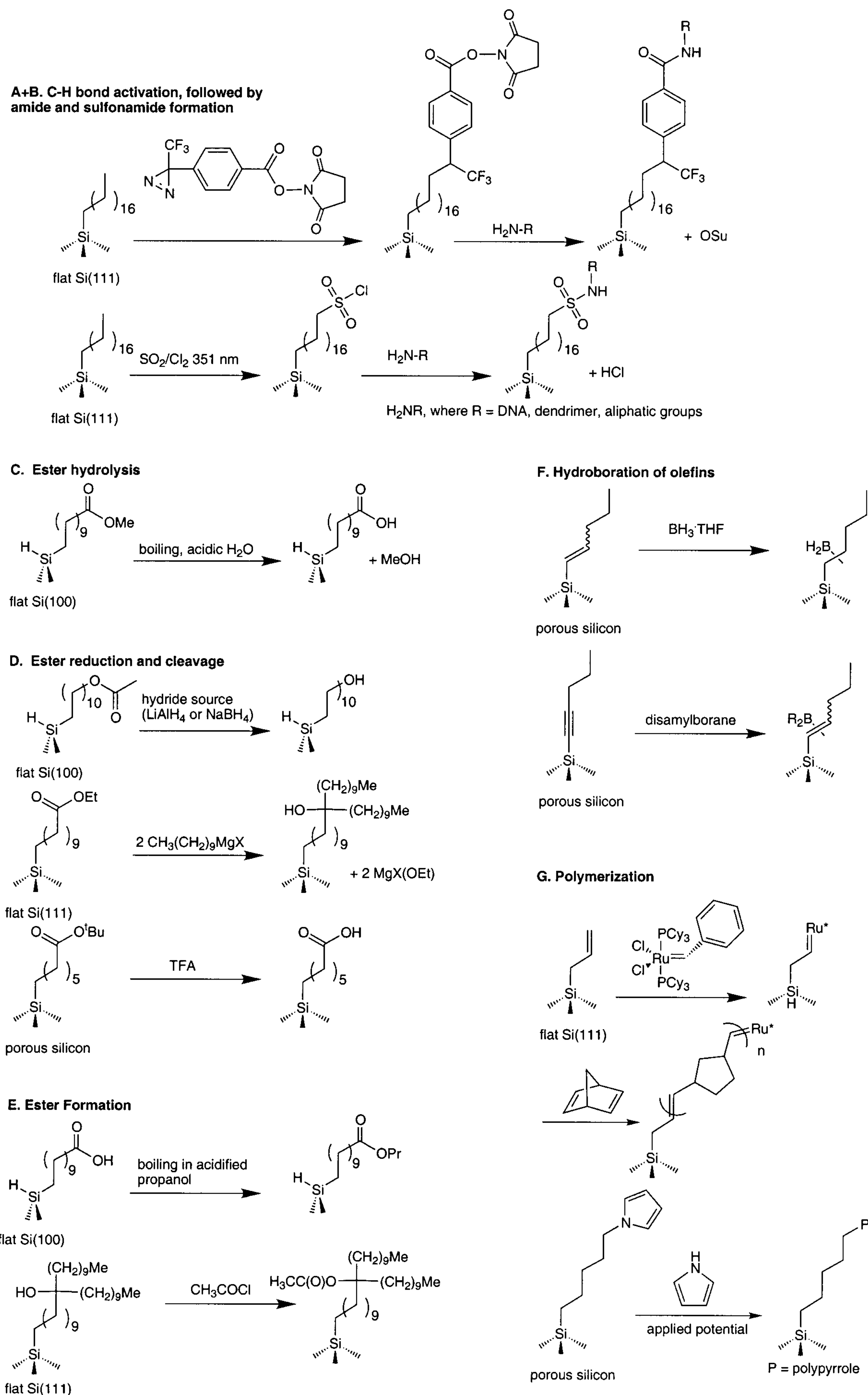

Figure 69. Outline of the secondary chemistry undertaken on functionalized silicon surfaces.

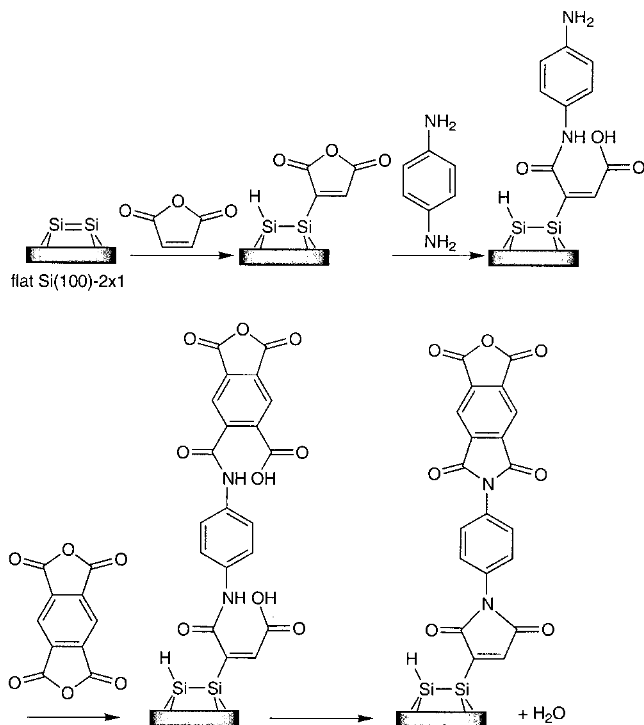

Figure 70. Amide bond formation and imide condensation on Si(100)-2 × 1 surfaces under UHV conditions.[193]

surface, Si(100)−$C_{11}H_{22}OC(O)CH_3$. Because this group could not be hydrolyzed under acidic aqueous conditions to produce the hydroxy-terminated surface, it was reduced with $LiAlH_4$ in boiling ether for 15 min.[80] Low contact angles with water and ATR-FTIR confirmed complete disappearance of all carbonyl groups, in line with release of the free hydroxy groups. A 0.5 M $NaBH_4$ solution in methoxyether, when heated to 85 °C for 30 min, can also lead to the alcohol-terminated surface, as substantiated by ATR-FT-IR.[192]

The addition of Grignard reagents to an ester-terminated surface, formed via UV-induced hydrosilylation of CH_2=$CHC_8H_{16}COOEt$ on the Si(111)−H surface, was shown to provide a useful route to carbon−carbon bond formation. A 1.0 M solution of decyl Grignard in diethyl ether resulted, in 24 h at 90 °C, in a tertiary alcohol as shown by the appearance of an O−H stretch at 3400 cm^{-1} in the ATR-FTIR spectrum and a 3-fold increase of intensity in the methylene stretching region.[192]

In an interesting application of a standard organic chemistry protecting group, a *tert*-butyl ester group was shown to be easily cleaved on a porous silicon surface with a trifluoroacetic acid (TFA)/dichloromethane solution, at room temperature as shown in Figure 69.[134] The surface, terminated with Si−$(CH_2)_6$-COO^tBu, yields the carboxylic acid surface Si−$(CH_2)_6$-COOH after treatment.

E. Ester Formation

The free carboxylic acid-terminated monolayer (prepared in section VII.C), Si(100)−$C_{10}H_{20}COOH$, was esterified by boiling in acidified 1-propanol for 30 min. The contact angles were very similar to those measured when the propyl ester-containing alkenes was utilized.[80] Acylation of a hydroxy-terminated surface with acetic anhydride did not go to completion, leading to only partial esterification.[80] Treatment of the tertiary alcohol, formed via the Grignard reduction of esters (section VII.D), with acetyl chloride at 50 °C for 14 h did result in good yields of the acetate termination.[192]

F. Hydroboration of Olefins

Alkyne hydrosilylation on porous silicon though Lewis acid chemistry (section IV.E) leads to alkenyl substitution, with a carbon−carbon double bond directly bonded to the surface.[114,115] The intense ν-(C=C) vibration, ∼1595 cm^{-1}, has the correct stretching frequency for a monosilicon-substituted C=C bond, but in order to definitively prove the chemical nature of this group, it was hydroborated with BH_3 in THF. If the apparent ν(C=C) vibration were to disappear, then it should correspond to the vinylic stretch. Indeed, soaking a pentenyl- or dodecenyl-terminated surface in 1.0 M BH_3·THF in THF at room temperature for 16 h results in quantitative reduction of the double bond, as observed by FTIR and ^{13}C solid-state NMR.[114,115] The ^{13}C NMR solid-state NMR spectra of a pentenyl-terminated porous silicon sample before and after hydroboration are shown in Figure 40. The two vinylic carbons, at ∼ δ 110 and 140 ppm in the spectrum, vanish after the hydroboration treatment, as would be expected for an alkene group. A similar procedure was applied to an alkyne-terminated porous surface.[135]

G. Polymerization

Instead of just a nanometer thick monolayer protecting the silicon surface, ring-opening metathesis polymerization (ROMP) has been shown to lead to a thick (up to 5.5 μm) film of polynorbornene on the Si(111) surface.[194] To provide the appropriate chemical handle through which polymerization can commence, a chlorinated Si(111) surface was exposed to allyl Grignard, $XMgCH_2CH$=CH_2, leading to an Si(111)−CH_2CH=CH_2 surface. Exposure of this surface to Grubb's catalyst [$(PCy_3)_2Cl_2Ru$=CHPH, Cy = cyclohexyl] and norbornene lead to ROMP. As shown in the SEM image in Figure 71, the entire surface is thoroughly covered with a 5.5 μm thick polynorbornene layer. By changing the concentration of norbornene monomer, the thickness of the layer can be controlled. The authors suggest that these polymer interfaces could be of interest for formation of metal−insulator−semiconductor structures or capacitive devices with defined thicknesses.

Electrochemical polymerization of pyrrole on a 5-(*N*-pyrrolyl)pentyl-terminated Si(100) surface proceeds smoothly.[126] The flat pyrrole-modified surface is 7−10 times smoother than polymerization on a native Si−H surface, as shown by AFM, suggesting much more uniform growth in the former due to a constant potential across the face of the crystal. The presence of the pyrrole interface appears to improve the electrical properties of the polymer/silicon interface and thus may prove to be a viable solution for device synthesis on silicon.[195]

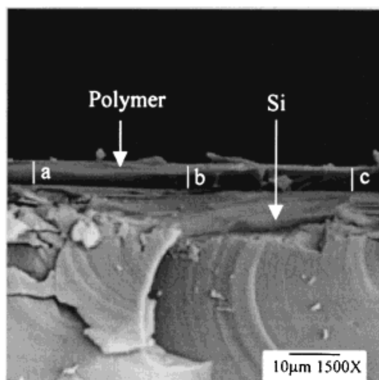

Figure 71. Cross-sectional SEM image of a polynorbornene-covered Si surface at 1500× magnification. The polymer film covers the entire Si substrate, and the estimated film thicknesses at points a, b, and c from the SEM image are 5.0, 5.5, and 5.4 μm, respectively. (Reprinted with permission from ref 194. Copyright 2001 American Chemical Society.) The authors are also thanked for permission to reprint this figure.

IX. Conclusions

From this incredible body of research, many generalizations can now be made about the organometallic surface chemistry of silicon and germanium. Still, more questions remain, especially concerning the nature of packing and bonding of organic groups in wet chemical reactions, the bonding and reactivity of the silicon–silicon and germanium–germanium dimers on the Si(100)-2 × 1 reconstructed surface, the stability of all these surfaces over the long term, their biocompatability, and many other important questions. The field is an extremely exciting one because of the close proximity between fundamental science and technological applications, and it is only a matter of time and circumstance before tailored organic interfaces reach their commercial potential.

X. Acknowledgments

I acknowledge the work, time, and care taken by my co-workers over the past 4 years at Purdue. I also thank the following agencies for their generous support: NSF (Career Award, 1999–2003), the Alfred P. Sloan Foundation (Research Fellow, 2000–2002), the Camille and Henry Dreyfus Foundation (New Faculty Award, 1997–2002), and Purdue University and the Purdue Research Foundation. J.M.B. is a Cottrell Teacher Scholar of Research Corporation (2000–2002). The researchers who permitted reprinting of their figures are also thanked wholeheartedly: Professors C. E. D. Chidsey, D. D. M. Wayner, S. F. Bent, R. J. Hamers, E. J. R. Sudhölter, G. A. Lopinski, R. A. Wolkow, C. M. Greenlief, Y. J. Chabal, N. S. Lewis, D. J. Doren, S. Jiang, and M. R. Linford and their co-workers.

XI. References

(1) Waltenburg, H. N.; Yates, J. T. *Chem. Rev.* **1995**, *95*, 1589.
(2) Hamers, R. J.; Wang, Y. *Chem. Rev.* **1996**, *96*, 1261.
(3) Campbell, S. A. *The Science and Engineering of Microelectronic Fabrication*; Oxford University Press: Oxford, 1996.
(4) *The National Technology Roadmap for Semiconductors*; Semiconductor Industry Association (SIA): San Jose, CA, 1997.
(5) Hasegawa, H.; Fujikura, H.; Okada, H. *MRS Bull.* **1999**, *24*, 25.
(6) Sailor, M. J.; Lee, E. J. *Adv. Mater.* **1997**, *9*, 783.
(7) Sze, S. M. *The Physics of Semiconductor Devices*, 2nd ed.; Wiley: New York, 1981.
(8) Albert, K. J.; Lewis, N. S.; Schauer, C. L.; Sotzing, G. A.; Stitzel, S. E.; Vaid, T. P.; Walt, D. R. *Chem. Rev.* **2000**, *100*, 2595.
(9) Freeman, W. M.; Robertson, D. J.; Vrana, K. E. *Biotechniques* **2000**, *29*, 1042.
(10) Hansen, K. M.; Ji, H. F.; Wu, G. H.; Datar, R.; Cote, R.; Majumdar, A.; Thundat, T. *Anal. Chem.* **2001**, *73*, 1567.
(11) Zee, F.; Judy, J. W. *Sensor Actuators B* **2001**, *72*, 120.
(12) Birkinshaw, K. *Int. Rev. Phys. Chem.* **1996**, *15*, 13.
(13) Eijkel, J. C. T.; Prak, A.; Cowen, S.; Craston, D. H.; Manz, A. *J. Chromatogr. A* **1998**, *815*, 265. Drott, J.; Lindstrom, K.; Rosengren, L.; Laurell, T. *J. Micromech. Microeng.* **1997**, *7*, 14.
(14) Weigl, B. H.; Yager, P. *Science* **1999**, *283*, 346.
(15) Maboudian, R. *Surf. Sci. Rep.* **1998**, *30*, 209.
(16) Buriak, J. M. *J. Chem. Soc., Chem. Commun.* **1999**, 1051. Bent, S. F. *J. Phys. Chem.*, in press. Bent, S. F. *Surf. Sci.*, in press.
(17) Sieval, A. B.; Linke, R.; Zuilhof, H.; Sudhölter, E. J. R. *Adv. Mater.* **2000**, *12*, 1457.
(18) Brook, M. A. *Silicon in Organic, Organometallic, and Polymer Chemistry*; Wiley: New York, 2000. *The Chemistry of Organic Silicon Compounds*; Patai, S., Rappoport, Z., Eds.; John Wiley and Sons: New York, 1989.
(19) Bardeen, J.; Brattain, W. H. *Phys. Rev.* **1948**, *71*, 230.
(20) Whall, T. E.; Parker, E. H. C. *J. Mater. Sci.: Mater. Electron.* **1995**, *6*, 249.
(21) Kubby, J. A.; Boland, J. *Surf. Sci. Rep.* **1996**, *26*, 249.
(22) Paul, D. J. *Adv. Mater.* **1999**, *11*, 191.
(23) Bardeen, J.; Brattain, W. H. *Phys. Rev. Lett.* **1948**, *74*, 230.
(24) Colace, L.; Masini, G.; Galluzzi, F.; Assanto, G. *Nucl. Instrum. Methods A* **2001**, *457*, 212.
(25) Hu, D. Q.; MacPherson, C. D.; Leung, K. T. *Surf. Sci.* **1992**, *273*, 21. MacPherson, C. D.; Hu, D. Q.; Doan, M.; Leung, K. T. *Surf. Sci.* **1994**, *310*, 231.
(26) For instance: Zanatta, J. P.; Ferret, P.; Duvaut, P.; Isselin, S.; Theret, G.; Rolland, G.; Million, A. *J. Cryst. Growth* **1998**, *185*, 1297. Ranke, W. *Surf. Sci.* **1995**, *342*, 281.
(27) Canham, L. T. *Appl. Phys. Lett.* **1990**, *57*, 1046.
(28) Halimaoui, A.; Oules, C.; Bomchil, G.; Bsiesy, A.; Gaspard, F.; Herino, R.; Ligeon, M.; Muller, F. *Appl. Phys. Lett.* **1991**, *59*, 304.
(29) McCord, P.; Yau, S. L.; Bard, A. J. *Science* **1992**, *257*, 68.
(30) Stewart, M. P.; Buriak, J. M. *Adv. Mater.* **2000**, *12*, 859.
(31) Fauchet, P. M. *J. Lumin.* **1996**, *70*, 294.
(32) Cullis, A. G.; Canham, L. T.; Calcott, P. D. J. *J. Appl. Phys.* **1997**, *82*, 909.
(33) Song, J. H.; Sailor, M. J. *Comments Inorg. Chem.* **1999**, *21*, 69.
(34) Lauerhaas, J. M.; Sailor, M. J. *Science* **1993**, *261*, 1567.
(35) Song, J. H.; Sailor, M. J. *J. Am. Chem. Soc.* **1998**, *120*, 2376.
(36) Allen, M. J.; Buriak, J. M. *J. Lumin.* **1999**, *80*, 29.
(37) Canham, L. T. In *Properties of Porous Silicon*; Canham, L. T., Ed.; INSPEC: London, 1997; 249.
(38) Sailor, M. J.; Heinrich, J. L.; Lauerhaas, J. M. *Semiconductor Nanoclusters*; Kamat, P. V., Meisel, D., Eds.; Elsevier: Amsterdam, 1996; Vol. 103, 209.
(39) Hamilton, B. *Semiconductor Sci. Technol.* **1995**, *10*, 1187.
(40) Sailor, M. J. In *Properties of Porous Silicon*; Canham, L. T., Ed.; INSPEC: London, 1997; 364.
(41) Lin, V. S.-Y.; Motesharei, K.; Dancil, K.-P. S.; Sailor, M. J.; Ghadiri, M. R. *Science* **1997**, *278*, 840.
(42) Janshoff, A.; Dancil, K.-P. S.; Steinem, C.; Greiner, D. P.; Lin, V. S.-Y.; Gurtner, C.; Motesharei, K.; Sailor, M. J.; Ghadiri, M. R. *J. Am. Chem. Soc.* **1998**, *120*, 12108.
(43) Letant, S. E.; Sailor, M. J. *Adv. Mater.* **2001**, *13*, 335.
(44) Letant, S. E.; Content, S.; Tan, T. T.; Zenhausern, F.; Sailor, M. J. *Sensor Actuators B* **2000**, *69*, 193.
(45) Thönissen, M.; Krüger, M.; Lerondel, G.; Romestain, R. In *Properties of Porous Silicon*; Canham, L. T., Ed.; INSPEC: London, 1997; 349. Van Belle, M. *Photonics Spectra* **1998**, *32*, *10*, 57.
(46) Wei, J.; Buriak, J. M.; Siuzdak, G. *Nature* **1999**, *399*, 243.
(47) Choi, H. C.; Buriak, J. M. *J. Chem. Soc., Chem. Commun.* **2000**, 1669.
(48) Miyazaki, S.; Sakamoto, K.; Shiba, K.; Horose, M. *Thin Solid Films* **1995**, *255*, 99.
(49) Chang, S. S.; Hummel, R. E. *J. Lumin.* **2000**, *86*, 33.
(50) Bayliss, S.; Zhang, Q.; Harris, P. *Appl. Surf. Sci.* **1996**, *102*, 390.
(51) Bond energies taken from: Walsh, R. *Acc. Chem. Res.* **1981**, *14*, 246. Dewar, M. J. S.; Friedham, G.; Grady, E. F.; Healy, J. J. P.; Stewart, J. P. *Organometallics* **1986**, *5*, 375. Walsh, R.; Becerra, R. In *The Chemistry of Organic Silicon Compounds*; Rappaport, Z., Apeloig, Y., Eds.; Wiley-Interscience: Chichester, 1998; Vol. 2, pp 153–180. Cotton, F. A.; Wilkinson, G.; Murillo, C. A.; Bochmann, M. *Advanced Inorganic Chemistry*, 6th ed.;

Wiley: New York, 1999. Glockling, F. *The Chemistry of Germanium*; Academic Press: New York, 1969.
(52) Higashi, G. S.; Chabal, Y. J.; Trucks, G. W.; Raghavachari, K. *Appl. Phys. Lett.* **1990**, *56*, 656.
(53) Higashi, G. S.; Becker, R. S.; Chabal, Y. J.; Becker, A. J. *Appl. Phys. Lett.* **1991**, *58*, 1656.
(54) Newton, T. A.; Boiani, J. A.; Hines, M. A. *Surf. Sci.* **1999**, *430*, 67.
(55) Dumas, P.; Chabal, Y.; Jakob, P. *Surf. Sci.* **1992**, *269/270*, 867.
(56) Halimaoui, A. In *Properties of Porous Silicon*; Canham, L. T., Ed.; INSPEC: London, 1997; 12.
(57) Kelly, M. T.; Chun, J. K. M.; Bocarsly, A. B. *Appl. Phys. Lett.* **1994**, *64*, 1693. Coffer, J. L. In *Properties of Porous Silicon*; Canham, L. T., Ed.; INSPEC: London, 1997; 23.
(58) Noguchi, N.; Suemune, I. *Appl. Phys. Lett.* **1994**, *62*, 1429. Anderson, O. K.; Frello, T.; Veje, E. *J. Appl. Phys.* **1995**, *78*, 6189.
(59) Anderson, R. C.; Muller, R. S.; Tobias, C. W. *J. Electrochem. Soc.* **1993**, *140*, 1393. Grosman, A.; Ortega, C. In *Properties of Porous Silicon*; Canham, L. T., Ed.; INSPEC: London, 1997; 145.
(60) Lehmann, V.; Gosele, U. *Appl. Phys. Lett.* **1991**, *58*, 856.
(61) Choi, K.; Buriak, J. M. *Langmuir* **2000**, *16*, 7737.
(62) Germanium-hydride stretches have been observed on flat Ge surfaces during in-situ electrochemistry/FTIR experiments: Maroun, F.; Ozanam, F.; Chazalviel, J. N. *J. Phys. Chem. B* **1999**, *103*, 5280.
(63) Bansal, A.; Li, X.; Lauermann, I.; Lewis, N. S.; Yi, S. I.; Weinberg, W. H. *J. Am. Chem. Soc.* **1996**, *118*, 7225.
(64) Okubo, T.; Tsuchiya, H.; Sadakata, M.; Yasuda, T.; Tanaka, K. *Appl. Surf. Sci.* **2001**, *171*, 252.
(65) He, J.; Patitsas, S. N.; Preston, K. F.; Wolkow, R. A.; Wayner, D. D. M. *Chem. Phys. Lett.* **1998**, *286*, 508.
(66) Zhu, X.-Y.; Boiadjiev, V.; Mulder, J. A.; Hsung, R. P.; Major, R. C. *Langmuir* **2000**, *16*, 6766.
(67) Luo, H.; Chidsey, C. E. D.; Chabal, Y. *Mater. Res. Soc. Proc.* **1997**, *477*, 415.
(68) Lauerhaas, J. M.; Sailor, M. J. *Mater. Res. Soc. Symp.* **1993**, *298*, 259.
(69) Lauerhaas, J. M.; Sailor, M. J. *Science* **1993**, *261*, 1567.
(70) Cullen, G. W.; Amick, J. A.; Gerlich, D. *J. Electrochem. Soc.* **1962**, *109*, 124.
(71) Lu, Z. H. *Appl. Phys. Lett.* **1996**, *68*, 22.
(72) Hamers, R. J.; Coulter, S. K.; Ellison, M. D.; Hovis, J. S.; Padowitz, D. D. F.; Schwartz, M. P.; Greenlief, C. M.; Russell, J. N. *Acc. Chem. Res.* **2000**, *33*, 617.
(73) Lopinski, G. P.; Moffatt, D. J.; Wayner, D. D. M.; Zgierski, M. Z.; Wolkow, R. A. *J. Am. Chem. Soc.* **1999**, *121*, 4532.
(74) Schwartz, M. P.; Ellison, M. D.; Coulter, S. K.; Hovis, J. S.; Hamers, R. J. *J. Am. Chem. Soc.* **2000**, *122*, 8529.
(75) (a) Hovis, J. S.; Hamers, R. J.; Greenlief, C. M. *Surf. Sci.* **1999**, *440*, 815. Other approaches towards the Ge(100)-2 $\times$ 1 surface: (b) Zhang, X.-J.; Xue, G.; Agarwarl, R.; Tsu, R.; Hasan, M. A.; Greene, J. E.; Rocket, A. *J. Vac. Sci. Technol. A* **1993**, *11*, 2553. (c) Gan, S.; Li, L.; Nguyen, T.; Qi, H.; Hicks, R. F.; Yang, M. *Surf. Sci.* **1998**, *395*, 69.
(76) Linford, M. R.; Chidsey, C. E. D. *J. Am. Chem. Soc.* **1993**, *115*, 12631. Linford, M. R.; Fenter, P.; Eisenberger, P. M.; Chidsey, C. E. D. *J. Am. Chem. Soc.* **1995**, *117*, 3145.
(77) Chatgilialoglu, C. *Acc. Chem. Res.* **1992**, *25*, 188.
(78) Labinger, J. A. In *Comprehensive Organic Synthesis*; Trost, B. M., Fleming, I., Eds.; Pergamon: New York, 1991; Vol. 8, p 699.
(79) Sung, M. M.; Kluth, J.; Yauw, O. W.; Maboudian, R. *Langmuir* **1997**, *13*, 6164.
(80) Sieval, A. B.; Demirel, A. L.; Nissink, J. W. M.; Linford, M. R.; van der Maas, J. H.; de Jeu, W. H.; Zuilhof, H.; Sudhölter, E. J. R. *Langmuir* **1998**, *14*, 1759.
(81) Sieval, A. B.; Vleeming, V.; Zuilhof, H.; Sudhölter, E. J. *Langmuir* **1999**, *15*, 8288.
(82) Sieval, A. B.; van den Hout, B.; Zuilhof, H.; Sudhölter, E. J. *Langmuir* **2000**, *16*, 2987.
(83) Sieval, A. B.; van den Hout, B.; Zuilhof, H.; Sudhölter, E. J. R. *Langmuir* **2001**, *17*, 2172.
(84) Zhang, L.; Wesley, K.; Jiang, S. *Langmuir* **2001**, *17*, 6275.
(85) Bateman, J. E.; Eagling, R. D.; Worrall, D. R.; Horrocks, B. R.; Houlton, A. *Angew. Chem., Int. Ed. Engl.* **1998**, *37*, 2683.
(86) Boukherroub, R.; Morin, S.; Wayner, D. D. M.; Bensebaa, F.; Sproule, G. I.; Baribeau, J.-M.; Lockwood, D. J. *Chem. Mater.* **2001**, *13*, 2002.
(87) Bateman, J. E.; Eagling, R. D.; Horrocks, B. R.; Houlton, A. *J. Phys. Chem. B* **2000**, *104*, 5557.
(88) Feng, W.; Miller, B. *Langmuir* **1999**, *15*, 3152.
(89) In footnote 33 of the second cited paper in ref 76, the authors note that the surface hydrosilylation of hexadecyne produces a small peak at 1600.8 cm^{-1} which they state suggests a surface-bound vinyl group. Indeed, Lewis-acid- and white-light-mediated hydrosilylation of dodecyne on porous silicon yields a strong ν-(C=C) vibration at 1595 cm^{-1}; see refs 103, 104, 114, and 115.
(90) Sieval, A. B.; Opitz, R.; Maas, H. P. A.; Schoeman, M. G.; Meijer, G.; Vergeldt, F. J.; Zuilhof, H.; Sudhölter, E. J. R. *Langmuir* **2000**, *16*, 10359.
(91) Buriak, J. M.; Stewart, M. P.; Allen, M. J. *Mater. Res. Soc. Symp. Proc.* **1998**, *536*, 173−178.
(92) Fleming, I. In *Comprehensive Organic Chemistry*; Jones, N., Ed.; Pergamon: New York, 1979; Vol. 3, p 568.
(93) Terry, J.; Linford, M. R.; Wigren, C.; Cao, R.; Pianetta, P.; Chidsey, C. E. D. *Appl. Phys. Lett.* **1997**, *71*, 1056−1058. Terry, J.; Mo, R.; Wigren, C.; Cao, R.; Mount, G.; Pianetta, P.; Linford, M. R.; Chidsey, C. E. D. *Nucl. Instrum. Methods Phys. Res., Sect. B* **1997**, *133*, 94. Terry, J.; Linford, M. R.; Wigren, C.; Cao, R.; Pianetta, P.; Chidsey, C. E. D. *J. Appl. Phys.* **1999**, *85*, 213.
(94) Cicero, R. L.; Linford, M. R.; Chidsey, C. E. D. *Langmuir* **2000**, *16*, 5688.
(95) Effenberger F.; Götz, G.; Bidlingmaier, B.; Wezstein, M. *Angew. Chem., Int. Ed. Engl.* **1998**, *37*, 2462.
(96) Burkhard, C. A.; Krieble, R. H. *J. Am. Chem. Soc.* **1947**, *69*, 2687.
(97) Kanabus-Kaminska, J. M.; Hawari, J. A.; Griller, D.; Chatgilialoglu, C. *J. Am. Chem. Soc.* **1987**, *109*, 5267−5268.
(98) Vondrak, T.; Zhu, X. Y. *Phys. Rev. Lett.* **1999**, *82*, 1967. Pusel, A.; Wetterauer, U.; Hess, P. *Phys. Rev. Lett.* **1998**, *81*, 645.
(99) Wojtyk, J. T. C.; Tomietto, M.; Boukherroub, R.; Wayner, D. D. M. *J. Am. Chem. Soc.* **2001**, *123*, 1535.
(100) Barrelet, C. J.; Robinson, D. B.; Cheng, J.; Hunt, T. P.; Quate, C. F.; Chidsey, C. E. D. *Langmuir* **2001**, *17*, 3460.
(101) Cheng, J.; Robinson, D. B.; Cicero, R. L.; Eberspacher, T.; Barrelet, C. J.; Chidsey, C. E. D. *J. Phys. Chem. B* **2001**, *105*, 10900.
(102) Leroy, E.; Küttel, O. M.; Schlapbach, L.; Giraud, L.; Jenny, T. *Appl. Phys. Lett.* **1998**, *73*, 1050.
(103) Stewart, M. P.; Buriak, J. M. *Angew. Chem., Int. Ed. Engl.* **1998**, *23*, 3257.
(104) Stewart, M. P.; Buriak, J. M. *J. Am. Chem. Soc.* **2001**, *123*, 7821.
(105) Canham, L. T. *Appl. Phys. Lett.* **1990**, *57*, 1049. Fauchet, P. M. *J. Lumin.* **1996**, *70*, 294.
(106) Lambert, J. B.; Zhao, Y.; Wu, H. *J. Org. Chem.* **1999**, *64*, 2729. Lambert, J. B. *Tetrahedron* **1990**, *46*, 2677. Lambert, J. B.; Zhao, Y.; Wu, H. *J. Org. Chem.* **1999**, *64*, 2729.
(107) Asao, N.; Yamamoto, Y. *Bull. Chem. Soc. Jpn.* **2000**, *73*, 1071.
(108) Lewis, L. N. *J. Am. Chem. Soc.* **1990**, *112*, 5998.
(109) Zazzera, L. A.; Evans, J. F.; Deruelle, M.; Tirrell, M.; Kessel C. R.; McKeown, P. *J. Electrochem. Soc.* **1997**, *144*, 2184.
(110) Buriak, J. M.; Holland, J. M.; Allen, M. J.; Stewart, M. P. *J. Solid State Chem.* **1999**, *147*, 251−258.
(111) Saghatelian, A.; Buriak, J.; Lin, V. S. Y.; Ghadiri, M. R. *Tetrahedron* **2001**, *57*, 5131,
(112) Hydrosilylation with Wilkinson's catalyst: Marciniec, B.; Gulinski, J. *J. Organomet. Chem.* **1993**, *446*, 15. Bis-silylation with palladium complexes: Ito, Y.; Suginome, M.; Murakami, M. *J. Org. Chem.* **1991**, *56*, 1948.
(113) For example: Nlate, S.; Ruiz, J.; Sartor, V.; Navarro, R.; Blais, J. C.; Astruc, D. *Chem.-Eur. J.* **2000**, *6*, 2544. Lewis, L. N.; Lewis, N.; Uriarte, R. J. *Adv. Chem. Ser.* **1992**, *230*, 541.
(114) Buriak, J. M.; Allen, M. A. *J. Am. Chem. Soc.* **1998**, *120*, 1339.
(115) Buriak, J. M.; Stewart, M. J.; Geders, T. W.; Allen, M. J.; Choi, H. C.; Smith, J.; Raftery, M. D.; Canham, L. T. *J. Am. Chem. Soc.* **1999**, *121*, 11491.
(116) Asao, N.; Sudo, T.; Yamamoto, Y. *J. Org. Chem.* **1996**, *61*, 7654. Sudo, T.; Asao, N.; Gevorgyan, V.; Yamamoto, Y. *J. Org. Chem.* **1999**, *64*, 2494.
(117) Oertle, K.; Wetter, H. *Tetrahedron Lett.* **1985**, *26*, 5511. Yamamoto, K.; Takemae, M. *Synlett* **1990**, 259.
(118) Asao et al. showed that $EtAlCl_2$ and $AlCl_3$ work equally well as catalysts for hydrosilylation of alkynes (see ref 116).
(119) Canham, L. T.; Reeves, C. L.; Newey, J. P.; Houlton, M. R.; Cox, T. I.; Buriak, J. M.; Stewart, M. P. *Adv. Mater.* **1999**, *11*, 1505.
(120) Canham, L. T.; Stewart, M. P.; Buriak, J. M.; Reeves, C. L.; Anderson, M.; Squire, E. K.; Snow, P. A. *Phys. Status Solidi A* **2000**, *182*, 521.
(121) Boukherroub, R.; Morin, S.; Bensebaa, F.; Wayner, D. D. M. *Langmuir* **1999**, *15*, 3831.
(122) Viellard, C.; Warntjes, M.; Ozanam, F.; Chazalviel, J.-N. *Proc. Electrochem. Soc.* **1996**, *95*, 250. Ozanam, F.; Vieillard, C.; Warntjes, M.; Dubois, T.; Pauly, M.; Chazalviel, J. N. *Can. J. Chem. Eng.* **1998**, *76*, 1020.
(123) Fidélis, A.; Ozanam, F.; Chazalviel, J.-N. *Surf. Sci.* **2000**, *444*, L7.
(124) Song, J. H.; Sailor, M. J. *J. Am. Chem. Soc.* **1998**, *120*, 2376.
(125) Song, J. H.; Sailor, M. J. *Inorg. Chem.* **1999**, *38*, 1503.
(126) Kim, N. Y.; Laibinis, P. E. *J. Am. Chem. Soc.* **1999**, *121*, 7162.
(127) Kim, N. Y.; Laibinis, P. E. *J. Am. Chem. Soc.* **1998**, *120*, 4516.
(128) Royea, W. J.; Juang, A.; Lewis, N. S. *Appl. Phys. Lett.* **2000**, *77*, 1988.
(129) He, J.; Patitsas, S. N.; Preston, K. F.; Wolkow, R. A.; Wayner, D. D. M. *Chem. Phys. Lett.* **1998**, *286*, 508.
(130) Yang, C. S.; Kauzlarich, S. M.; Wang, Y. C.; Lee, H. W. H. *J. Cluster Sci.* **2000**, *11*, 423. Mayeri, D.; Phillips, B. L.; Augustine, M. P.; Kauzlarich, S. M. *Chem. Mater.* **2001**, *13*, 765. Yang, C. S.; Bley, R. A.; Kauzlarich, S. M.; Lee, H. W. H.; Delgado, G. R. *J. Am. Chem. Soc.* **1999**, *121*, 5191.

(131) Taylor, B. R.; Kauzlarich, S. M.; Delgado, G. R.; Lee, H. W. H. *Chem. Mater.* **1999**, *11*, 2493.
(132) Yang, C. S.; Kauzlarich, S. M.; Wang, Y. C. *Chem. Mater.* **1999**, *11*, 3666.
(133) Henry de Villeneuve, C.; Pinson, J.; Bernard, M. C.; Allongue, P. *J. Phys. Chem. B* **1997**, *101*, 2415.
(134) Gurtner, C.; Wun, A. W.; Sailor, M. J. *Angew. Chem., Int. Ed.* **1999**, *38*, 1966.
(135) Robins, E. G.; Stewart, M. P.; Buriak, J. M. *J. Chem. Soc., Chem. Commun.* **1999**, 2479.
(136) Jouikov, V. V. *Russ. Chem. Rev.* **1997**, *66*, 509. Jouikov, V.; Salaheev, G. *Electrochim. Acta* **1996**, *41*, 2623. Kunai, A.; Ohnishi, O.; Sakurai, T.; Ishikawa, M. *Chem. Lett.* **1995**, 1051.
(137) *Cationic Polymerization*; Faust, R., Shaffer, T. D., Eds.; American Chemical Society: Washington, DC, 1997; Vol. 665.
(138) Linford, M. R. U.S. Patent 6,132,801, issued October 17, 2000.
(139) Niederhauser, T. L.; Jiang, G.; Lua, Y.-Y.; Dorff, M. J.; Woolley, A. T.; Asplund, M. C.; Berges, D. A.; Linford, M. R. *Langmuir* **2001**, *17*, 5889.
(140) Niederhauser, T. L.; Lua, Y.-Y.; Sun, Y.; Jiang, G.; Strossman, G. S.; Pianetta, P.; Linford, M. R. *Chem. Mater.*, in press.
(141) Amick, J. A.; Cullen, G. W.; Gerlich, D. *J. Electrochem. Soc.* **1962**, *109*, 127.
(142) Gerlich, D.; Cullen, G. W.; Amick, J. A. *J. Electrochem. Soc.* **1962**, *109*, 133.
(143) He, J.; Lu, Z.-H.; Mitchell, S. A.; Wayner, D. D. M. *J. Am. Chem. Soc.* **1998**, *120*, 2660.
(144) Bozack, M. J.; Taylor, P. A.; Choyke, W. J.; Yates, J. T. *Surf. Sci.* **1986**, *177*, L933. Bozack, M. J.; Choyke, W. J.; Muehlhoff, L.; Yates, J. T. *Surf. Sci.* **1986**, *176*, 547. Bozack, M. J.; Choyke, W. J.; Muelhoff, L.; Yates, J. T. *J. Appl. Phys.* **1986**, *60*, 3750. Yoshinobu, J.; Tsuda, H.; Onchi, M.; Nishijima, M. *J. Chem. Phys.* **1987**, *87*, 7332. Cheng, C. C.; Wallace, R. M.; Taylor, P. A.; Choyke, W. J.; Yates, J. T. *J. Appl. Phys.* **1990**, *67*, 3693. Clemen, L.; Wallace, R. M.; Taylor, P. A.; Dresser, M. J.; Choyke, W. J.; Weinberg, W. H.; Yates, J. T. *Surf. Sci.* **1992**, *268*, 205. Craig, B. I.; Smith, P. V. *Surf. Sci.* **1992**, *276*, 174. Craig, B. I.; Smith, P. V. *Surf. Sci.* **1993**, *285*, 295. Huang, C.; Widdra, W.; Weinberg, W. H. *Surf. Sci.* **1994**, *315*, L953. Imamura, Y.; Morikawa, Y.; Yamasaki, T.; Nakatsuji, H. *Surf. Sci.* **1995**, *341*, L1091. Widdra, W.; Huang, C.; Yi, S. I.; Weinberg, W. H. *J. Chem. Phys.* **1996**, *105*, 5605. Gokhale, P.; Trischberger, D.; Menzel, W.; Widdra, H.; Dröge, H.-P.; Steinrück, U.; Birkenheuer, U.; Gutdeutsch; Rösch, N. *J. Chem. Phys.* **1998**, *108*, 5554. Borovsky, B.; Krueger, M.; Ganz, E. *Phys. Rev. B* **1998**, *57*, R4269. Alavi, S.; Rousseau, R.; Seideman, T. *J. Chem. Phys.* **2000**, *113*, 4412. Hofer, W. A.; Fisher, A. J.; Lopinski, G. P.; Wolkow, R. A. *Phys. Rev. B* **2001**, *63*, 5314. Birkenheuer, U.; Gutdeutsch, U.; Rosch, N. *Surf. Sci.* **1998**, *409*, 213.
(145) Konecny, R.; Doren, D. J. *Surf. Sci* **1998**, *417*, 169. Imamura, Y.; Morikawa, Y.; Yamasaki, T.; Nakatsuji, H. *Surf. Sci.* **1995**, *341*, L1091. Liu, Q.; Hoffmann, R. J. *J. Am. Chem. Soc.* **1995**, *117*, 4082. Fisher, A. J.; Blöchl, P. E.; Briggs, G. A. D. *Surf. Sci.* **1997**, *374*, 298. Pan, W.; Zhu, T.; Yang, W. *J. Chem. Phys.* **1997**, *107*, 3981.
(146) Taylor, P. A.; Wallace, R. M.; Cheng, C. C.; Weinberg, W. H.; Dresser, M. J.; Choyke, W. J. Yates, J. T. *J. Am. Chem. Soc.* **1992**, *114*, 6754. Huang, C.; Widdra, W.; Wang, X. S.; Weinberg, W. H. *J. Vac. Sci. Technol. A* **1993**, *11*, 2250. Liu, Q.; Hoffman, R. *J. Am. Chem. Soc.* **1995**, *117*, 4082. Terborg, R.; Baumgartel, P.; Lindsay, R.; Schaff, O.; Giessel, T.; Hoeft, J. T.; Polcik, M.; Toomes, R. L.; Kulkarni, S.; Bradshaw, A. M.; Woodruff, D. P. *Phys. Rev. B* **2000**, *61*, 16697.
(147) Examples of computational studies of the [2+2] cycloaddition reaction of alkenes and alkynes: Fisher, A. J.; Blochl, P. E.; Briggs, G. A. D. *Surf. Sci.* **1997**, *374*, 298. Silvestrelli, P. L.; Toigo, F. F.; Ancilotto, F. *J. Chem. Phys.* **2001**, *114*, 8539. Hofer, W. A.; Fisher, A. J.; Wolkow, R. A. *Surf. Sci.* **2001**, *475*, 83. Cho, J. H.; Kleinman, L.; Chan, C. T.; Kim, K. S. *Phys. Rev. B* **2001**, *6307*, 3306.
(148) Morikawa, Y. *Phys. Rev. B* **2001**, *63*, 3405. Sorescu, D. C.; Jordan, K. D. *J. Phys. Chem. B* **2000**, *104*, 8259. Tanida, Y.; Tsukada, M. *Appl. Surf. Sci.* **2000**, *159*, 19.
(149) Woodward, R. B.; Hoffmann, R. *The Conservation of Orbital Symmetry*; Academic Press: New York, 1970.
(150) Liu, H.; Hamers, R. J. *J. Am. Chem. Soc.* **1997**, *119*, 7593.
(151) Chahdi, D. J. *Phys. Rev. Lett.* **1979**, *43*, 43.
(152) Yates, J. T. *Science* **1998**, *279*, 335.
(153) Hamers, R. J.; Hovis, J. S.; Lee, S.; Liu, H.; Shan, J. *J. Phys. Chem. B* **1997**, *101*, 1489.
(154) Liu, H. B.; Hamers, R. J. *Surf. Sci.* **1998**, *416*, 354.
(155) Hovis, J. S.; Hamers, R. J. *J. Phys. Chem. B* **1997**, *101*, 9581.
(156) Hovis, J. S.; Hamers, R. J. *J. Phys. Chem. B* **1998**, *102*, 687.
(157) Hovis, J. S.; Lee, S.; Liu, H.; Hamers, R. J. *J. Vac. Sci. Technol. B.* **1997**, *15*, 1153.
(158) Padowitz, D. F.; Hamers, R. J. *J. Phys. Chem. B* **1998**, *102*, 8541.
(159) Kiskinova, M.; Yates, J. T. *Surf. Sci.* **1995**, *325*, 1.
(160) Lopinski, G. P.; Moffatt, D. J.; Wayner, D. D. M.; Wolkow, R. A. *J. Am. Chem. Soc.* **2000**, *122*, 3548.
(161) Lopinski, G. P.; Moffatt, D. D. J.; Wayner, D. D. M.; Wolkow, R. A. *Nature* **1998**, *392*, 909.
(162) Armstrong, J. L.; White, J. M. *J. Vac. Sci. Technol. A* **1997**, *15*, 1146.
(163) Armstrong, J. L.; Pyant, E. D.; White, J. M. *J. Vac. Sci. Technol. A* **1998**, *16*, 123.
(164) Barriocanal, J. A.; Doren, D. J. *J. Am. Chem. Soc.*, in press.
(165) Ellison, M. D.; Hamers, R. J. *J. Phys. Chem. B.* **1999**, *103*, 6243.
(166) Konecny, R.; Doren, D. *J. Am. Chem. Soc.* **1997**, *119*, 11098.
(167) Teplyakov, A. V.; Kong, M. J.; Bent, S. F. *J. Am. Chem. Soc.* **1997**, *119*, 11100.
(168) Teplyakov, A. V.; Kong, M. J.; Bent, S. F. *J. Chem. Phys.* **1998**, *108*, 4599.
(169) Hovis, J. S.; Liu, H. B.; Hamers, R. J. *J. Phys. Chem. B* **1998**, *102*, 6873.
(170) Choi, C. H.; Gordon, M. S. *J. Am. Chem. Soc.* **1999**, *121*, 11311.
(171) Wang, G. T.; Mui, C.; Musgrave, C. B.; Bent, S. F. *J. Phys. Chem. B* **1999**, *103*, 6803.
(172) Kong, M. J.; Teplyakov, A. V.; Jagmohan, J.; Lyubovitsky, J. G.; Mui, C.; Bent, S. F. *J. Phys. Chem. B* **2000**, *104*, 3000.
(173) Borovsky, B.; Krueger, M.; Ganz, E. *Phys. Rev. B* **1998**, *57*, R4269. Lopinski, G. P.; Fortier, T. M.; Moffatt, D. J.; Wolkow, R. A. *J. Vac. Sci. Technol. A* **1998**, *16*, 1037. Craig, B. I. *Surf. Sci.* **1993**, *280*, L279. Jeonng, H. D.; Ryu, S.; Lee, Y. S.; Kim, S. *Surf. Sci.* **1995**, *344*, L1226. Kong, M. J.; Teplyakov, A. V.; Lyubovitsky, J. G.; Bent, S. F. *Surf. Sci.* **1998**, *411*, 286.
(174) Teplyakov, A. T.; Kong, M. J.; Bent, S. F. *J. Chem. Phys.* **1998**, *108*, 4599.
(175) Bronikowski, M. J.; Hamers, R. J. *J. Vac. Sci. Technol. A* **1995**, *13*, 777.
(176) Kong, M. J.; Lee, S. S.; Lyubovitsky, J.; Bent, S. F. *Chem. Phys. Lett.* **1996**, *263*, 1.
(177) Colaiainni, M. L.; Chen, P. J.; Gutleben, H.; Yates, J. T. *Chem. Phys. Lett.* **1992**, *191*, 561.
(178) Gutlteben, H.; Lucas, S. R.; Cheng, C. C.; Choyke, W. J.; Yates, J. T. *Surf. Sci.* **1991**, *257*, 146.
(179) Nyffenegger, R. M.; Penner, R. M. *Chem. Rev.* **1997**, *97*, 1195.
(180) Abeln, G. C.; Lee, S. Y.; Lyding, J. W.; Thompson, D. S.; Moore, J. S. *Appl. Phys. Lett.* **1997**, *70*, 2747.
(181) Abeln, G. C.; Hersam, M. C.; Thompson, D. S.; Hwang, S.-T.; Choi, H.; Moore, J. S.; Lyding, J. W. *J. Vac. Sci. Technol. B* **1998**, *16*, 3874. Hersam, M. C.; Guisinger, N. P.; Lyding, J. W. *J. Vac. Sci. Technol. A* **2000**, *18*, 1349.
(182) Lopinski, G. P.; Wayner, D. D. M.; Wolkow, R. A. *Nature* **2000**, *406*, 48.
(183) Lee, S. W.; Hovis, J. S.; Coulter, S. K.; Hamers, R. J.; Greenlief, C. M. *Surf. Sci.* **2000**, *462*, 6. Hamers, R. J.; Hovis, C. M.; Greenlief, C. M.; Padowitz, D. F. *Jpn. J. Appl. Phys.* **1999**, *38*, 3879.
(184) Lal, P.; Teplyakov, A. V.; Noah, Y.; Kong, M. J.; Wang, G. T.; Bent, S. F. *J. Chem. Phys.* **1999**, *110*, 10545.
(185) Wang, G. T.; Mui, C.; Musgrave, C. B.; Bent, S. F. *J. Phys. Chem. B* **2001**, *105*, 12559.
(186) Teplyakov, A. V.; Lal, P.; Noah, Y. A.; Bent, S. F. *J. Am. Chem. Soc.* **1998**, *120*, 7377.
(187) Kobayashi, Y.; Isaka, H.; Ogino, T. *Appl. Surf. Sci.* **1998**, *132*, 314. Patthey, L.; Bullock, E. L.; Abukawa, T.; Kono, S.; Johansson, L. S. O. *Phys. Rev. Lett.* **1995**, *75*, 2538. Iwawaki, F.; Tomitori, M.; Nishikawa, O. *Surf. Sci.* **1992**, *266*, 285. Tomitori, M.; Watanabe, K.; Kobayashi, M.; Nishikawa, O. *J. Vac. Sci. Technol. B* **1994**, *12*, 2022. Guo, L. W.; Huang, Q.; Li, Y. K.; Ma, S. L.; Peng, C. S.; Zhou, J. M. *Surf. Sci.* **1998**, *406*, L592. Liu, F.; Wu, F.; Lagally, M. G. *Chem. Rev.* **1997**, *97*, 1045.
(188) Mui, C.; Bent, S. F.; Musgrave, C. B. *J. Phys. Chem. A* **2000**, *104*, 2457.
(189) Toscano, M.; Russo, N. *J. Mol. Catal.* **1989**, *55*, 101. Toscano, M. *Surf. Sci.* **1991**, *251*, 894.
(190) Wagner, P.; Nock, S.; Spudich, J.; Volkmuth, W. D.; Chu, S.; Cicero, R. L.; Wade, C. P.; Linford, M. R.; Chidsey, C. E. D. *J. Struct. Biol.* **1997**, *119*, 189.
(191) Cicero, R. L.; Wagner, P.; Linford, M. R.; Hawker, C. J.; Waymouth, R. M.; Chidsey, C. E. D. *Polym. Prepr.* **1997**, *38*, 904.
(192) Boukherroub, R.; Wayner, D. D. M. *J. Am. Chem. Soc.* **1999**, *121*, 11513.
(193) Bitzer, T.; Richardson, N. V. *Appl. Surf. Sci.* **1999**, *144*−*145*, 339. Bitzer, T.; Rada, T.; Richardson, N. V. *J. Phys. Chem. B* **2001**, *105*, 4535.
(194) Juang, A.; Scherman, O. A.; Grubbs, R. H.; Lewis, N. S. *Langmuir* **2001**, *17*, 1321.
(195) Vermeir, I. E.; Kim, N. Y.; Laibinis, P. E. *Appl. Phys. Lett.* **1999**, *74*, 3860.

CR000064S